Regulation of Amino Acid Homeostasis in the Brain Interstitial Fluid

---

Dissertation

zur

Erlangung der naturwissenschaftlichen Doktorwürde (Dr. sc. nat.)

vorgelegt der

Mathematisch-naturwissenschaftlichen Fakultät

der

Universität Zürich

von

ELENA DOLGODILINA

aus

WEISSRUSSLAND

Promotionskomitee

Prof. Dr. Francois Verrey
Prof. Dr. Carsten A. Wagner
Prof. Dr. Jean-Marc Fritschy
Prof. Dr. Britta Engelhardt

Zürich, 2015

Никогда и ничего не просите!
Никогда и ничего, и в особенности
у тех, кто сильнее вас.
Сами предложат и сами все дадут!
М. А. Булгаков, «Мастер и Маргарита»

Table of contents

1. Summary

Homeostatic control of the surrounding microenvironment is a requirement for proper neuronal function. Their high metabolism requires an efficient supply of nutrients (sugars, amino acids, nucleosides, etc.) and removal of potentially toxic metabolites. A central role in balancing these two processes belongs to the barriers of the central nervous system (CNS). The Blood Brain barrier (BBB) is a dynamic interface between the peripheral circulation and the CNS that tightly regulates transport of compounds into and out of the brain. According to the currently accepted hypothesis the BBB plays a significant role in the production of the brain interstitial fluid (ISF) that directly surrounds neurons and other brain cells. However, since the ISF is only ~ 20% of the total brain volume and is distributed throughout the brain, it is difficult to sample unlike the cerebrospinal fluid (CSF). Therefore, rather less is known about its content. Amino acids (AA) are vitally necessary compounds with multiple functions. Additionally, in the CNS AAs are neurotransmitters or neurotransmitter precursors. For example, glutamine (Gln) serves as a precursor for both the major excitatory (glutamate) and inhibitory (γ-aminobutyric acid (GABA)) neurotransmitters and as a result levels are altered during some pathologies. The conditionally essential AA Gln is the most abundant AA in plasma and CSF. Moreover, in CSF Gln concentration is ~ 80% of that in plasma, while all other standard AAs are ~ 10-fold less concentrated [1]. Nevertheless, data about concentrations of Gln and other AAs in brain ISF are infrequent and inconsistent. The following Gln transporters: LAT1 (SLC7A5), SNAT2 (SLC38A2), SNAT3 (SLC38A3), and SNAT5 (SLC38A5), are significantly expressed in the BBB [2]. Moreover, LAT1 and SNAT3 have been shown to be localized on both luminal and abluminal membranes of BBB endothelial cells [3].

For my dissertation I focused on the brain ISF AAs (in particular Gln) and possible mechanisms of regulation by BBB expressed amino acid transporters (AAT)s. Using *in vivo* intracranial microdialysis in awake freely moving mice we determined the levels of 14 standard and 2 non-standard AA. For all AAs a ~10 fold concentration gradient between ISF and CSF was observed. Furthermore the acute administration of valine by intraperitoneal (IP) injection caused a significant increase of its concentration not only in plasma, but also in the brain ISF. In contrast, $^{15}N_2$ Gln (hGln) IP administration resulted in an elevation only in plasma, but not ISF. Nonetheless this labeled form of Gln represented ~ 4% of total Gln in microdialysate samples. Thus, we demonstrated efficient transendothelial transport of both AA from the blood. Competitive inhibition of system L and system A AATs in the brain by inhibitors (2-aminobicyclo-(2,2,1)-heptane-2-carboxylic acid (BCH) and α-(methylamino)-isobutyric acid

(MeAIB), respectively) introduced via the microdialysis probe led to Gln increase in the brain ISF. The Gln elevation produced due to BCH infusion was twice higher than that caused by MeAIB. To study whether Gln was released from brain cells or its raise in ISF was due to increased BBB transport, IP injection of $^{15}N_2$ Gln was combined with BCH administration. The data showed a significant increase of hGln in the brain ISF in presence of BCH in comparison to its IP administration alone indicating that brain perfusion with BCH increased Gln influx via the BBB, presumably by transstimulating Gln uptake via obligatory exchanger LAT1.

Since a high level of *Snat5* mRNA was found in BBB its localization in brain endothelial cells (BEC) membranes was studied. Unfortunately, an antibody-dependent approach did not allow distinction of SNAT5 in the BBB endothelium.

Therefore, first of all, a steep AA concentration gradient between the brain ISF and CSF was demonstrated. Second, the data are consistent with LAT1 playing a major role in the regulation of Gln in brain ISF. Since LAT1 is an obligatory exchanger, we suggest it acts together with BBB expressed SNAT3 as key regulators of Gln in brain ISF. We consider that studies using inducible endothelial specific SNAT3 knockout animals will clarify the contributions of BBB expressed SNAT3 in Gln ISF homeostasis.

2. Zusammenfassung

Homöostatische Kontrolle der angrenzenden Mikroumgebung ist eine Voraussetzung für korrekte neuronale Funktion. Der hohe Metabolismus von Neuronen erfordert eine effiziente Nährstoffversorgung (Zucker, Aminosäuren, Nukleoside, etc.) und Beseitigung von potentiell toxischen Metaboliten. Eine zentrale Rolle für die Balance zwischen diesen beiden Prozessen nehmen die Schranken des Zentralnervensystems (ZNS) ein. Die Blut-Hirn-Schranke (BHS) ist eine dynamische Verbindung zwischen der peripheren Zirkulation und dem ZNS, welche den Stoffaustausch ins und aus dem Gehirn heraus eng reguliert. Gemäss der aktuell akzeptierten Hypothese spielt die BHS eine bedeutende Rolle für die Produktion der interstitiellen Flüssigkeit des Gehirns (ISF), welche Neuronen und andere Gehirnzellen direkt umgibt. Die ISF macht nur ~ 20% des gesamten Gehirnvolumens aus und sie ist im ganzen Gehirn verteilt. Im Gegensatz zur Zerebrospinalflüssigkeit (ZSF) ist es deshalb schwierig Proben der ISF zu nehmen, weswegen weniger über deren Zusammensetzung bekannt ist. Aminosäuren (AS) sind lebensnotwendige Komponenten mit mannigfaltigen Funktionen. Im ZNS operieren AS auch als Neurotransmitter oder als deren Vorstufen. Glutamin (Gln) dient beispielsweise als Vorstufe für den wichtigsten exzitatorischen (Glutamat) sowie den inhibitorischen (γ-Aminobuttersäure (GABA)) Neurotransmitter, wobei deren Konzentrationen in manchen Krankheitsbildern verändert sind. In dem Plasma und in der ZSF ist die konditionell essentielle Aminosäure Gln die höchstkonzentrierte Aminosäure. In der ZSF beträgt die Gln Konzentration ~ 80% des Plasmalevels, während alle anderen Standardaminosäuren ~ 10-fach niedriger konzentriert sind [1]. Daten über Aminosäure Konzentrationen in der ISF des Gehirns sind jedoch selten und inkonsistent. Die Gln Transporter LAT1 (SLC7A5), SNAT2 (SLC38A2), SNAT3 (SLC38A3) und SNAT5 (SLC38A5) sind in der BHS massgeblich exprimiert [2]. Des weiteren ist gezeigt worden, dass LAT1 und SNAT3 auf der luminalen wie auch der abluminalen Membran von BHS Endothelialzellen lokalisiert [3].

Für meine Dissertation fokussierte ich auf AS der ISF des Gehirns (vor allem Gln) und mögliche Mechanismen der Regulation durch die in der BHS exprimierten Aminosäure Transporter (AST). Wir bestimmten die Konzentrationen von 14 kanonischen und 2 nichtkanonischen AS mit Hilfe von *in vivo* intrakranieller Mikrodialyse in wachen, frei-beweglichen Mäusen. Es konnte für alle AS ein 10-facher Konzentrationsgradient zwischen ISF und ZSF beobachtet werden. Des weiteren führte die intraperitoneale (IP) Injektion von Valin zu einem markanten Anstieg der Konzentration dieser Aminosäure nicht nur in Plasma, sondern auch in der ISF des Gehirns. Hingegen resultierte die IP Applikation von $^{15}N_2$ Gln (hGln) nur zu einem Anstieg im

Plasma, nicht jedoch in der ISF. Gleichzeitig repräsentierte diese markierte Form von Gln dennoch ~ 4% des totalen Gln der Mikrodialyse Proben. Somit zeigten wir einen effizienten transendothelialen Transport beider AS vom Blut. Kompetitive Hemmung der System-L und System-A Transporter im Gehirn durch Inhibitoren (2-Aminobicyclo-(2,2,1)heptan-2-carbonsäure (BCH) und α-Methylamino-isobuttersäure (MeAIB) beziehungsweise), welche durch die Mikrodialyse-Probe appliziert wurden, führten zu einem Gln Anstieg in der ISF des Gehirns. BCH führte hierbei zu einem doppelt so hohen Gln Anstieg wie MeAIB. Die IP Injektion von $^{15}N_2$ Gln (hGln) wurde mit einer BCH Applikation kombiniert, um zu eruieren, ob Gln aus Gehirnzellen freigesetzt wurde oder ob der Gln Transport über die BHS erhöht wurde. Die Daten zeigen einen signifikanten Anstieg von hGln in der ISF des Gehirns in der Präsenz von BCH verglichen mit der alleinigen hGln Applikation, was auf eine erhöhte Gln Zufuhr über die BHS hinweist, vermutlich durch Transstimulation des Gln Transportes via dem obligaten Austauscher LAT1.

Die Lokalisierung von SNAT5 in Membranen der Endothelzellen des Gehirns wurde untersucht, da hohe Levels von *Snat5* mRNA in der BHS gefunden wurden. Leider gelang der Nachweis von SNAT5 in der BHS durch eine auf Antikörper-basierte Methode nicht.

Abschliessend, konnten wir zeigen zuerst, dass ein steiler AS Konzentrationsgradient zwischen der ISF des Gehirns und der ZSF herrscht. Zweitens, stimmen die Daten damit überein, dass LAT1 eine Hauptrolle in der Regulation von Gln in der ISF des Gehirns spielt. Da LAT1 zwingend ein Austauscher ist, schlagen wir vor, dass LAT1 zusammen mit SNAT3 als Hauptregulator von Gln in der ISF des Gehirns agiert. Wir nehmen an, dass Studien mit induzierbaren Endothel-spezifischen SNAT3 Knockout Mäusen den Beitrag, welcher SNAT3 in der Gln Homöostase der ISF leistet, klären werden.

3. Introduction

3.1. Barriers of the CNS

The central nervous system (CNS) integrates diverse information obtained both from external as well as internal environment and coordinates adequate responses of the whole body to the challenges. The brain is the organ with the most complex organization in the body and controls under normal conditions all other organs and vital processes. Neurons, glial cells (oligodendrocytes, astrocytes, microglia) and pericytes together occupy the major brain volume (80%), while the brain endothelial cells represent not more than 3% of the total brain volume [4, 5]. The excitability of neurons together with the specificity of their anatomical structure allows them to receive, process and transmit information. These nervous system functions are associated with changes in membrane potential and, consequently, ion concentration and chemical gradients in the extracellular fluid. Additionally, these functions are highly energy intensive and as a result 15-20% of the body's basal metabolic rate is due to brain metabolism [6]. Homeostatic control of the microenvironment of neurons is an essential requirement for normal physiological function. Conversely, the demanding brain metabolism requires a constant supply of nutrients and oxygen from the blood and the consequent removal of metabolic wastes.

A crucial role in the establishment and maintenance of normal homeostasis in the extracellular brain milieu is carried out by the barriers of the CNS (Figure 1): the Blood-Brain Barrier (BBB) protects the brain from possible changes within blood plasma, while the blood-CSF barrier (BCSFB) and the arachnoid barrier separate cerebrospinal fluid (CSF) from the blood [7, 8].

Interestingly, there is an additional barrier between the brain interstitial fluid (ISF) and the CSF, formed by neuroependymal cells during early development [9]. The main role of this barrier might be the establishment of a special environment for the developing brain. For instance, small molecules such as sucrose can penetrate the barrier, while large molecules like proteins cannot. However, in the adult organisms ependymal cells lining the ventricles are joined only by gap junctions that allows free communication between ISF and CSF.

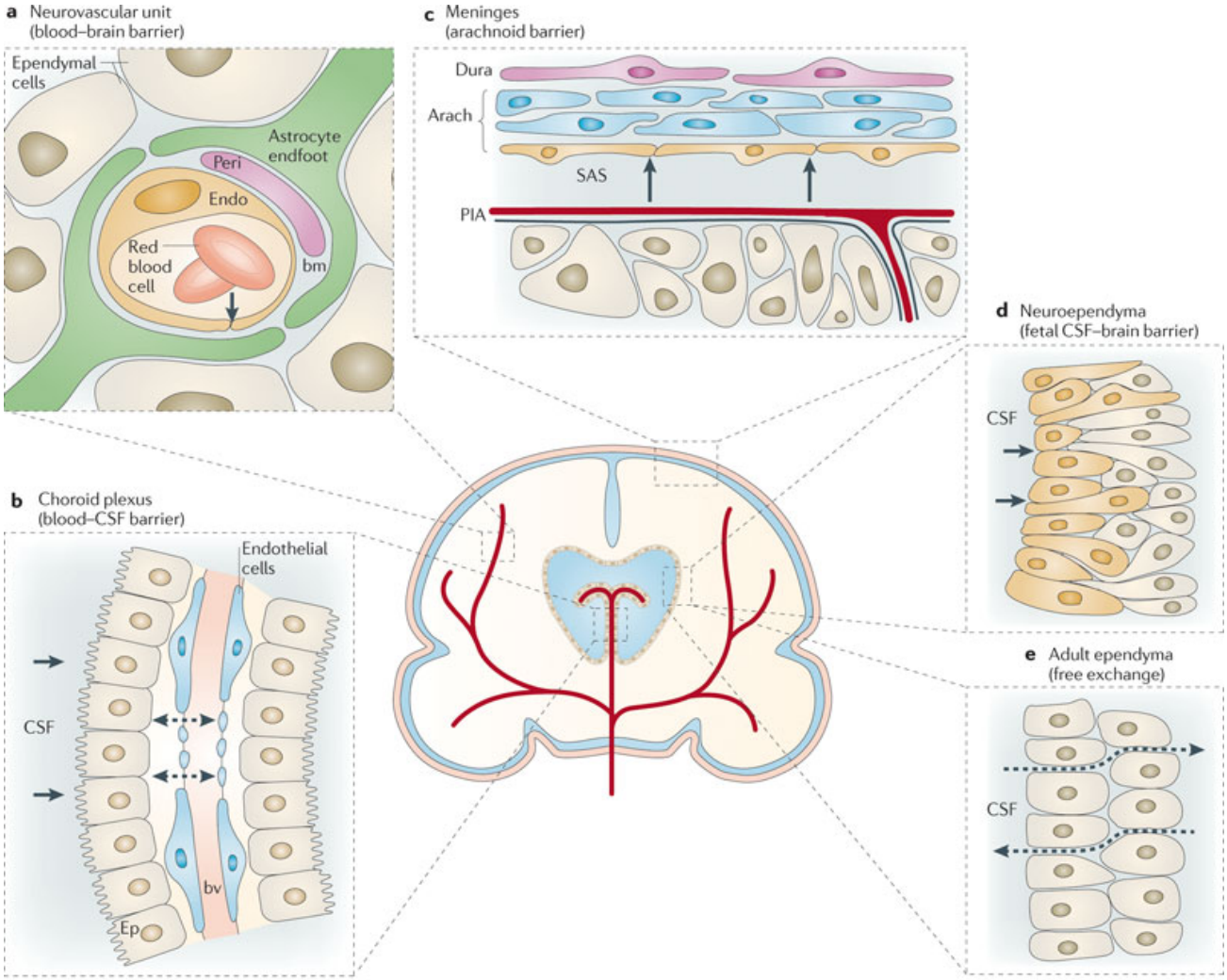

Figure 1. Barriers of the CNS (source [10])
A. The BBB is composed of the endothelial cells (Endo) of cerebral microvasculature, which together with pericytes (Peri) are surrounded by the basement membrane (bm). All together the mentioned structures are wrapped in astrocytic processes.
B. Choroid plexus epithelial cells (Ep) form the BCSF barrier. The endothelial cells of CP are fenestrated and substance exchange (dashed arrows) between blood vessel (bv) and CSF takes place.
C. The outer layer of the arachnoid membrane (Arach) has tight junctions (TJ) and establishes the barrier between subarachnoid space (SAS), containing CSF, and the overlaying structures. The blood vessels between the arachnoid membrane and the pial surface (PIA) also have TJ (not shown).
D. Neuroependymal cells are connected by strap junctions (arrows) and form the barrier at the early stages of development.
E. Ependymal cells in the adults do not form proper barrier and molecules can freely exchange (dotted arrows)
The black arrow indicates presence of TJ.

The arachnoid barrier is composed of two layers, separated by trabeculae. Epithelial cells of the outer layer have tight junctions (TJ), which prevent free diffusion of molecules into the subarachnoid fluid, while cells of the inner layer are linked by “punctate” junctions and provide the main route for CSF drainage [11]. Conversely, the major communication interfaces between blood and brain extracellular fluid (ECF), which includes brain ISF and CSF, are represented by

surfaces of the BCSFB and BBB. The BCSF barrier consists of epithelial cells, while the BBB is composed of endothelial cells. Despite the fact that brain endothelial cells are the anatomical and functional units of the BBB, these cells must closely cooperate with other cell types in the brain such as neurons, glial cells, and pericytes in order to maintain their specific structural features and regulate the neuronal microenvironment properly. Consequently, the concept of neurovascular unit (NVU) was introduced to describe the close structure-functional association of brain endothelium, extracellular basement membranes, pericytes, astrocytes, microglia, and neurons [12]. Despite the differences in morphology, expression profile of molecule subsets and functions, the BBB and BCSFB share many similarities in structural organization.

3.1.1. Junctional complexes as a basement for the barrier function

One of the distinguishing structural features of both barriers is the presence of complicated, well-organized junctional complexes, which include TJ and adherens junctions (AJ) (Figure 2). TJ and AJ include transmembrane as well as cytoplasmic proteins, which link the complexes to the actin cytoskeleton [13].

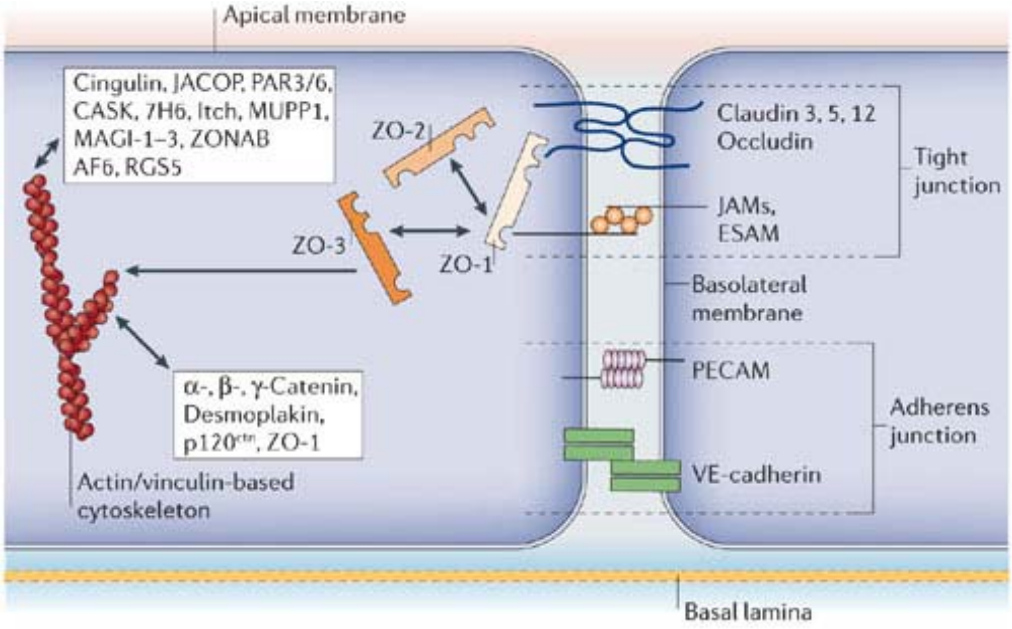

Figure 2. Structure of tight junctions (TJ) (source [14])
A simplified scheme of TJ structure of brain endothelial cells is presented. The principal organization of junctional complexes is similar for endothelial and epithelial cells and includes a transmembrane component (occludin, claudins, junctional adhesion molecules and/or adherent proteins) and a cytoplasmic component (first and second-order adaptor proteins). The main difference between the BBB and BCSFB is the set of claudins expressed by each barrier.

Occludin, claudins and junctional adhesion molecules (JAM-A, B and C) belong to the transmembrane component of TJ. Occludin is a phospho-protein, which consists of two

extracellular loops, four trans-membrane domains and three cytoplasmic domains. The N-terminal domain plays an essential role in TJ assembly, since upon its deletion TJ are still formed, but paracellular diffusion increases significantly, while C-terminus anchors the protein to the cytoskeleton via *zonula occludenes* (ZO) proteins [13, 14] and interacts with regulatory proteins. A range of kinases and phosphatases regulate occludin's conformation and, thus, TJ association [15, 16]. Claudins belong to a family of 24 small transmembrane phospho-proteins and are essential for the formation of barrier properties [17]. Homophilic claudin-claudin interactions between neighboring cells create a skeleton for TJ formation. All members of the family possess two extracellular loops that determine diffusion of different sized molecules. Thus, expression of a subset of claudins determines paracellular ion movement and as a result transepithelial electrical resistance (TEER) of barriers. Difference in expressed claudins between BBB and BCSFB is considered to be the main reason for differences in their TEER and function [12, 17-21]. A long C-terminal domain interacts with cytoplasmic proteins, particularly, ZO proteins [13]. JAMs (JAM-A, JAM-B, JAM-C, JAM-4 and JAM-L) are glycoproteins with two immunoglobulin folds in the extracellular domain. These proteins form heterodimers in TJ complexes [22]. Their role in TJs is still under investigation, however due to the presence of C-terminal sites for interactions with different cytoplasmic proteins such as ZO-1 and cingulin, JAMs are believed to assign the position of ZO-1 and occludin proteins in TJs [23]. The cytoplasmic component of TJs includes a wide range of proteins, which are different in size and function, and that together form a cytoplasmic plaque. The following proteins are referred to the first class of plaque proteins: adaptor proteins ZO proteins; Ca^{2+} dependent serine protein kinase (CASK); membrane-associated guanylate kinase with inverted orientation of protein-protein interaction domains (MAGI-1, MAGI-2, MAGI-3); the portioning defective proteins (PAR3, PAR6). The second class of plaque proteins consists of regulatory and signaling proteins and their regulators (for instance, the regulator of G-protein signaling 5 (RGS5)) [14]. The ZO proteins (ZO-1, ZO-2, ZO-3) are membrane associated gunylate kinases (MAGUK) with many protein-protein interaction sites, and their main function is to anchor transmembrane TJ proteins to the cytoskeleton. Interaction with actin occurs either directly via binding sites or via a myosin-like protein called cingulin. Additionally, ZO proteins control the spatial distribution of claudins [13].

Adherens junctions (AJs) stabilize cell-cell interaction in the junctional complexes. Cadherins are transmembrane proteins of AJs, while the cytosolic component is presented by catenins. Cadherin-10 and vascular endothelial cadherin 5 (VE-Cadherin 5) are expressed in the BBB and BCSFB. Moreover, VE cadherin is additionally expressed in brain microvessels without barrier

properties [13]. The C-terminal domain of cadherins links to catenins: α, β, χ and p120. β or p120 catenins can bind directly to cadherins and via α catenin link the whole complex to the actin. The effect of AJ on integrity of junctional complexes happens via VE-cadherin, which has been reported to promote claudin 5 expression [24], or via β-catenin through the Wnt signaling pathway [25].

3.1.2. Blood-Cerebrospinal Fluid Barrier

The BCSFB is a monolayer of polarized choroid plexus epithelial (CPE) cells that produce cerebrospinal fluid (CSF). The choroid plexuses (CP) are leaf-like intensively vascularized structures located in the walls of four brain ventricles with a combined surface area of 200 cm^2 in human. The blood vessels of CP are leaky and allow the fluent exchange of substances, while epithelial cells possess TJ [11, 13]. Two morphologically different parts of CP – epithelial monolayer and stroma – come from different embryonic layers, the ectoderm and the mesoderm, respectively [26]. During the development the formation of CP is reported to start around E10 for mice, since at this time transthyretin (Ttr), known as the CP marker, is expressed. Ttr, Wnt, the transcription factor, Otx2, as well as, the BMP and Notch signaling pathways are reported to be important for CP formation and differentiation [27]. As soon as CP is determined as a structure consequent morphological changes take place and finally result in the formation of mature structures. The CP is considered to be the most important source of vital substances from the blood into the brain during early development [9]. CPE cells have TJs on the apical side and due to this fact are able to a certain extent control the flow of substances from blood into the CSF. CPE cells are known to express claudin 1, 2, 3 (the most abundant) and 11[15, 21, 28] and this set of molecules is believed to determine CP epithelium as “leaky” type that secretes large fluid volumes with little energy consumption [11, 13]. As a result, TEER values for BCSFB are in the range of 50-150 Ω/cm^2. Additionally, ZO proteins of CP (ZO-1, 2 and 3) are relatively short and concentrated close to the apical (CSF) side of the tissue, while in BBB they are localized at cell-to-cell interfaces. Among AJ molecules epithelial cells of BCSF barrier express mainly cadherin-10 and catenins α and β [13].

3.1.3. Blood-Brain Barrier

BBB is an extensive network of cerebral microvessels, which tightly regulates the access of diverse substances from blood into the brain and transport of metabolites in the opposite direction. Interestingly, the total surface area of brain microvessels in the human brain is about

15-25 m^2, while their total length reaches 600 km [29]. The process of the BBB formation starts during the early stages of development (for mice E10, for rats E11), when vascular sprouts invade the neuroectoderm and give rise to new vessels during a process called angiogenesis [30]. When these sprouts initially enter the ectoderm, they do have TJs, but are permeable to small molecules, however possibly still not macromolecules. However, by E18 (rats) the TJs become complex and by birth are associated with the protoplasmic face (P-face) and are tight to small polar molecules [30]. The BBB of E21 rats already demonstrates high TEER levels [31]. Thus, BBB maturation is a progressive process that is complete by birth, while angiogenesis continues to P20 (for example, in rats). The process of the BBB maturation is believed to be initiated by signals from neuronal progenitor cells [32], however for the further induction of the brain endothelial phenotype signals from astrocytes, pericytes, and microglia are also essential [33, 34]. Both BBB formation and angiogenesis are controlled by Wnt/β-catenin signaling [25], while Hedgehog pathway plays an important role in maturation [35]. Brain endothelial cells (BEC) of adult organisms possess several distinguishing structural features that differ them from endothelial cells in the rest of the body. First, the presence of well-organized TJ complexes is unique. The BBB expresses claudins 3, 5, 12 and probably 1 and this combination of proteins is believed to be associated with high TEER values (1500-8000 Ω/cm^2) [36]. The expression of claudin 5 is believed to be essential for proper barrier function. For example, in claudin 5 knock-out mice brain microvessels develop normally and do not have morphological changes, but are permeable to substances with molecular weight less than 800 D. Interestingly, these mice die 10 h after birth and increased BBB permeability for small molecules might be involved in their early death [17]. Out of five known JAMs JAM-A, JAM-B and JAM-C are found in TJ of the BBB [14]. AJ components cadherins (VE-Cadherin 5, cadherin-10) and catenins (α, β, χ and p120) are expressed in brain endothelial cells [13, 37]. Second, the cerebral endothelium has increased number of mitochondria comprising 10-14% of total cell volume in comparison with other endothelial cells (2-6% total cell volume) [38, 39]. The high number of mitochondria is a necessary source of energy for the maintenance of the chemical gradients existing across the BBB. Finally, cerebral endothelial cells contain reduced numbers of vesicles, which results in the limited transcellular movement of substances [40, 41]. The BBB performs a dual function in living organisms, since, on the one hand, it protects the brain from possible strong chemical fluctuations in blood, but, on the other hand, it provides a constant supply for the brain of vitally necessary substances. Several main pathways exist to deliver compounds into the brain and to remove metabolic products from the brain (Figure 3).

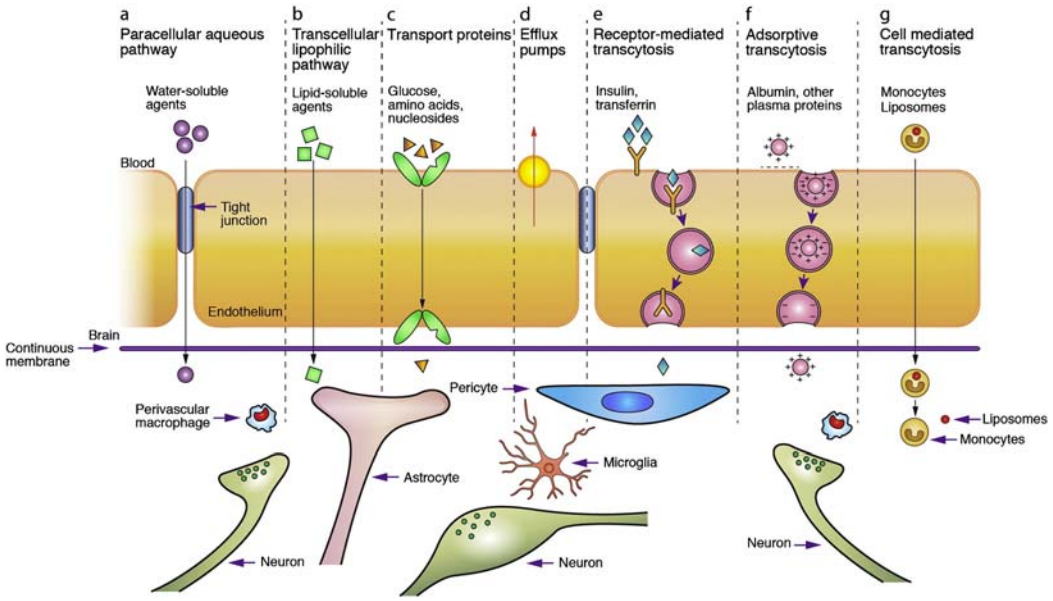

Figure 3. Transport pathways across the BBB (source [42])
A. Paracellular transport; B. Passive diffusion of lipid soluble molecules; C. Carrier-mediated influx via solute carriers (SLCs); D. Active efflux mediated by ABC-transporters; E. Receptor-mediated transcytosis; F. Adsorptive transcytosis; G. Cell-mediated transcytosis.

Substances can enter the brain via the BBB paracellularly or transcellularly. The presence of complex well-organized TJs almost completely restricts paracellular transport and only few substances (for example, water or dissolved in plasma gases such as O_2, CO_2) can diffuse into the brain in this way. For instance, it has been shown that under normal conditions the BBB is impermeable to chemicals with a molecular weight (MW) of 562 Da or larger [17]. Therefore, most compounds have to cross the brain endothelium either passively or actively to reach the brain. Generally passive diffusion takes place for lipophilic substances that fulfill certain criteria:

1. MW less than 500 Da;
2. high lipid solubility and have $logP_{oct}$ in the range 2-4;
3. Polar surface area (PSA) must be lower than 80 A^2;
4. The cumulative number of hydrogen bounds is less than 7 [8, 43-45].

Additionally, positively charged molecules penetrate the BBB more efficiently than negatively charged molecules due to the negatively charged glycocalix and phosphate groups of lipid bilayer. As a result, for instance, many lipophilic molecules (ethanol, nicotine, caffeine) as well as steroid hormones passively diffuse through the BEC. The majority of all other compounds, which do not meet the mentioned above requirements like, for instance, sugars or amino acids, are transcellularly transported across the BBB by carrier-mediated transport, active efflux transport, or by receptor-mediated, or adsorptive transcytosis. Carrier-mediated and active efflux types of transport are mediated by special proteins and happen passively (along the concentration

gradient) or actively, using ATP (primarily) or electrochemical gradient (secondarily) as energy source. Around 36 genes of Solute Carriers (SLC) family (see the detailed description in the section 3.4.) are significantly expressed in the BBB [46, 47] and their main function is to deliver amino acids, sugars, nucleosides and some other small charged essential compounds into or out of the CNS. Some of SLC members are expressed on both membranes of endothelial cells, while others are found only on luminal (blood-facing) or abluminal (brain-facing) sides of the BBB, which results in preferential transport of some substances from blood to the brain or from the brain to blood. Active efflux transport is performed by members of ATP-binding cassette (ABC) family, which use the chemical energy of ATP to pump diverse lipid-soluble compounds from CNS [8]. These proteins transport both potentially dangerous xenobiotics, as well as, drugs. The following ABC members are reported to be expressed in the BBB: P-glycoprotein (Pgp, Multidrug Resistance Protein, ABC B1), the Multidrug Resistance-Assosiated proteins (MRPs, ABC C1, 2, 4, 5 and possibly 3 and 6), Breast Cancer Resistance Protein (BRCP, ABC G2), ABC A1, ABC G1 (both cholesterol transporters) and ABC A2 (connected with drug resistance). Transcytosis represents a special pathway, which allows macromolecules such as proteins, and peptides to get into the CNS and can be receptor or adsorptive mediated. Molecules as transferrin, insulin, lipoprotein bind to their receptors expressed on BBB; then the complex ligand-receptor is pinched from the cell membrane as a vesicle and internalized. After acidification of the endosome, the ligand-receptor complex disassociates and the ligand is released on the opposite side of endothelial cells [48]. If there are no cerebral endothelial cell receptors for a protein or if proteins contain positively charged sites, they still can be transported into the CNS. Positive residues on a protein interact with the negatively charged membrane surface and trigger pinocytosis. This adsorptive-mediated transcytosis (AMT) has a lower affinity, but higher capacity than a receptor-mediated (RMT). AMT was described for cell penetrating peptides [49] and considered to be as a potential way for new drug delivery technologies [50]. Finally, under normal conditions lymphocytes and monocytes cross the BBB by a process, called diapedesis. In diapedisis a mononuclear cell creates an opening on the luminal membrane of BEC, enters the cell, closes the opening and only afterwards exits the endothelial cell through the abluminal side [51]. During this process the TJ are not damaged, however during inflammatory processes disruption of tight junctions takes place and agranulocytes enter the CNS not only by a transcellular path, but as well paracellularly [52, 53].
Thus, the BBB is not only a physical barrier between blood and CNS due to the presence of well-structured TJs, but also a transport barrier by reason of specific diverse transport mechanisms. Moreover endothelial cells are characterized by the expression of a wide range of

enzymes involved in the disposition of drugs and xenobiotics [54], which allows the BBB additionally functioning as a metabolic barrier.

3.1.3.1 Components of neurovascular unit (NVU)

Neurovascular unit (NVU) defines structure-functional interactions between vascular cells, extracellular basement membrane, pericytes, astrocytes, microglia and neurons [12].

Extracellular basement membrane

The extracellular basement membrane (EBM) is a thin layer of 20-200 nm, which surrounds endothelial cells and pericytes. It is composed of fibronectin, laminin (411, 421 and 511), collagen type IV, heparan sulfate proteoglycans (perlecan, agrin) and the nidogens [55, 56]. Endothelial cells, astrocytes and leptomeningial cells produce different laminin chains (α4 and 5, α1, α2). Collagen type IV was demonstrated to be essential for structural integrity of small vessels [57, 58]. The basement membrane is suggested to function as an anchor for endothelial cells [12], as well as, to be involved in TJ maintenance. Minor components of the EBM such as collagen types VII, XV and XVIII, fibulin 1 and 2, and thrombospondin 1 and 2 are believed to also play a role in the structure and function of the EBM [56].

Pericytes

Pericytes are contractile, motile cells that wrap the capillaries in a tunic-like fashion [37], and are separated from endothelial cells and astrocytic endfeet by a thin basement membrane [55]. The ratio of pericytes to endothelial cells varies, depending on the species. For instance, in rat brain this ratio is 1:5, while in mouse brain 1:4 and in human brain is 1:3-4 [37]. One of specific features of pericytes is their pluripotentiality, which allows them to differentiate into several cell types (fibroblasts, smooth muscle cells, macrophages), depending on the signaling molecules in the microenvironment. The following molecules are used as markers for brain pericytes: PDGFR-β receptor, desmin, γ-glutamyl transpeptidase, Sca-1, nestin, ATP-sensitive potassium channel (kir6.1). Additionally, during the development a positive staining for proteoglycan, NG2, is a good surface pericytic marker [56]. Interaction of pericytic PDGFR-β receptor with platelet-derived growth factor B (PDGFR-B), expressed by BEC, is required for recruitment and proliferation of pericytes [55].

Being contractile cells, pericytes control the diameter of capillaries and, thus, regulate the blood flow [59, 60]. Moreover, pericytes were shown to regulate the development and transport

activity of the BBB [61]. Interestingly, if pericytes are differentiated by TGFβ, they decrease barrier properties of the BBB, while differentiation by BFGF causes an increase of the BBB resistance [55].

Astrocytes

Astrocytes are star-shaped glial cells with multiple processes that have dilated end-feet almost completely wrapping the cerebral microvessels as well as forming contacts with the neuronal synapses [37]. Astrocytes represent around 20% of total glial cell population in the human brain [4]. The intermediate filament glial fibrillary acidic protein (GFAP) and S100 calcium binding protein B (s100β) are considered to be typical astrocytic markers. Based on GFAP staining cortical astrocytes can be subdivided into four different morphological groups: protoplasmic, interlaminar, polarized and fibrillary [62]. It is interesting to note that glial cells establish the BBB in invertebrates (such as insects, crustacea, representatives of molluscan class Cephalopoda moluscs) as well as in primitive vertebrates (cartilaginous fish (sharks, rays, skates)) [63]. As evidenced by the presence of an intermediate barrier formed by pericytes and smooth muscles in cephalopods; during evolution a shift of the barrier functions from glial to endothelial cells took place [64]. Factors such as the need for an ionic homeostasis around central integrating synapses, a physical barrier to protect the brain ISF from plasma fluctuations, and the separation between neurotransmitters in the CNS and the peripheral nervous system (PNS) may have driven the evolution of the BBB as a multitasking barrier formed by endothelial cells. However, the remnants of a glial barrier (ependymo-glial barriers formed by tanycytes, retinal pigment epithelium,) are still present in the modern mammalian CNS [7]. In the mammalian brain astrocytes perform multiple functions such as the regulation of water and ion transport, matching oxygen and glucose transport to neuronal activity (metabolic coupling to neuronal activity), control of proliferation of stem cells and the number of synapses [14, 65-71]. Due to close association of astrocytes with endothelial cells, it is not surprising that they have significant impact on the BBB maintenance [14, 69]. For instance, co-culture of brain endothelial cells with astrocytes or with astrocyte-conditioned media leads to the improvement of such barrier features as TJ formation and as a result higher TEER values and an increase in expression of characteristic BBB enzymatic and transport systems [72-79]. Some factors released by astrocytes that induce barrier properties in BEC have been identified. Such astrocytic derived factors as glial-derived neurotrophic factor (GDNF), basic fibroblast growth factor (bFGF), angiopoetin-1 (ANG-1), angiotensinogen, and interleukin-6 were shown to induce certain barrier properties [14, 34, 69, 79-83].

Microglia

Microglia, which are specialized macrophages of haemotopoetic origin in the CNS, are another type of glial cells (7% of total glial cells) [4]. Microglial cells are innate immune cells with special ramified branches, by which they communicate with surrounding neurons and other glial cells [84]. Evidence has been recently obtained about the importance of the resident microglia in angiogenesis, vascularization of the CNS and the regulation of the BBB properties during embryogenesis and disease [36, 85, 86]. Additionally, microglia become activated by brain injury and immunological stimuli to undergo several alternations from a resting state to an activated state [87]. Activated microglia produce many pro-inflammatory mediators (cytokines, chemokines, reactive oxygen species (ROS) and nitric oxide) that are involved in the clearance of pathogen infectious [84]. Microglia activation and consequent neuroinflamation are reported to be involved in the progression of neurodegenerative diseases (Alzheimer disease (AD), multiple sclerosis (MS)) and impairments of the BBB [88].

Neurons

Neurons are highly metabolic active cells, which closely cooperate with astrocytes, and are not more than 10-20 nm distant from capillaries [89]. This close cooperation allows the neurovascular and neurometabolic coupling that maintains an adequate energy supply to neurons under conditions of increased neuronal activity. Neurovascular coupling, or heperemia, is the coupling of vessel diameter and, consequently, blood flow with nutrients, including glucose, to regions of high neuronal activity [90-92] It has been shown that active neurons communicate with brain endothelial cells via astrocytes and, as a result, vasodilation takes place [93]. Neurometabolic coupling occurs between neurons and astrocytes, when increased neuronal activity elevates glutamate (Glu) concentration in the brain ISF. The consequent Glu up-take by astrocytes leads to an increased glucose metabolism and, as a result, lactate production, which is released by glial cells and consumed by neurons for further breakdown [66, 94-96]. Interestingly, Leybaert suggested distinguishing another type of coupling between neurons and endothelial cells, which can be called the neurobarrier coupling [97]. In this case increased neuronal activity causes changes in glucose transport through the BBB according to the increased metabolic demands. It has been shown that seizure induction leads to acute increase of glucose transport through the BBB in the rat brain [98]. Moreover in the earlier studies increased GLUT1 expression following chronic seizures was detected [99]. Since BEC have an intracellular pool of *Glut1* mRNA, which is ~40% of the total *Glut1* mRNA [100], redistribution of this mRNA in response to neuronal activation is suggested to be a mechanism for the rapid

increase of glucose transport via the BBB [101]. The phospholipase C (PLC) pathway (via level of inositol triphosphate (InsP3), Ca^{2+}, diacyl glycerol (DG)) or the protein kinase C (PKC) pathway, which are both known to be involved in astrocytes and endothelial cell interactions, may be also signaling pathways for neurobarrier coupling [102, 103]. Thus, it can be suggested that neurons might regulate expression of other molecules in the BBB.

3.1.4. Circumventricular organs

A group of specialized structures, the circumventricular organs (CVO), is localized along the midline of the brain ventricles and, thus, takes a strategically important position [104]. In early studies with intravital administration of dyes, such as trypan blue, these organs were shown to be stained in contrast to the rest of the brain. The following eight structures are referred to CVO in mammals: the subfornical organ (SFO), organum vasculosum of the lamina terminalis (OVLT), median eminence (ME), neurohypophysis (posterior pituitary), intermediate lobe of pituitary, pineal gland (PI), subcomissural organ (SCO), area postrema (AP) [105]. Some authors classify CP as CVO, but it is not a generally accepted point of view [104]. All CVOs are surrounded on their ventricular surface by ependymal cells, which have an irregular, flattened or elongated shape with only few cilia. The CVOs are highly vascularized with extensive perivascular spaces. However, their capillaries in contrast to the BBB are fenestrated, which allows substances to exchange with the blood [104]. Nevertheless, the CVOs are isolated from the CNS due to the presence of TJ between ependymal cells of the CVOs and tanycytes, which are specialized ependymal cells that lack cilia, but have multiple long processes [30, 105]. This barrier established by tanycytes is regarded as a remnant of the glial barrier [7, 105]. The CVOs are subdivided into ependymal (SCO) and paraependymal organs (all the rest) [104]. Ependymal organs are composed of one or more layers of ependymal cells, which can be modified and vascularized. Paraependymal organs additionally include subependymal elements and are further classified into sensory and secretory organs. The sensory organs (SFO, OVLT, AP) sense and deliver information to other brain regions. The secretory organs (neurohypophysis, median eminence, PI) secrete hormones and glycoproteins into the blood stream based on messages from peripheral organs and the brain environment, and thus, regulate the function of the whole body [104, 106-108]. For instance, hypothalamic peptide hormones are released via neurohypophysis and median eminence and affect anterior pituitary function and several organ systems (renal, reproductive, cardiovascular) [108]. It is important to note that the SCO also exhibits secretory activity [104, 108].

Generally, CVOs can be named as “windows of the brain” that allow communication between the CNS and blood and the rest of the body [105]. The CVO are involved in a number of functions such as maintenance of the body fluid balance, blood pressure, temperature, respiration, energy balance, mediation of immune responses, pain modulation, protection against ingested toxic substances, biological rhythms, reproduction, parental behavior, lactation, growth, sleep, and arousal and attention [105]. These broad functions are possible due to the presence of receptors for a number of humoral factors in the CVO: angiotensin II, atrial natriuretic peptide, relaxin [104]. Additionally, the direct exchange of substances makes the control over the whole body possible. Thus, the absence of the BBB in CVOs allows the CNS to detect changes in peripheral circulation.

3.2. Fluids of the CNS

Conditionally the brain volume can be subdivided into two large compartments – the parenchymal, or cellular, that occupies more than 60% of total brain volume and the fluid one, which includes blood of cerebral vessels and extracellular fluid (ECF) [109]. Brain ECF is represented by two fluids, which have different origin and are spatially separated – cerebrospinal fluid (CSF) and brain interstitial fluid (ISF).

3.2.1. CSF: formation and control of secretion

The CSF is a clear colorless fluid that is mainly produced by CPE with ~25% contribution of ISF across ependymal cells of ventricles [110-112]. The estimated CSF volume in the adult human is around 125-150 mL (or 8-9% of total brain volume), the majority of which is in the cortical and cerebellar subarachnoid spaces and the basal cisterns of the brain, while ventricles contain only 23 mL [11]. Rates of CSF production are rapid and vary for different species, for example, for mice this parameter is 0.325 μl/min, for rats it is 2.1 μl/min and for human roughly 350 μl/min [113]. Another important parameter of CSF formation is a turnover rate (the volume of CSF produced in 24 hours divided by the volume of the CSF space). Human CSF is renewed about 4 times per day, while for young adult rats this parameter reaches 11 times. The CSF turnover rate decreases with age [110]. The process of CSF production includes two main steps: the passive filtration of fluid across capillaries of CP stroma and following after this active secretion across CPE ([110]; Figure 4).

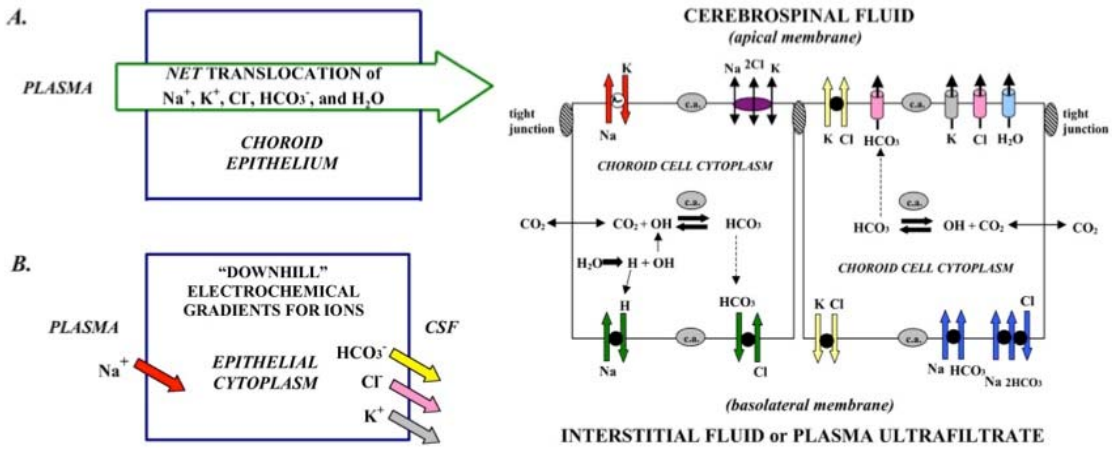

Figure 4. CSF formation (source [110])
A. General route of secretion; B. Ion movements; C. Ion transporters and channels involved in CSF secretion

During the first step the plasma filtrate is formed due to the fenestrated nature of choroidal capillaries in contrast to the majority of brain capillaries [114]. Filtration rate is proportional to the hydrostatic pressure gradient between the blood and the fluid of CP interstitium. As a result, high levels of intracranial pressure (ICP) as well as reduced blood flow to the CP are known to reduce plasma filtration. With mean arterial pressure of 100 mm Hg and normal CSF hydrodynamic parameters (pressure around 10 mm Hg) a sufficient volume of plasma filtrate is formed and reaches basolateral surface of CPE for the next step of CSF production [115]. The epithelial cells of CP possess apical TJs (chapter 3.1.1.), which restrict the free movement of substances from the newly formed plasma filtrate into the CSF. CPE are not only structurally polarized cells, but also functionally polarized. The expression of different transporter sets on apical and basolateral membranes is necessary for CSF production. Basically, the net transport of Na^+, Cl^-, K^+, HCO_3^- and water from plasma to CPE and then to CSF leads to CSF production [110]. The Na^+/H^+ and HCO_3^-/Cl^- (SLC4A2, anion exchanger 2, AE2) exchangers as well as Na^+/ HCO_3^- cotransporter (SLC4A7, NBCn1, NBC2) and Na^+-dependent HCO_3^-/Cl^- exchanger (SLC4A10, NBCn2/NBCE) are expressed on basolateral membrane of CPE and bring Na^+, Cl^- and HCO_3^- into epithelial cells. The driving force for the Na^+-coupled transporters is the Na^+ ion gradient formed due the constant Na^+ discharge into the CSF at the apical cell membrane [116-118]. While the activity of cellular carbonic anhydrase leads to the HCO_3^- generation, which drives Cl^- transport into the cell [119, 120]. The apically localized Na/K/ATPase, K^+/Cl^- (SLC12A7, KCC4) and $Na^+/K^+/2Cl^-$(SLC12A2; NKCC1) cotransporters, Na^+/HCO_3^- exchanger (SLC4A5, NBCe2, NBC4) as well as K, HCO_3 and Cl channels release ions into the newly formed hypertonic CSF. The Na/K/ATPase is the most important Na^+ extruder and provides the driving force for secretion. Three ATPase subunits are detected in CPE: a1 (ATP1A1), b1

(ATP1B1) and b2 (ATP1B2) [121]. Due to the higher concentrations of K^+, HCO_3^- and Cl^- inside the CPE than in the ventricle space, their release is along their concentration gradients [116, 122-126]. Water diffusion through mainly expressed apically aquaporin-1 (AQP1) channels occurs according to chemical potential gradient and completes CSF secretion [127].

The CSF, formed in the lateral, third and fourth ventricles, flows through the subarachnoid space around the brain and drains through the superior sagittal sinus and the nasal pathway (Figure 5). The direction of CSF flow is mainly determined by the cisterna magna and the cisterna basalis. The cisterna magna directs CSF flow back and upward around the cerebellum or forward around the brain stem to the cisterna basalis. In turn, from the cisterna basalis CSF moves into two different directions. In the first case, it flows forward and then directly drains through the anterior part of the sinus. Alternatively, the CSF progresses back between the cerebrum and cerebellum, where it joins the fluid at the back of the brain, which moves upwards around the cerebellum from the cisterna magna, and then drains in the superior saggital sinus, from where it exudes into the venous system [109]. Historically valve-like structures, the arachnoid granulations, of the subarachnoid space have been considered to be the main outflow route for CSF from the CNS into the venous sinus. The driving forces are the hydrostatic gradient and colloid osmotic pressure between CSF and venous blood [128]. However, based on experiments with various animal models (rats, pig, sheep, non-human primate) over last years this point of view is changing [129-134]. Currently, the olfactory and optic nerves, cribriform plate, nasal submucosa and cervical lymphatics are regarded as the main routes for CSF drainage from the brain. For instance, around 50% of CSF is drained along the olfactory nerves to the nasal submucosa, which is enriched with blood vessels and lymph pathways [132, 135]. Generally, the flow rate for CSF is roughly 1500 times less than the blood flow in the brain [109].

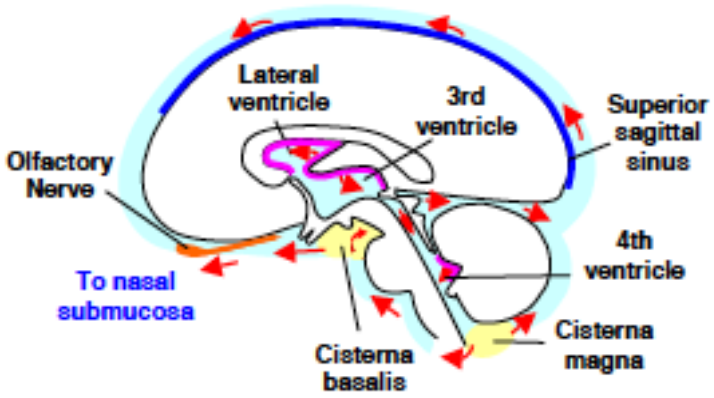

Figure 5. Direction of CSF flow in the brain (source [109])
Choroid plexus (CP) produces CSF, which moves around the brain (red arrows) towards cisterna magna and cisterna basalis (yellow) and drained through the superior saggitalis sinus and the nasal pathway (blue)

The CSF performs a number of important functions in living organisms. First, it plays an important protective role, surrounding the brain and, thus, reducing effective brain weight, as well as, decreasing possibility of mechanical injury. Since it originates as a plasma filtrate, the CSF is also a source of nutrients for the CNS. Finally, a main function of the CSF is the removal of waste metabolite products and excess neurotransmitters from the brain [110].

3.2.2. ISF: origin and regulation of production

The brain interstitial fluid (ISF) is a direct microenvironment for cells in the brain. The ISF occupies 12-18% of total brain volume; in human brain the ISF volume is around 200-250 mL [109]. ISF is a sizeable volume fraction and its volume changes in response to such factors as active neuronal activity and glial cells swelling.

There are three main hypotheses concerning the origin of the brain ISF. According to the first theory, the ISF is believed to be a fraction of the CSF flow. In this case part of ventricular CSF flows into the subarachnoid space (SAS), from where it moves along ventral perivascular channels back to the brain, simultaneously permeating through the parenchyma, and then flows out the brain along venular perivascular spaces [136] Thus, in this case ISF is a recycled CSF with different substances, including possible toxic wastes, which have been excreted by the brain. The second hypothesis states that the water produced during intensive oxidation of the brain's main energy fuel, glucose, is the source of the brain ISF. However, the formed fluid is estimated to be only 10% of the required volume and additionally lacks ions. Finally, the third hypothesis is that the ISF originates from the BBB, which has a surface area of ~ 25 m^2. In this case water and ions come from plasma and the polarized distribution of transporters in BEC regulates the composition of the formed ISF. As in case of CSF secretion, the net transport of such ions as Na^+, Cl^-, K^+, HCO_3^- is key for ISF formation (see section 3.2.1). The $Na^+/K^+/2Cl^-$ cotransporter (SLC12A2, NKCC1), localized on luminal (plasma facing) membranes, provides the flux of Na^+ and Cl^- ions into the BEC [137]. Additionally, the two isoforms of Na^+/H^+ exchanger (SLC9A1 (NHE1) and SLC9A2 (NHE2)), possibly involved in intracellular pH control, are localized on the same membrane. The driving force for not only Na^+, but also for other ions and water movement is provided by the activity of the mainly abluminally positioned Na/K/ATPase (ATP1 family) [138, 139]. Three alpha-(ATP1A1-3) and two beta-(ATP1B1-2) subunit isoforms are found in the rat endothelium, therefore six isoforms of the enzymes can be expressed in the BBB [121]. Some other transporters and channels such as chloride-bicarbonate exchanger (SLC4A1), potassium channels Kv1 and Kir2 are localized on both endothelial membranes [140, 141]. The Cl^-/HCO_3^- exchanger is believed to participate in endothelial cell

regulation of pH. *In vitro* experiments with acid loaded BEC demonstrated that small acid load is neutralized by HCO_3^- influx via Cl^-/HCO_3^- exchanger, while a large acid load is eliminated due to Na^+/H^+ exchanger [142]. Since changes in K^+ concentration impacts resting membrane potential, maintenance of its homeostasis is required for proper neuronal function. However, there are still open questions about K^+ flux through the BBB. Potassium transporters and channels localized on the BBB membranes are believed to efflux K^+ from the brain and, thus, lower its concentrations in the ISF [143]. On the other hand, potassium mainly fluxes into CPE during CSF secretion (Figure 4), however its levels are around 2.5-3 mM. Therefore, the BBB is believed to play if not the main, but at least a partial role in high K^+ levels in CSF. However, a detailed investigation is still required. The comparative analysis of ISF in animals at different levels of organization gives additional evidence for the brain endothelium as a main producer of ISF. For example, the cuttlefish *Sepia*, which lacks CP, ventricles, or CSF, has brain microvessels, the BBB at capillary level, and an ISF flow rate similar to those of rat [136]. Thus, currently ISF is regarded as a mixed fluid, produced mainly by the BBB with minor contribution from active brain cell metabolism and recycled CSF.

Multiple experiments injecting different sized radiolabeled substances into the brain parenchyma have been carried out to test whether the ISF is a static or dynamically flowing fluid. Since clearance from the brain of administrated molecules does not depend on size, the main route of tracers' distribution in the brain parenchyma is convective flow, rather than a simple diffusion [144]. The estimated rate of the ISF secretion is ~ 0.1-0.3 µl/g*min in the rat brain, which is approximately 10 times less than CSF secretion rate, while the surface area of the BBB is ~1000 greater than CP [144, 145]. Consequently, ISF has lower turnover rate than CSF (10 h vs 2.5h) [128]. The main pathways for ISF flow in the brain are the perivascular spaces and the white matter tracts [146, 147]. Ventricular-cisternal perfusion of horse-radish peroxidase (HRP) [148, 149] or administration of radiolabeled inulin [150] and injection studies [151, 152] identified the paravascular ISF circulation route (Figure 6). ISF is formed partially from flow of the CSF into the brain along arteries penetrating the outer surface of the brain and back out along large-caliber draining veins. Interestingly, recent studies with different molecular weight fluorescent substances administrated into the lateral ventricle or cisterna magna of transgenic mice not only confirmed the described ISF circulation route, but also demonstrated significant difference in brain parenchyma penetration for compounds, depending on the molecular size and applied route of injection [153]. Paravascular ISF circulation is most probably driven by difference in pulse pressures between para-arterial and para-venous pathways [149, 154, 155]. Investigation of the mechanisms involved in coupling of para-arterial CSF flux into the brain interstitium and

paravenous ISF clearance might be important for future CNS drug development. For instance, studies in AQP4 knock-out mice showed that abolishment of this water channel leads to a significant decrease of clearance from the brain parenchyma and the authors suggest that astroglial water transport is essential for ISF clearance [153]. Along these lines, the described ISF paravascular route is important for the fast exchange between CSF and ISF.

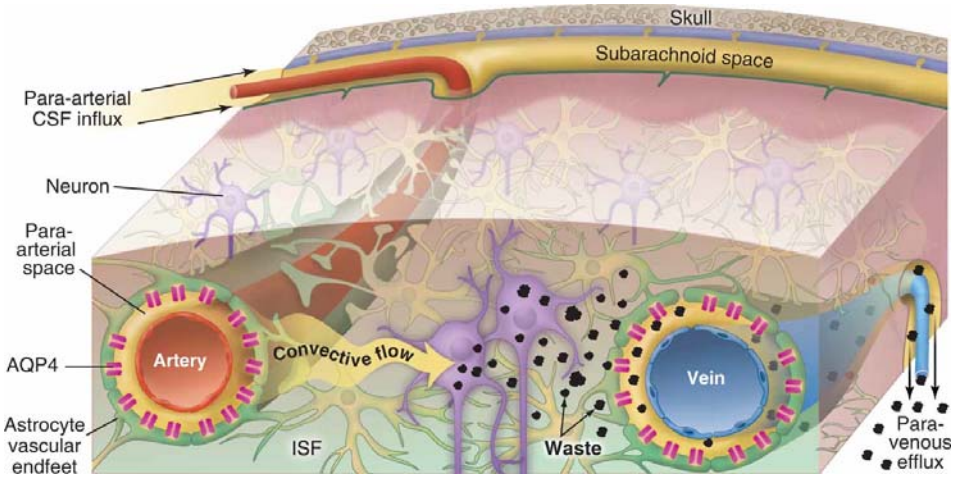

Figure 6. Suggested paravascular ISF route (source [156])
Para-arterial CSF flux together with paravenous ISF clearance are suggested to serve as lymphatic system in the brain and to be called "glymphatic" system [153]

Another possible exchange mechanism between these two fluids is diffusion, which is a slow process that operates over short distances. Diffusion occurs according to concentrations gradient and depends on volume fraction, tortuosity and chemical molecular weight [157-159]. Ependymal cells lining the ventricles walls do not have proper TJs and as a result exchange between CSF and ISF takes place in both directions. Since diffusion of compounds is dependent on molecular weight, for example, it has been estimated that 109 hours are required for albumin (MW 66.5 kDa) to diffuse one cm [160, 161]. Thus, ISF bulk flow might become more important than diffusion in larger brains.

ISF flow is believed to eliminate concentration gradients in brain tissue. However, the brain is an active structurally and functionally heterogeneous organ and the latest measurements of basal neurotransmitter concentrations in different nuclei with high spatial resolution demonstrated the existence of gradients. Statistically significant difference in dopamine concentrations between the ventral tegmental area and the red nucleus of the midbrain region was detected in awake rats. Glutamate was distributed in similar pattern, but with rather higher variability [162].

3.2.3. CSF and ISF content

There is a substantial amount of data in the literature about CSF content (Table 1), which is consistent for different species. CSF is a fluid, originated from plasma and, consequently, it is not surprising that ion concentrations in these two fluids are very comparable.

Solute	Plasma	CSF
Ions, mmol/L		
Na^+	152	141
K^+	4.7	2.9
Ca^{2+}	1.3	1.1
Mg^{2+}	1.5-2.0	2.0-2.5
Cl^-	110	113
HCO_3^-	24	22
Osmolarity, mOsm	290	290
pH	7.4	7.3
Glucose, mg/dL	70-120	45-80
Total amino acids, µmol/L	3200	820
Alanine (Ala)	328.4	31.3
Aspartate (Asp)	5.3	2.3
Arginine (Arg)	80.9	22.4
Asparagine (Asn)	111.7	13.5
Cysteine (Cys)	123.7	<2
Glutamate (Glu)	61.3	26.1
Glutamine (Gln)	641.0	552.0
Glycine (Gly)	282.7	5.9
Histidine (His)	79.8	12.3
Isoleucine (Ile)	76.7	6.2
Leucine (Leu)	155.3	14.8
Lysine (Lys)	170.7	20.8
Methionine (Met)	27.7	2.5
Phenylalanine (Phe)	64.0	9.9
Proline (Pro)	323.7	<2.0
Serine (Ser)	139.7	29.5
Threonine (Thr)	165.5	35.5
Tryptophan (Trp)	49.6	<2.0
Tyrosine (Tyr)	73.0	9.5
Valine (Val)	308.6	19.9
Total protein, mg/dL		
Albumin	4000	20.0
Immunoglobulin G	1000	2.6
Transferrin	230	1.4

Table 1. Content of different solutes in plasma and CSF
Three letter abbreviations for AA are provided. The table was adapted from [163, 164]

Levels of such ions as Mg^{2+} and Cl^- are higher in CSF than in plasma, while for K^+ the situation is opposite. Potassium levels are tightly regulated, which can be explained by its importance for neuronal depolarization and astrocytic swelling [165, 166]. For nutrients, such as glucose and amino acids (AAs), a gradient between the CSF and plasma is observed. CSF glucose levels represent ~2/3 of plasma glucose in healthy subjects. The concentration of most proteinogenic AAs (alanine, asparagine, histidine, isoleucine, leucine, lysine, methionine, phenylalanine, tyrosine, valine) are 10X lower in CSF than in plasma, while for tryptophan, glycine, cysteine and proline this difference reaches up to 20-160 times (Table 1). Interestingly, glutamine (Gln) is the only AA, for which CSF levels represent 80% of plasma values [1]. Generally, the CSF is characterized by lower levels of proteins in comparison to plasma. Nevertheless, albumin, the most abundant plasma protein, is also the most common protein in CSF and represents 56-76% of total CSF proteins [163]. Among the proteins normally found in the CSF are lipocalin-type prostaglandin-D-synthetase (L-PGDS, or previously known as β-trace protein), immunoglobulin G (IgG), transthyretin and transferrin.

Unfortunately, unlike for CSF there is not much known about solutes content of the brain ISF. CSF level of K^+ correlates well with the measured in the brain ISF of ~ 3.3 mmol/L by microelectrode in anesthetized rats. The data about nutrient concentrations in the ISF show a lot of variation. For example, reported glucose levels in the ISF are in the range of 0.35-1 mmol/L in striatum, when measured by microelectrode, and between 0.3-0.5 mmol/L in the same brain region as estimated by *in vivo* microdialysis in freely moving animals [167-169]. Additionally, there is an almost ten fold difference in glucose concentration between cortical and striatal regions, when determined by the same method (Table 2). Glucose levels of 1.6 mmol/L are also reported in the brain ISF in non-epileptic areas of conscious patients with complex partial seizures [170]. It is intriguing to note a gradient in glucose concentration not only between hippocampal ISF and plasma (ISF/plasma ratio is 0.13), but also between ISF and CSF (ISF/CSF is 0.19) in rats (Table 2). There were also several attempts to determine concentration of different amino acids in the brain ISF, particularly, glutamine (Gln) and such neurotransmitters as glutamate (Glu) and GABA. Lerma and co-authors collected fractions at different flow rates during microdialysis in hippocampal region of the anaesthetized rats, determined concentrations of AAs in the collected fractions and then estimated the actual concentrations in the ISF using a non-liner model [171]. The reported level of Gln in the ISF was approximately 190 μmol/L and the authors observed a concentration gradient between ISF and plasma (ISF/plasma is 0.23), as well as, between ISF and CSF (ISF/CSF is 0.37) (Table 2). Additionally, the level of the major excitatory neurotransmitter, Glu, in the rat hippocampus was 2.9 μmol/L, while the concentration

of the major inhibitory neurotransmitter, GABA, was ~ 0.8 µmol/L. In the later microdialysis experiments Gln level was determined as 385 µmol/L in the cortico-striatal ISF [172]. This concentration is two times higher than reported by Lerma, but still lower than in CSF. In the same study Kanamori also reported no difference in Gln concentration between such brain regions as hippocampus, somato-sensory cortex and thalamus in the fractions collected at the same flow rate [172]. Recent microdialysis studies testing Glu and GABA concentrations in the rat brain ISF report levels of 1.8-5.6 µmol/L and 0.0327 µmol/L, respectively, depending on the brain region. Thus, Glu level in the ISF determined by Lerma is in a good agreement with the current studies, while GABA level may be overestimated [171]. Therefore, contemporary experimental data demonstrate a difference in the solute content between ISF and CSF and, moreover, provide evidence of possible gradient between the ISF in different brain regions.

Compartment	Substance			
	Glucose, mmol/L	Glutamine, µmol/L	Glutamate, µmol/L	GABA, µmol/L
Plasma	5.9[A]-7.7[A,B]	563.3[K]/834.6[L]	49.7[K]/159.6[L]	ND
CSF	5.2[C]	549.5[K]/523.6[L]	16.9[K]/11.4[L]	ND
ISF				
Cortex	2.4[I]/3.3[D]			
Striatum	0.3-0.5[E,F]/0.35-1[J]	385.0[M]	1.1[O]/3.0[N]	0.033[Q]/0.0643[P]
Hippocampus	1.0[G]	193.4[L]	2.9[L]	0.8[L]
Hypothalamus	0.7/1.4[H]			

Table 2. Solute concentrations in different fluid compartments in the brain
Glucose concentrations in plasma of fasted and fed awake rats (A [173]) and normoglemic anaesthetized rats (B [174]), CSF (C [175]) and ISF in different brain regions determined by microdialysis (in neocortex of anaesthetized rats (D [176]); striatum of awake rats (E [168] and F [169]); hippocampus of freely moving rats (G [177]); hypothalamus of freely moving fasted and fed rats (H [173])) or by a microelectrode (in cingulate cortex (I [174]) and striatum (J [167])
Glutamine levels in plasma (rats K [178] and L [171]), CSF (rats K [178] and L [171]) and brain ISF in different regions evaluated by microdialysis (cortico-striatal region of awake rats (M [172]) and hippocampus of anaesthetized rats (L [171])).
Glutamate concentrations in plasma (rats K [178] and L [171]), CSF (rats K [178] and L [171]) and ISF determined by microdialysis (hippocampus of anaesthetized rats (L [171]); striatum of freely moving rats (N [179])) or by push-pull perfusion sampling (O [162]).
GABA concentrations determined in ISF by microdialysis in striatum (non-hibernating squirrels (P [180]), hippocampus (anaesthetized rats (L [171]) and basal forebrain (nucleus accumbens (Q [181])

3.3. Amino acids

Amino acids (AA) are a class of organic compounds with amine (-NH_2) and carboxylic acid (-COOH) functional groups and a side chain. Currently more than 500 AA are known to occur in nature (Figure 7) [182]. Depending on which carbon atom the two groups are attached, AAs are classified as α-, β-, γ- or δ-amino acids. The α-amino acids have particular importance in the

living organisms, since they are building blocks for proteins. Further, α-amino acids are stereoisomeric chemicals, which occur as D- or L-isomer, but with the exception of a few bacterial proteins, only L-amino acids are found in proteins [183]. For instance, 21% of total body weight in humans is composed of proteins and, thus, AAs [184]. The recommended daily consumption of essential and non-essential AAs is 0.18 g/kg and 0.48 g/kg, respectively [185]. There are 23 proteinogenic AAs, out of which 20 are encoded by genetic code.

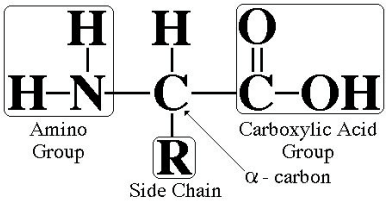

Figure 7. General structure of α-amino acid (un-ionized form).
The source of figure is http://www.hcc.mnscu.edu/chem/V.27/pageid17100.html)

3.3.1. Classification

There are several different AA classification systems, for example, according to the polarity of the side chain proteinogenic AA are subdivided into three groups: nonpolar, polar, or charged (positively or negatively) (Figure 8). Classification by the chemical structure of a side chain, or R-group, results in the following AA groups: aliphatic (Ala, Gly, Ile, Leu, Pro, Val), aromatic (Phe, Trp, Tyr), acidic, which posses extra -COOH group (Asp, Glu), basic with two $–NH_2$ groups (Arg, His, Lys), hydroxylic (Ser, Thr) and sulfur-containing (Cys, Met, Tau). Another important type of AA classification is based on their necessity in nitrogen balance and growth. Correspondingly, AAs are divided into two groups – essential (indispensible) or non-essential (dispensable). Essential AA either cannot be synthesized *de novo* in the organism or are produced, but in insufficient amounts compared to the body needs, and as a result must be supplied with the food. For humans His, Ile, Leu, Lys, Met, Phe, Thr, Trp and Val are essential amino acids. Additionally, Arg, Cys, Tyr are essential in children [186]. Non-essential amino acids are synthesized *de novo* in the organism in adequate amounts. It is important to note that under specific conditions some non-essential AA can become conditionally essential. For instance, Gln is regarded to be a conditionally essential AA, since under such conditions as stress, major trauma, sepsis, this AA must be additionally supplied [187].

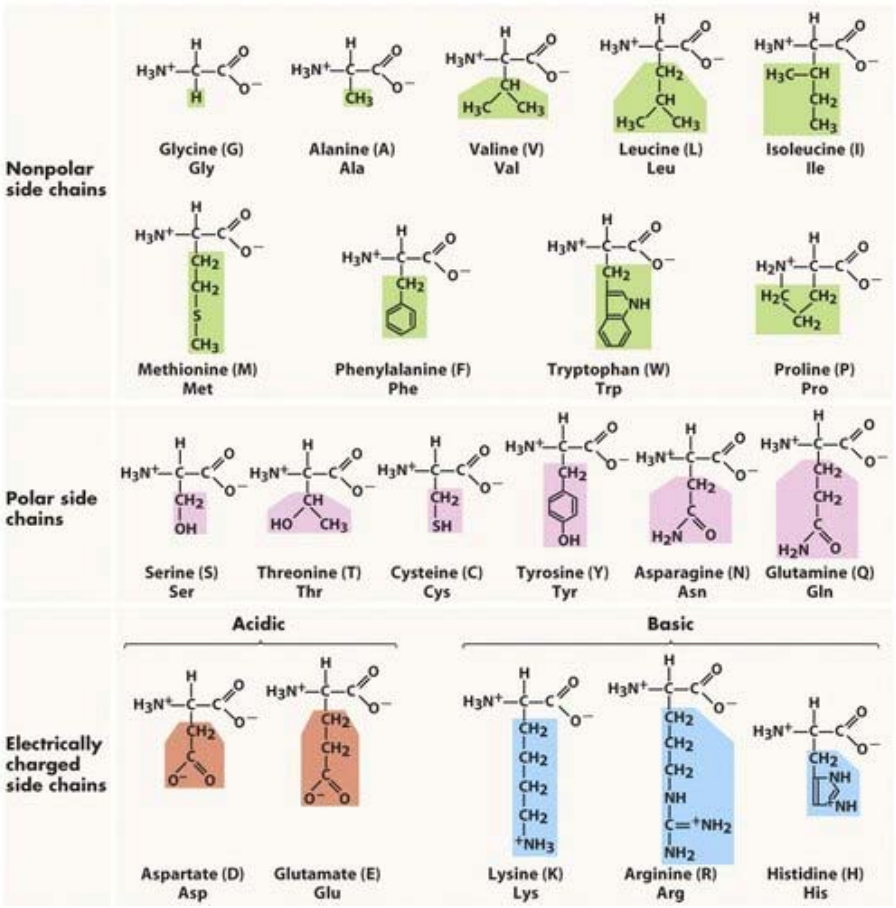

Figure 8. Classification of 20 α-proteinogenic AAs based on the charge of the side chain (R). Trivial names as well as one and three letter abbreviations for AAs are provided (the figure is taken from http://www.uic.edu/classes/bios/bios100/lectures/aminoacids01.jpg)

3.3.2. Roles of amino acids in the whole organism and the CNS

While serving as building blocks for proteins is one of the most important functions of AA, it is not their exclusive role in organisms. Additionally, AAs perform energetic, metabolic, structural, protective, and regulatory functions. For instance, Gln is an energetic fuel for actively proliferating cells, including cancer cells, while Ala is involved in gluconeogenesis and Glu in the Krebs cycle [187-190]. The complete catabolism of an AA produces acetyl-CoA, which is oxidized to CO_2 and H_2O, however, during this process multiple intermediate metabolites are formed. Thus, some AAs are precursors for the synthesis of other AAs. For example, Thr is involved in Gly synthesis, and Glu in Gln, Cit and Arg synthesis, Ile and Val in Ala and Gln production, and Gln is a source for Arg, Asn, Cit, Orn, and Pro [187, 191, 192]. Additionally, AAs are an important source of nitrogen, for example, Gln is considered to be a nitrogen reservoir, while Ala and Asp are transaminated to pyruvate and oxaloacetate, respectively [189,

192, 193]. On the other hand, ammonia detoxification occurs via the urea cycle, in which such AA as Cit, Asp, Arg and Orn are synthesized [194]. Furthermore, AAs are precursors for other compounds such as nucleotide bases, e.g., Gln, Gly and Asp participate in biosynthesis of purines and pyrimidines. While Gly along with succinyl-CoA forms the heme ring in hemoglobin. Additionally, AAs are also important structural components in proteins, for example, His maintains the structure of hemoglobin [183, 192]. Some AAs, like Arg, are themselves antioxidants [195], while others form dipeptides (creatine formed by Arg and Gly) or tripeptides (glutathione consists of Cys, Glu and Gly) with antioxidant properties [196, 197]. Furthermore, AA or their metabolites can perform regulatory functions in cells. For instance, Arg and Gln were shown to regulate gene expression *in vitro,* and potentially *in vivo* [193, 198-203], moreover these AAs along with Leu (via mTORC1 pathway) regulate protein turnover in cells [204-207]. Other AAs directly control enzyme activity, for example, Ala inhibits pyruvate kinase regulating gluconeogenesis and glucolysis [208].

In addition, AAs can affect the whole body's function, e.g. AA or AA metabolites function as neurotransmitters. For instance, nitric oxide (NO) is a product of Arg metabolism with well-known neurotransmitter functions [209-211] and Gly, GABA, Asp, and Glu are classical CNS neurotransmitters [212]. Gly is an inhibitory neurotransmitter, which binds glycine inhibitory receptors in the spinal cord and brainstem [213, 214]. However, it is also a co-agonist of N-methyl-D-aspartate (NMDA) sensitive glutamate receptors in the cortex, hippocampus, cerebellum and brainstem [215]. Gly is released from the presynaptic membrane to the synaptic cleft and then either transferred into presynaptic neurons or transported into astrocytes by Glyt1 (SLC6A9) and Glyt2 (SLC6A5) [216]. There is a special glycine cleavage system (GCS) in astrocytes, which effectively degrades glycine and, thus, provides the gradient for glycine movement from ISF into the cells [217-219]. Unfortunately, the data about Gly alterations as a result of various pathological conditions are inconsistent. For example, a Japanese group showed a correlation between extracellular Gly concentrations and ischemic injury in mice with altered GCS [220]. However, data concerning Gly concentrations in the CSF of patients with Parkinson disease (PD) are unclear. In most cases Gly levels were reported to be unaltered, however two groups reported elevated Gly concentrations in CSF and one group observed decreased levels [221].

GABA is a major inhibitory neurotransmitter in the CNS. This γAA is reported to serve as the primary inhibitory neurotransmitter for 20% to 44% of cortical neurons [222, 223]. GABA is formed from glutamate in the reaction catalyzed by glutamic acid decarboxylase (GAD) and, thus, is involved in glutamate/GABA-glutamine cycle (Figure 9). GABA is metabolized to

succinate by actions of GABA-transaminase (GABA-T) and succinic semialdehyde dehydrogenase (SSADH) [224]. It binds to its ionotropic receptors, GABA(A) and GABA(C), which are ligand-gated chloride channels, and a metabotropic receptor, GABA(B) [225]. The reported GABA levels in the brain ISF vary from 30-100 to 800 nmol/l, depending on the region and detection method used [162, 171, 181]. GABA-transporters are localized both on neurons and glial cells. They function to terminate GABA-ergic transmission, maintain low ambient extracellular concentrations of GABA and recycle GABA for re-use by neurons. Plasma membrane localized GABA transporters belong to the SLC6 family and in mammals they are: SLC6A1 (GAT1 in mouse, rat and human), SLC6A11 (GAT4 in mouse; GAT3 in rat and human), SLC6A12 (GAT2 in mouse; BGT-1 in rat and human preferable transports betaine) and SLC6A13 (GAT3 in mouse; GAT2 in rat) [226]. Reduced GABA levels in CSF and brain hippocampal ISF were reported in patients with epileptic syndromes [227, 228]. In some studies GABA levels in CSF were found to be decreased in patients with PD, while others reported these levels to be normal [221].

Aspartate and glutamate are both excitatory neurotransmitters. The ability of Asp to result in depolarization was shown on feline spinal motoneurons and observed to be similar to glutamate [229]. Aspartate was found to co-localize with glutamate in synaptic vesicles and to be released by exocytosis. It is not easy to differentiate glutamate and aspartate neurotransmission since both neurotransmitters affect many of the same receptors and share many presynaptic mechanisms. Furthermore, Asp is believed to be similarly distributed as Glu, but in lower concentrations. Distribution of possible asparaginic synapses is thought to be limited in the brain (to certain cortical, hippocampal and cerebellar neurons) and, thus, in excitatory neurotransmission Asp is considered to play minor role in comparison with Glu [230, 231]. In cells aspartate is used for conversion of 2-oxoglutarate to glutamate by aspartate aminotransferase [232]. Aspartate levels in brain ISF were estimated to be approximately 2 μmol/L [171].

Glutamate, the major CNS excitatory neurotransmitter, is involved in learning and memory, and synapse induction and elimination during the development. The following families of glutamate receptors are expressed in the CNS: N-methyl-D-aspartate (NMDA), α-amino-3-hydroxy-5-methyl-4-isoxazole propionic acid (AMPA), kainate and metabotropic [233]. Since Glu demonstrates an “excitotoxicity” effect on neurons [234], after release into the synaptic cleft the Glu concentration must be rapidly brought to basal levels by re-uptake either by pre-, or post-synaptic cells or other non-neuronal cells. Several Glu transporters are expressed in mammalian CNS: EAAT2 (GLT-1; SLC1A2), EAAT1 (GLAST; SLC1A3), EAAT3 (EAAC1; SLC1A1), EAAT4, EAAT5 [235-238]. Members of SLC1 family co-transport $1H^+$, $3Na^+$ and $1K^+$ with one

molecule of substrate [239-242], while representative of SLC7 family acts in electroneutral manner, exchanging 1 Glu for 1 Cys [243, 244]. It is interesting to note that EAAT4 and EAAT5 have the largest chloride conductance [245, 246] and due to this may function mainly as inhibitory glutamate receptors [247, 248]. The mentioned transporters are detected in neurons (EAAT3; EAAT4) [249-254], astrocytes (EAAT1, EAAT2) [253, 255-260] or in several cell types. For instance, EAAT2 is found not only in astrocytes, but also in retinal neurons [261] as well as on growing axons [262] and axonal terminals in CA1 region of hippocampus [263-266], EAAT3 is highly expressed not only in neurons, but also in endothelial cells [2] and EAAT4 is additionally expressed in cerebellar Purkinje [236]. Simultaneously, EAAT5 is preferentially expressed in retina [235, 267].

Consideration of the glutamate/GABA-glutamine cycle (Figure 9) is essential for understanding neurotransmitter homeostasis in the brain ISF. Neurons lack pyruvate-carboxylase and cannot synthesize Glu and GABA *de novo* from glucose [268-272], as a result, an alternative mechanism exists in the CNS to restore pools of these two important neurotransmitters [273].

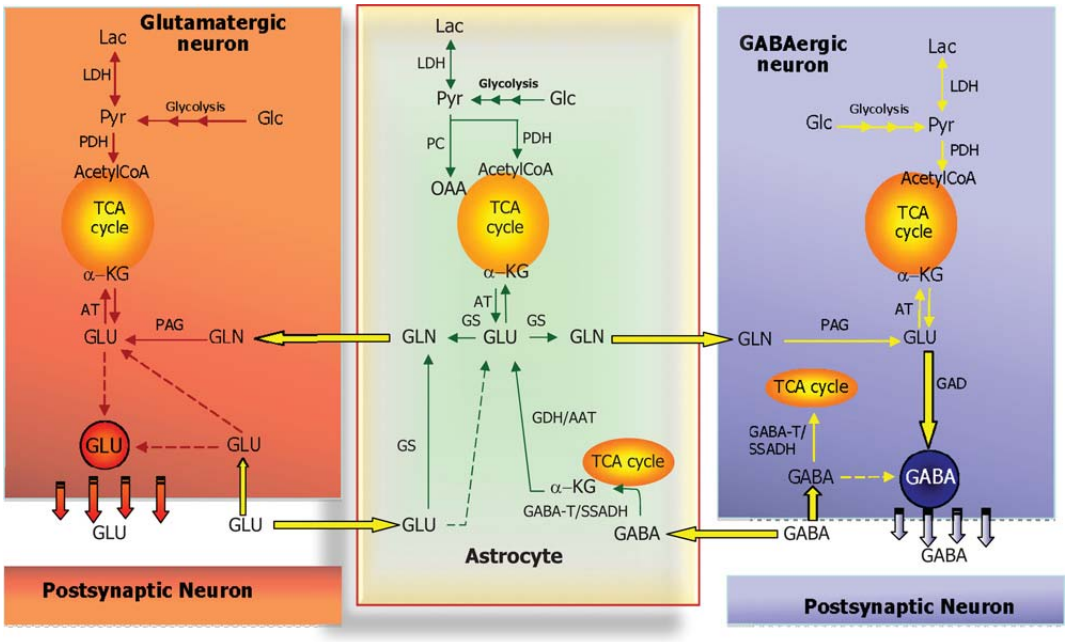

Figure 9. Glutamate/GABA-glutamine cycle (source [274])

In glutamatergic synapses released Glu is taken up by glutamate transporters expressed on astrocytes and metabolized by glutamine synthetase (GS) to Gln [273]. Newly produced Gln is released from astrocytes via system N transporters of SLC38 family – SLC38A3 and SLC38A5 – and then taken up by neurons [275-280]. Since LAT2 (SLC7A8) and ASCT2 (SLC1A5) were identified in cultured astrocytes, these transporters might also mediate Gln flux from astrocytes [281]. System A transporters – SLC38A1 and SLC38A2 – uptake Gln into neurons, where it is

transformed to Glu by phosphate-activated glutaminase (PAG) and, thus, the cycle starts again [277, 278, 282-284]. In case of GABAergic synapses the sequence of events is similar, released GABA is taken up by astrocytes via membrane-expressed transporters, as described above. In astrocytes consequent action of GABA-T and SSADH enzymes leads to succinate synthesis from GABA. Citrate is formed from succinate via the tricarboxylic acid cycle (TCA), next citrate is transformed to α-ketoglutarate, from which Glu is synthesized. Astrocytic GS produces Gln from Glu, which is released into the extracellular space via system N transporters. Then Gln is taken up by neurons, where it is metabolized by PAG to Glu, which glutamate decarboxylase (GAD) converts to GABA [273].

Glu levels in the brain ISF in animals are reported as ~ 3 μmol/L (see table 2) and they are reported to be affected during some pathologies: elevated Glu levels were shown in animal models with Huntington disease [285] and epilepsy [286-289], while decreased glutamatergic neurotransmission was observed in patients suffering from Alzheimer disease [290] or animals with cerebral ischemia [291, 292]. It is important to note that disturbances in Glu levels do not occur alone and usually are a result of an improperly functioning glutamate-glutamine cycle. Moreover, three groups described decreased levels of Glu in CSF from PD patients [221], while most investigators found levels to be normal [221].

Taurine (2-aminoethanesulphonic acid (Tau)) is a non-standard AA heterogeneously distributed in mammalian brain [293-295]. Tau is released from cells under hypoosmotic stimuli and regulates cell volume [296-299]. On the other hand, release of Tau was reported in the feline cerebral cortex as a response to stimulation of the reticular formation [300]. Currently, Tau is regarded as neuromodulator and neurotransmitter in the brain [301]. Application of Tau causes increase of Cl^- conductance and evokes hyperpolarization in neurons [302, 303]. Tau is released in response to NMDA and high concentrations of K^+ [304-309] and impacts the release of neurotransmitter AAs and intracellular Ca^{2+} homeostasis [301, 310]. Tau uptake is carried out by the transporter TauT (SLC6A6), which is expressed in neurons and astrocytes (at least under culture conditions), as well as, in the BBB [2, 311, 312]. Tau is reported to be protective against the neurotoxicity caused by Glu [313] and is suggested to be an inhibitory neurotransmitter like Gly. Nevertheless, the target of Tau action and the origin of its release must still be identified. As determined in rat striatum by microdialysis, Tau levels in brain ISF are ~25 μmol/L [314]. However, this level is higher than any other neurotransmitters. Two groups reported decreased Tau concentrations in CSF of patients suffering from PD, while three other groups made the opposite observation [221]. Interestingly, decreased basal Tau in brain ISF was suggested to be a good predictor of an irreversible lesion after ischemia [291].

AAs are essential in the CNS not only as neurotransmitters, but also as precursors for neurotransmitters. Trp, Phe and Tyr are precursors for the synthesis of the monoamine neurotransmitter, serotonin, and the catecholamines: dopamine (DA), norepinephrine (NE), and epinephrine (Figure 10**)** [315, 316]. Neurotransmitter synthesis and release rates are directly influenced by brain concentrations of the respective AA precursors (Trp, Phe, Tyr), which in turn depend on plasma AA concentrations [317, 318]

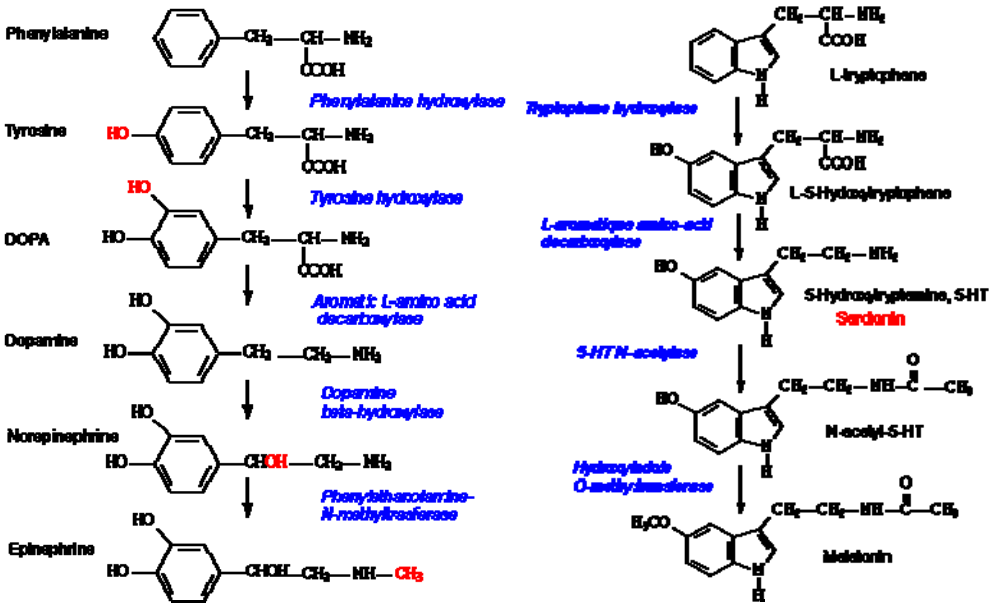

Figure 10. Biosynthetic pathways of catecholamines and serotonin from aromatic amino acids in the brain (source of the pathways is http://www.pharmacorama.com)

Glutamine is the most abundant AA not only in plasma, but also in CSF and brain ISF (Table 2). In addition to roles in gene expression regulation, and energetic and metabolic pathways (gluconeogenesis, urea cycle, lipogenesis), protein synthesis, and cell proliferation; in the CNS Gln is a precursor for Glu and GABA neurotransmitters [192, 193]. Reported Gln levels in the brain ISF vary from 190 to 390 μmol/L (Table 2). Since this AA is involved in synthesis of Glu and GABA via glutamate/GABA-glutamine cycle, it is not surprising that increased Gln levels are found in such cases as Huntington disease, ischemia and epilepsy [285, 286, 291, 319]. In most PD patients Gln levels in CSF are normal, while only one group reported increased levels in PD [221]. Levine observed a trend for increased Gln in the CSF of depressed patients in contrast to healthy subjects [320]. Brain Gln levels are also affected during a group of neurological disorders, called hyperammonemic encephalopathies. Viral or toxic liver damage (fulminant hepatic failure (FHF)) is accompanied by secondary complication, called hyperammonemia, or hepatic encephalopathy (HE), which can develop into brain edema and

mortality in patients with acute HE [321-323]. During HE, NH_3 and Gln are the key elevated metabolites. In patients with HE and experimental animals cerebral Gln levels increase 3-4 fold compared to normal values [322, 324-330]. Elevated Gln levels in liver and extrahepatic tissues are called hyperammonemia [322]. Extreme ammonia challenge of experimental FHF animal models leads to a maximal increase in brain ISF Gln to ~ 2.5 mmol/L, which is in a good agreement with CSF Gln levels reported for patients with FHF [331, 332]. The development of brain edema is considered to be caused by Gln accumulation in glial cells due to osmotic properties of Gln and cerebral hyperemia [322, 333, 334]. Disturbances in Gln concentrations in the brain during HE might be an additional reason for excessive extrasynaptic accumulation of Glu and increased synaptic release of GABA, since these three AA are involved in glutamate/GABA-glutamine cycle [321]. Moreover, elevated Gln brain concentrations favor the influx of aromatic AA (Trp, Tyr) into the brain via transporter proteins expressed in the BBB and, consequently, result in changes of serotonin and dopamine levels [321, 326].

3.4. Amino acid transporters

AAs are vital chemicals involved in many cellular functions; however, to perform these diverse functions, AAs must get inside cells. Since AAs are polar molecules, they cannot directly cross the cell membrane lipid bilayer and, thus, are transported via special transporters. Amino acid transporters (AAT) belong to a superfamily of Solute Carrier (SLC) proteins, which control exchange through membranes of different substances such as nutrients, hormones, neurotransmitters, metabolites, inorganic cations and anions, organic anions, bile salts, essential metals, vitamins, biogenic amines, nucleosides, fatty acids, lipids, drugs, and toxins [335]. Currently this superfamily includes ~400 genes, assigned to 52 different families based on protein structure, comprising the largest group of ATP-independent transporters. They are further categorized by substrate specificity, subcellular localization and mechanism of transport (http://SLC.bioparadigms.org/). All SLC family members have in common a structural motif of one or more transmembrane (TM) domains. SLC transporters are localized in various cell compartments: mitochondria, vesicles, peroxisomes, lysosomes and cellular membranes [335]. Products of more than 50 SLC family genes are AATs. They are distributed in nine families (there is an additional SLC3 family with two members, which are the accessory proteins for heterodimeric AATs). AATs use passive or active transport (Figure 11), e.g. facilitated diffusion is a passive transport in which AAs are moved along their concentration gradient. Examples of SLC family members, which use this mechanism, are the AATs transporting aromatic AAs, e.g. SLC16A10 (TAT1), or large neutral AA (LNAA), e.g. SLC43A1 (LAT3) and SLC43A2

(LAT4). An active transporter uses the concentration gradient of another compound or ion as driving force for translocation. The AA substrate transport occurs either in the same (symport) or opposite (antiport) direction as the molecule providing the driving force. Heterodimeric AATs such as SLC7A5 (LAT1) and SLC7A8 (LAT2) are obligatory exchangers that catalyze the sequential influx and efflux of AA substrates. Many transporters, e.g. SLC38A1 (SNAT1), SLC38A2 (SNAT2) and SLC38A4 (SNAT4) couple Na^+ transport to provide a driving force for the symport of AA substrates. In contrast, other classes of AATs symport one ion type and antiport another type of ion. An example is the neurotransmitters (Glu and Asp) transporters, SLC1A1 (EAAT3), SLC1A2 (EAAT2), SLC1A3 (EAAT1), SLC1A6 (EAAT4) and SLC1A7 (EAAT5), which symport 1 AA, 3 Na^+ and 1 H^+ and antiport K^+. There are also some heteromeric AATs that in absence of Na^+ act as exchangers and in presence of Na^+ may function as symporters. For instance, SLC7A6 (y^+LAT1) and SLC7A7 (y^+LAT2) can exchange cationic AA (Arg, Lys) for neutral AAs, while in the presence of Na^+ they might symport this ion together with neutral AA (Gln, Leu) [336].

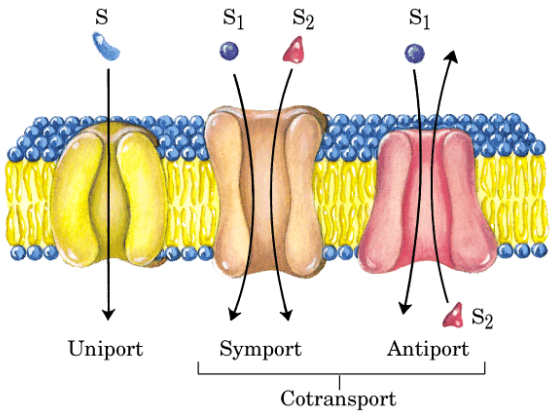

Figure 11. Types of transport carried out by AAT.
Uniport is a passive transport that occurs along the concentration gradient. Co-transport is a type of an active transport, when as the source of energy for transport the concentration gradient of other chemical is used. If the transported molecule and co-transportes molecule move in the same direction, the transporter is called symporter, if in opposite direction, then it is anti-porter (exchanger). The figure is taken from [183]

The first studies of AA transport date back to 1960, when different AA transport systems were described in Erhlich cells [337-339]. It became clear that these transport systems transported groups of AAs rather than individual AAs. The following systems were identified: system L, which prefers Leu and other large hydrophobic neutral AA, system A prefers Ala and other polar small AA, and system ASC, which transports mainly Ala, Ser and Cys. The studies of AA transport over the next decades identified similar systems in different cell types and characterized them in terms of substrate selectivity, thermodynamic properties, inhibitors, etc.

[337, 340, 341]. A nomenclature was introduced to simplify the naming of AA transport systems, in which X stands for anionic, Y for cationic and Z for neutral (zwitterioninc) AAs [342]. This nomenclature was suggested to be useful for AAT systems that can transport both neutral and anionic AA. Lowercase acronyms indicate Na^+-independent transporters and uppercase acronyms are used for Na^+-dependent transporters. Moreover, superscript 0 indicates transport of neutral AA and is used alone or in combination with + or -, depending on the net charge of AA transported. A major step in the study of AATs occurred when the first GABA [343] and cationic AATs were cloned [344, 345]. Cloning and the consequent expression of mammalian transporter genes in simple expression systems, such as ***Xenopus laevis*** oocytes, began a new era in the field of AAT studies. This work resulted in the assignment of SLC genes to the already identified AAT systems and improved characterization of transport activities (substrate preferences, pH dependence, etc.). Currently most SLC genes coding AATs localized in cellular membranes have been assigned by substrate preferences, sensitivity to inhibitors, and transport mechanism to 18 AAT systems: A, ASC, asc, B^0, $B^{0,+}$, $b^{0,+}$, β, Gly, IMINO, L, N, PAT, PROT, T, X_{AG}^-, X_C^-, y^+ and y^+L [336, 346]. Nevertheless, there are AATs that are not assigned to any AAT system. One example is a SLC7A13 (AGT1, XAT2) transporter, associated with an unidentified heavy chain, that is expressed in kidney and preferentially transports Glu and Asp in Na^+-independent manner [347]. AGT1 is suggested to act as an exchanger or uniporter. Moreover, AATs are also expressed in mitochondria (members of SLC 25 family: SLC25A12, 13, 15, 18, 22 and 38) and vesicles (SLC32A1) (http://SLC.bioparadigms.org/).

3.4.1. Amino acid transporters involved in glutamine transport in the brain

There are seven AAT systems involved in Gln transport in mammalian cells: system A (SNAT1, SNAT2, SNAT4), system ASC (ASCT2), system B^0 (B^0AT1, B^0AT2), system $B^{0,+}$ ($ATB^{0,+}$), system L (LAT1, LAT2), system N (SNAT3, SNAT5) and system y^+L (y^+LAT1, y^+LAT2) [278, 348, 349]. Since Gln plays an important role in the CNS as a precursor for two main neurotransmitters, Glu and GABA, Gln transporters are widely expressed in the brain. However, to understand Gln homeostasis it is necessary to know which AATs are expressed in which cell types. The data about Gln AATs in the brain are presented in Table 3.

AAT system	Transporter	Transport type	Km, uM	Neurons	Astrocytes	BBB	BCSF
A	SLC38A1 (SNAT1, ATA1, NAT2, SAT1) SLC38A2 (SNAT2, ATA2, SAT2) SLC38A4 (SNAT4, ATA3, NAT3, PAAT)	AA^0/Na^+ → symport	300[1]-489[2] 1650[3]-1800[4] nf	+[1] +[14] ?	–[1] +[14,20] ?	–[23] +[23];AB[31] ?	? ? ?
ASC	SLC1A5 (ASCT2/AAAT)	AA^0/Na^+ ⇌ AA^0/Na^+ antiport	70[5]	–[15]	+[5,28],– [15]	+[23];AB[32]	?
B^0	SLC6A15 (B0AT2, SBAT1, NTT73, V 7-3)	AA^0/Na^+ → symport	5300[6]	+[16]	+[16]	?	?
L	SLC7A5/SLC3A2 (LAT1/4F2hc) SLC7A8/SLC3A2 (LAT2/4F2hc)	AA^0 ⇌ AA^0 antiport	1600[7]-2200[8] 151[9], 275[10], 318[11]	+[17] +[17]	+[17] +[17,28]	+[23,24]; AB&L[29,30,31] +[23]; AB&L[31, 32]	+[27];A, B[27] ?
N	SLC38A3 (SNAT3, SN1) SLC38A5 (SNAT5, SN2) SLC38A7 (SNAT7)	AA^0/Na^+ ⇌ H^+ symport/antiport AA^0/Na^+ → symport	900[12] 990[4] nd	? ? +[18]	+[21,28] +[22] –[18]	+[21,23]; AB&L[30] +[23,25];AB[32] ?	+[26,27];A[27] +[27];A[27] ?
y^+L	SLC7A6/SLC3A2 (y^+LAT2/4F2hc) SLC7A7/SLC3A2 (y^+LAT1/4F2hc)	AA^0/Na^+ → symport or AA^+ ⇌ AA^0 antiport	295[13] nf	+[13] +[19]	+[13] ?	+[23]; AB&L[32] +[23]; AB&L[32]	+[26]/? ?

Table 3. Glutamine amino acid transporters expressed in the brain
Km parameter for Gln transport for different AAT is from: 1 – [350], 2 – [283], 3 – [351], 4 – [352], 5 – [353], 6 – [354], 7 –[355], 8 – [356], 9 – [357], 10 – [358], 11 – [359], 12 – [360], 13 – [361]; in some case Km was not determined (nd) or not found (nf).
AAT is detected (+) or not detected (–) in different brain cells by PCR, *in situ* hybridization, immunofluorescence or by several methods simultaneously: 1 – [350], 5 – [353], 13 – [361], 14 – [362], 15 – [363], 16 –[364], 17 –[365], 18 – [366], 19 – [367], 20 – [368], 21 – [276], 22 – [279], 23 –[2], 24 – [369], 25 – [370], 26 – [46], 27 – [371], 28 – [281].
Since BBB endothelial cells and BCSFB epithelial cells are polarized cells, AAT can be expressed on abluminal (AB) and/or luminal (L) membranes of the BBB and on apical (A) and/or basal (B) sides of the BCSF barrier. In the table data about localization on membranes of the BBB or BCSF barriers are presented; data were obtained from transport studies *in situ* perfusion (27 – [371]), isolated membrane vesicles (31 – [372], 32 – [373]) or by antibody-dependent methods (29 – [374], 30 – [3]).
? – the information is not available

Thus, six AAT systems can be potentially involved in the regulation of Gln concentrations in the brain.

System A includes three well-described members, SLC38A1 (SNAT1), SLC38A2 (SNAT2) and SLC38A4 (SNAT4), which are sodium dependent electrogenic transporters [375]. This system was originally described by Oxender in 1963 and the name system A was given due to a substrate preference for Ala and other small aliphatic AA, including Gln [339]. A nonmetabolizable AA analog, α-(methylamino)-isobutyric acid (MeAIB), is a substrate for system A and efficiently competes with other natural substrates [339, 376, 377]. System A is pH sensitive and is regulated by a number of factors including hormones, starvation, and hypertonic conditions [368, 378]. SNAT1 was the first member of system A cloned based on the sequence

homology with the vesicular inhibitory AAT [283]. This AAT is highly enriched in neurons and believed to play an important role in the glutamate/GABA-glutamine cycle [277, 278, 283]. Moreover, SNAT1 was found in luminal membranes of ependymal cells and large diameter vessels in the brain, but not in the BBB [2, 3, 350]. SNAT2 and SNAT4 were identified a bit later [351, 379]. SNAT2 is found in many different organs, including the brain, where it was identified in neurons and the BBB [2, 351, 362, 375]. Expression of SNAT2 in astrocytes was confirmed by immunofluorescence as well as PCR [362, 368]. However based on immunofluorescence studies in the brain tissue SNAT2 appears less expressed in astrocytes than in neurons [368]. In the BBB SNAT2 is believed to efflux AAs from the brain to blood [139, 372, 373, 380]. So far, SNAT4 is found to be expressed in liver, skeletal muscle, pancreas and kidney, but not in the brain [375].

B^0AT2 (SLC6A15) also known as SBAT1, NTT73 or V 7-3 was identified the first time in 1992 [381]. B^0AT2 is a Na^+-dependent AA transporter with wide substrate specificity (Met, Pro, Val, Ile, Leu) expressed in neurons and astrocytes [354, 382]. This transporter is a low affinity Gln transporter and is thought to be more important for branched chain AA than Gln transport *in vivo* [364].

System N is another transport system highly expressed in the brain and participating in Gln transport. This system was originally characterized as a pH and Na^+-dependent system, preferring Gln, Asn, and His [352, 383, 384]. The stoichiometry of system N transport is cotransport of 1 Na^+ and AA and simultaneous antiport of H^+, as a result the transport is electroneutral and pH dependent [280, 385]. Thus, both pH and substrate concentration can determine the transport direction. On the one hand, it has been observed that cells transfected with SNAT3 needed ~400 μmol/L Gln in the medium to maintain intracellular pH ~ 7.4. In this case efflux of AA occurred together with H^+ movement in opposite direction [386]. This mechanism might have particular importance *in vivo*, since, in astrocytes during synaptic transmission intracellular pH increases due to the action of Na^+/HCO^{3-} cotransporter, as result, system N transporter mediates efflux of Gln into the brain ISF to bring H^+ into the cell and normalize pH [387, 388]. On the other hand, depending on the substrate concentration in the uptake solution SNAT5 expressed in oocytes either influx or efflux Gln [352]. Thus, system N is believed to provide net movement of amino acids across the plasma membrane into and out of the cells. In contrast to system A, members of system N do not accept MeAIB as a substrate and the transport is Li^+ tolerant [383, 384, 389]. Currently, the system includes two members SNAT3 and SNAT5. However, the recently described transporter SNAT7 despite co-transporting 1AA : 1 Na^+ was suggested to be a new member of the system N due to its substrate specificity.

SNAT3, which was cloned in 1999 from a rat brain cDNA library, was the first identified member [386]. SNAT3 is expressed in liver, kidney, brain, retina, pancreas and adipose tissue [375, 390] and was found in astrocytes as well as in the BBB and BCSFB [2, 46, 276, 281, 391]. SNAT5 was cloned in 2001 and was identified in stomach, brain, retina, liver, lung, small intestine, spleen, colon, kidney, and pancreas [375, 390, 392]. In the brain, SNAT5 is found in astrocytes, BBB and BCSFB [2, 279, 370, 391]. SNAT7 was recently identified in neurons [366]. Originally, system N was believed to be expressed exclusively on abluminal BBB membranes [372, 373], however, functional experiments by Ennis together with recent localization studies by Ruderisch and co-workers showed SNAT3 localizes on both luminal and abluminal BBB membranes [3, 393]. Such localization of SNAT3 in the BBB might have a strategically important role for regulation of Gln flux in the brain.

The ASC (Ala, Ser, Cys) system was identified in the 1960s and described as an exchanger capable of mediating net influx or efflux [339, 394]. ASC system transporters are electroneutral Na^+-dependent exchangers, since an obligatory AA exchange occurs together with Na^+/Na^+ exchange [353, 395]. However, recently Zander and co-authors based on experiments and computational modeling suggested that two Na^+ must be co-transported with AA and, thus, electrogenic character of the transport [396]. ASCT2 transports Gln and its mRNA was identified in astroglial primary cultures during attempts to clone a new member of EAAT/ASCT family. ASCT2 is expressed in lung, skeletal muscle, large intestine, kidney, testis, adipose tissue [395]. High levels of ASCT2 mRNA are detected in primary cultures of astrocytes, while levels are lower in embryonic and adult brain [281, 353]. Recent immunostaining studies did not detect ASCT2 signal in astrocytes, nor in neurons [363]. This AAT was shown to be essential for Gln efflux from cultured astrocytes *in vitro*, however *in vivo* its impact is not clear. ASCT2 was also detected in freshly isolated BEC and is expected to be localized on abluminal membranes [2, 372, 373].

System L and y^+L are heteromeric AATs, which perform their functions only in association with heavy chain, 4F2hc (CD98) [397]. Members of system L mediate Gln exchange, rather than net uptake in a Na^+-independent manner. L system was described in 1960s as transporting large neutral hydrophobic AA as well as 2-aminobicyclo-(2,2,1)-heptane-2-carboxylic acid (BCH) [339, 398] . The light chain, which interacts with 4F2hc, in order to form functioning system L was independently identified by two groups and named LAT1 [356, 399]. Then another member of the system was identified and named as LAT2 [357-359, 400]. LAT2 demonstrates broader substrate selectivity as well as higher apparent affinity for such AAs as phenylalanine and glutamine when compared with LAT1 [358]. LAT1 is widely expressed in such organs as

spleen, brain, thymus, testis, skin, liver, placenta, skeletal muscle, stomach [397, 401]. However, it is important to note that the BBB has the highest expression of LAT1, which is localized on both membranes [2, 3, 369, 372, 374]. LAT1 was detected in primary cultures of neurons and astrocytes, although *in vivo* the highest LAT1 expression levels occur at birth [365]. LAT2 is found in kidney, small intestine, testis, prostate, ovary, brain, skeletal muscle, and placenta [401]. LAT2 has the same expression pattern as LAT1 in neurons and astrocytes with decreased expression in adulthood [365]. This AAT is highly expressed in cultured astrocytes [402]. In the BBB LAT2 is detected at lower levels than LAT1 [2]. LAT2 is suggested to localize on both BBB membranes [372, 373].

The y^+L system was identified as transporting positively charged and neutral amino acids in erythrocytes [403]. The transport of dibasic AA occurs in Na^+-independent manner, while in the presence of Na^+ this system transports neutral AA, including Gln [404]. This system currently includes two members y^+LAT1 and y^+LAT2 [405, 406]. y^+LAT1 is expressed mainly in kidney and small intestine, however it is still detected in liver, spleen, leucocytes, pancreas, epididymis, testis, placenta, ovary, lung, thyroid [397, 401]. Generally, y^+LAT1 is poorly expressed in the brain, its RNA was found in neuronal cell line and the BBB [2, 367]. y^+LAT2 is detected in small intestine, kidney, lung, thymus and heart, while in the brain, testis and parotids its mRNA is more abundant [397]. y^+LAT2 is highly expressed in cultured neurons and astrocytes, as well as in embryonic brains, but in the adult brain level is decreased [361]. This AAT is found in both barriers, the BBB and BCSFB [2, 46]. Members of y^+L system believed to be localized on both, luminal and abluminal, membranes of the BBB [373].

Taken together all the mentioned above facts, the net Gln movement in the CNS might be regulated by 12 identified AATs (Table 3). Interestingly, these AATs have overlapping expression patterns in neurons, astrocytes, BBB, and BCSFB cells. While some AATs like SNAT1, are expressed mainly in neurons, others are preferentially found in astrocytes and BBB (SNAT3, SNAT5). Whereas, other AATs like SNAT2, are expressed in all three CNS cell types. Thus, in the CNS Gln homeostasis is controlled simultaneously not only by different AATs, but also by different cells, and investigation of the role of each AAT in this complex regulation is not a trivial task.

3.5. Thesis projects

1. SNAT5 localization in the BBB

In this project we attempted to localize SNAT5 in the brain endothelial cells based on antibody-dependent approaches.

2. Investigation of AA concentrations in the brain ISF and possible mechanisms of their regulation

Here we compared levels of 16 different AAs in the brain ISF, CSF and plasma and discovered the existence of concentration gradients between all these three fluid compartments. Next we investigated possible mechanisms of Gln concentration regulation in the brain ISF under several different challenges (competitive inhibitor infusion into the brain ISF and/or peripheral bolus AA IP injection). The results of this project are summarized in the manuscript "Brain interstitial fluid glutamine homeostasis is controlled by blood-brain barrier SLC7A5/LAT1 amino acid transporter".

4. SNAT5 localization in brain endothelial cells

4.1. Materials and Methods

4.1.1 Antibodies

Table 4 summarizes information about anti-mSNAT5 antibodies as well as other primary and secondary antibodies used for western blot and immunofluorescence studies.

Antibody	Epitope/immunogen	Host	Manufacturer and catalog #	Dilutions	
				WB	IF
Primary polyclonal and monoclonal					
Anti-mouse Snat5 Q-15	near N terminus of mSnat5	goat	Santa Cruz (SC), sc-50682	1:1000	1:200
Anti-rat Snat5	residues 1-100 of rSnat5 (N-terminus)	rabbit	Abcam, ab72717	1:1000	1:200
Anti-mouse Snat5 11595	CPTTRNPATGRKPVQ (N-terminus)	goat	Everest Biology (EB)	1:100-1:500	1:50-1:200
Anti-mouse Snat5 11596	CDVSHNDTVVEAEQAP (extracellular loop)	goat	Everest Biology (EB)	1:500	1:50-1:100
Anti-mouse Snat3	MEIPRQTEMVELVPNGKC (N-terminus)	rabbit	Pineda, Berlin, Germany	1:500	1:200
Anti-laminin	Full length human protein	chicken	Abcam, ab14055	-	1:200
Anti- mouse anti-glucose transporter 1 (Glut1)	Full length human protein	sheep	Abcam, ab 54263	-	1:200
Anti-mouse glyceraldehyde-3-phosphate dehydrogenase (GAPDH)	GAPDH from rabbit muscle	mouse	Merck Millipore, MAB 374	1:7000	-
Anti-mouse β-actin	Ac-DDDIAALVIDDGSGK conjugated to KHL (N terminus)	mouse	Sigma Aldrich, A5316	1:5000	-
Anti-mouse Glut1	Synthetic human peptide (C-terminus)	mouse	Abcam, ab40084	1:1000	1:200
Anti-mouse anti-glial fibrillary acidic protein (GFAP)	Purified GFAP (porcine spinal cord)	mouse	Merck Millipore, MAB360, clone GA5	1:500	-
Anti-mouse GFAP	Enriched bovine glial filaments	rat	Invitrogen, 13-0300	-	1:100
Secondary					
Anti-mouse, AP conjugate	-	donkey	Promega, S372B	1:10000	-
Anti-mouse, HRP conjugate	-	goat	Promega, W402B	1:10000	-
Anti-rabbit, AP conjugate	-	goat	Promega, S373B	1:10000	-
Anti-goat, HRP conjugate	Whole goat IgG	donkey	Santa Cruz, sc-2020	1:10000	-
Streptavidin, HRP conjugate			Thermoscientific, PIERCE, 21130	1:20000	-
Anti-goat DyLight 488 conjugated	-	donkey	Abcam, ab-96935	-	1:400-1:1000
Anti-goat Alexa 594 conjugated	Gamma Ig heavy and light chains	donkey	Life technologies, A 11058	-	1:500
Anti-rabbit Alexa 488 conjugated	Gamma Ig heavy and light chains	goat	Life technologies, A 11008	-	1:400
Anti-rabbit Alexa 594 conjugated	Gamma Ig heavy and light chains	donkey	Life technologies, A 21207	-	1:400
Anti-chicken DyLight 549	-	goat	Jackson Immunoresearch Lab. Inc, 103-505-155	-	1:400
Anti-chicken DyLight 649	-	donkey	Jackson Immunoresearch Lab. Inc, 703-496-155	-	1:400
Anti-rat DyLight 594	-	donkey	Abcam, ab-102262	-	1:1000

Table 4. Primary and secondary antibodies used for western blot and immunofluorescence assays.

4.1.2 HEK 293T cell-line

Human embryonic kidney cells (HEK293T) were kindly provided by Dr. D. Schümperli from University of Bern. Cells were routinely cultured in Dulbecco's Modified Eagle Medium (DMEM, catalog no. E15-810, GE Healthcare) supplemented with 10% fetal bovine serum FBS (Sigma-Aldrich), 2 mM L-Glutamine and 1% non essential amino acids at standard cell culture conditions

(37°C, 95% relative humidity and 5% CO_2). At 80-90% confluence, cells were passaged with 0.25% trypsin in PBS and at a final density of 10%.

4.1.3 Animals

All experiments were performed with male C57BL/6J mice (Charles River (Crl), Germany) that were handled in accordance with the Swiss federal and cantonal law and with the approval of the Cantonal Veterinary Office Zürich.

4.1.4 Vectors and transfection

The mouse *Snat5* coding sequence was subcloned in the pLCPX (part of N631511, Clontech, Lab. Inc, USA) or peGFP-C1 (N 6084-1, Clontech Lab. Inc., USA) vectors. The vectors and constructs were prepared by transforming DH5α E.coli cells, followed by maxi or midi-prep DNA extraction kit (Qiagen).

For transfection HEK293T cells were seeded at $2 \cdot 10^6$ cells per well in 6 well plate (N92406, TPP Techno Plastic Products AG, Switzerland) and allowed to attach overnight. The next day, before transfection cells were washed twice with Optimem medium (11058021, Gibco, Life Technologies) and then kept in 1 mL of the same medium. The transfection was performed using X-treme GENE 9 transfection reagent (06365787001, Roche Diagnostics, Mannheim, Germany) as follows: 9 uL of X-treme GENE 9 in Optimem and 3 ug of DNA of interest (pLCPX, pLCPX-mSnat5, peGFP-C1 or mSnat5-eGFPC1) in Optimem were incubated separately for 5 min at room temperature, next mixed and incubated for 30 min, added to 800 uL DMEM and then applied to HEK cells. After 24 hours the cell medium was replaced by complete medium and 48 or 72 hours later HEK cells were used for lysate preparation or fixed for immunocytochemistry.

4.1.5 Cell lysate preparation

For lysate preparation transfected HEK cells were washed three times with ice-cold PBS, scraped in 1 mL of ice-cold PBS and centrifuged at 800 g for 1 min at 4°C. The cell pellet was homogenized by vigorous pipetting in 200 µL of ice-cold mannitol buffer (300 mM mannitol, 2 mM EDTA, 20 mM HEPES-Tris, pH 7) containing complete EDTA-free proteinase inhibitor cocktail (Roche Diagnostics, Mannheim, Germany) and 2 mM phenylmethanesulfonylfluoride (PMSF) and incubated for 30 min on ice. Cell debris was pelleted with centrifugation at 100 g for 10 min at 4°C. Part of the supernatant was used for determination of protein concentration, while the rest was centrifuged at 41000 rpm (RP45A rotor, SORVALL RC M120EX) for 1 hour

at 4°C. The supernatant containing the cytosolic fraction was kept for further analysis. The pellet that mainly contained membrane proteins was resuspended in 200 uL of resuspension buffer (mannitol buffer supplemented with 0.1% triton-X 100 and 0.5% Na^+-deoxycholate). The protein concentration for all samples was determined using the BCA protein assay kit (Thermo Scientific).

4.1.6 Cell surface biotinylation

HEK cells were transfected as described above and grown on 6 cm dishes for 48 hours. Cells were washed once with 3 mL PBS, incubated with the same volume of biotin (EZ-link sulfo-NHS-LC-Biotin, 21335, PIERCE, Thermoscientific) solution for 40 min at 4°C, followed by 100 mM glycine for 20 min. Cells were washed once with PBS for 20 min, scraped in 1 mL of PBS, transferred to an eppendorf tube and pelleted at 1000g for 1 min at 4°C. The supernatant was aspirated, cells were lysed in 100 uL of Radio-Immunoprecipitation Assay (RIPA) buffer (150 mM NaCl, 50 mM Tris pH 7.4, 1% NP-40, 0.5% Na^+-Deoxycholate) for 40 min on ice and centrifuged for 10 min at 2040 g at 4°C. Twenty percent of the supernatant (5 uL) was saved for western-blotting analysis. The remaining supernatant was added to pre-washed streptavidin agarose beads (original volume 50 uL; 20347 PIERCE, Thermoscientific), rocked overnight at 4°C and then pelleted at 943 g for 30 seconds. The supernatant (non-biotinylated proteins) was saved for western blotting, while the pellet was washed three times for 10 min with 1 mL of IP buffer (50 mM NaCl, 50 mM HEPES, pH 7.4, 1% NP-40, 5 mM EDTA) and finally once with 1 ml of PBS. Twenty microliter of 2x Lammli buffer containing DTT was added to the biotinylated protein pellets and samples were incubated for 40 min at 60°C and stored at -20°C for further analysis.

4.1.7 Tissue lysate preparation

Tissues (brains or pancreas) were homogenized in ice-cold homogenization buffer (200 mM mannitol, 80 mM HEPES, 41 mM KOH, 1 tablet complete EDTA-free proteinase inhibitor cocktail (Roche Diagnostics, Mannheim, Germany), pH 7.5) using a disperser (Polytron PT 1200C, Kinematica AG, Switzerland). Homogenates were sonicated (Labsonic 1510, Bender&Hobein, Switzerland) and centrifuged for 20 min, 2000 rpm at 4°C. Part of the supernatants was kept for western-blotting as total lysate sample, the rest was ultracentrifuged for 1 h 41000 rpm (RP45A rotor, SORVALL RC M120EX) at 4°C. The supernatant containing the cytosolic fraction was saved, and the pellet containing the membrane proteins was dissolved

in homogenization buffer and further sonicated. Protein concentrations were determined as mentioned above.

4.1.8 Brain microvessels isolation

After decapitation 5-10 brains were collected in buffer A (103 mM NaCl, 4.7 mM KCl, 2.5 mM $CaCl_2$, 1.2 mM KH_2PO4, 1.2 mM $MgSO_4$, 15 mM HEPES, pH 7.4) containing complete EDTA-free proteinase inhibitor cocktail and cerebella were removed. Then homogenization was performed using a Dounce glass homogenizer with 55 up and down strokes in 8 ml of buffer B (buffer A supplemented with 25 mM $NaHCO_3$, 10 mM glucose, 1 mM Na^+ pyruvate and 10 g/L dextran). The homogenate was mixed with 16 mL of 26% dextran, centrifuged at 5600 g at 4°C for 10 min. The pellet was resuspended in 10 mL of fresh buffer B, filtered through a 60 µm nylon mesh and centrifuged at 3000 g at 4°C for 10 min. The pellet containing brain microvessels was used for lysate preparation or immunofluorescence.

4.1.9 Brain microvessels lysate preparation

Lysates from the brain microvessls were prepared as previously described (3.1.6). The pellet enriched with microvessels was resuspended in 1 mL of homogenization buffer and homogenized with a disperser (Polytron PT 1200C, Kinematica AG, Switzerland) on ice for 15 sec each 15 min during 1 hour. Homogenates were centrifuged at 10000 g at 4°C for 10 min. Part of each homogenate was saved for western-blotting as a total lysate fraction, while the rest was ultracentrifuged for 90 min at 41000 rpm (RP45A rotor, SORVALL RC M120EX) at 4°C. The newly formed supernatant was kept as cytosolic fraction, and the pellet was resuspended in 50 µl of resuspension buffer (3.1.6).

4.1.10 Gel-electrophoresis and Western Blotting

For SDS-PAGE separation, 20 or 50 µg of cell, tissue or microvessel lysates were diluted with 4x Lämmli buffer, containing 100 mM dithiothreitol (DTT) (Juro Supply, Lucerne) and incubated for 5 min at 95°C or for 30 min at 25°C. Biotinylated samples from cell surface biotinylation were prepared as described (3.1.5). For SDS-PAGE separation, 10 µL of unbound fraction (10% total volume) was mixed with 15 µL of RIPA buffer and 25 µL of 2x Lämmli buffer containing DTT and incubated for 40 min at 65°C. For the total fraction samples, 5 uL (20% total volume) were treated in the same way using 20 µL RIPA buffer and 25 µL of 2x Lämmli buffer. Samples were loaded on 8.5% or 10% polyacrylamide gels. After separation,

proteins were transferred to PVDF membranes (Immobilion-P, Millipore) and blocked for 1 h at room temperature (RT) in either 2% TOP-BLOCK in TBS, 0.1% Triton X-100 (TBS-T) or 5% milk in TBS, 0.1% Tween-20 (TBS-t) and incubated overnight at 4°C with the primary antibody diluted in 1% TOP-BLOCK in TBS-T or 5% milk in TBS-t. Washes were performed with either TBS-T or TBS-t, respectively. Secondary antibodies diluted in 1% TOP-BLOCK in TBS-T or 5% milk in TBS-t were incubated with the blot for 1 hour at RT. For probing with several antibodies membranes were stripped with glycine, pH 2.2 (Abcam protocol stripping for reprobing), blocked and reprobed with the necessary antibody. Detection was performed by chemiluminescence and visualised with Immobilion Western Chemiluminescent horseradish peroxidase (HRP) substrate (Millipore) or CDP-Star (Roche) on a Fuji LAS-4000 camera (Bucher Biotec, Basel, Switzerland).

4.1.11 Immunocytochemistry

Transfected HEK cells were grown on polyester transwell inserts (3470, Transwell Costar, Corning Inc, USA) for 48 hours and fixed in 3% PFA, 0.1% TritonX100 for 10 min. Afterwards the filters were washed once in ice-cold PBS, 0.1% SDS in PBS for 5 minutes, washed once with PBS, 0.1% Triton-X (PBS-T) and blocked with serum from the host species of secondary antibody at 10% serum, PBS-T (blocking buffer) for 1 hour at RT. All wash steps were in PBS-T. Primary and secondary antibodies were diluted in blocking buffer and incubated for 1 hour, RT. Nuclei were labeled with Diamidino-2-Phenylindole Dihydrochloride (DAPI, Life Technologies) diluted 1:5000 in the same buffer as antibodies. All the incubation steps were performed in humidified chambers. Finally, filter pieces were mounted with DAKO Glycergel (DAKO North America, Inc., USA) on slides and examined under the fluorescent microscope Nikon eclipse TE 300.

4.1.12 Immunofluorescence on free-floating sections

Mice were anesthetized with ketamine (ketanarkon)/xylazin (Streuli Pharma AG, Uznach, Switzerland) cocktail (10 mg and 1 mg/ mL/100g, respectively) and perfused with PBS, pH 7.4, followed by fixation in 2% PFA and 0.2% glutaraldehyde in PBS. Then the brains were post-fixed for 2 h, kept in PBS overnight and stored in 0.02% PFA, 4°C. For immunofluorescent staining, brains were cut sagittaly into 20 μm sections using a vibrating microtome (Leica VT 1000S; Leica, Heerbrugg, Switzerland). Sections were agitated in PBS 0.5% Triton X-100 for 30 minutes, blocked for 10 minutes (Protein Block Serum-Free; Dako, Carpinteria, CA, USA),

and incubated with primary antibodies overnight at 4°C. All wash steps were done in PBS with agitation. The next day sections were incubated with secondary antibodies for 30 – 45 min, followed by 10 minutes in 4% PFA. Nuclei were counterstained with PO-PRO-1 iodide (1:400; Invitrogen) for 5 min. Sections were mounted on polylysine slides (Menzel Gläser, Thermoscientific, Braunschweig, Germany) in a Vectashield mounting medium (Vector Laboratories, Burlingame, CA, USA) and then examined under a Leica TCS SP2 confocal laser scanning microscope (Leica) using a 63x objective (oil, numerical aperture of 1.4, pinhole set to 1.0 airy unit).

4.1.13 Immunofluorescence on paraffin sections

Deeply anaesthetized mice were transcardially perfused with ice-cold PBS, pH 7.4, then brains were collected, incubated in 4% PFA in PBS at 4°C overnight. Paraformaldehyde-fixed brains were paraffinized (Shandon Xylene Substitute, Thermoscientific), cut coronally into 5 µm thick slices using a microtome (RM 2235, Leica), mounted on polylysine slides and kept at +4°C for staining. Paraffin slides were deparaffinized for immunofluorescence (Microm/Histocam AG, Thermoscientific).

Antigen retrieval was performed using the proteinase K antigen retrieval method (incubation of sections in proteinase K solution (proteinase K 20 µg/ml in 50 mM Tris base 1.0 mM EDTA, 0.5 % Triton X-100, pH 8.0)) at 37°C for 10 min. Slices were blocked for 1 h at RT using blocking buffer (5.0% donkey or goat serum in PBS, 0.3 % Triton X-100). Blocked slices were incubated overnight at 4°C in incubation buffer (PBS, 1% BSA, 0.3% Triton X-100) containing primary antibodies. Secondary antibody incubations were carried out for 1-2 h at RT. PBS was used for washes between incubation with primary and secondary antibodies. Nuclear counterstaining was performed with DAPI (1:500), brain sections were mounted with DAKO-Glycergel with coverslips and examined as previously described.

4.1.14 Immunofluorescence on isolated microvessels

Pellet enriched with microvessels (3.1.7) was resuspended in PBS, and a small drop of suspension carefully distributed on a slide (Superfrost Plus, Menzel Gläser, Thermoscientific, Braunschweig, Germany) and incubated at RT for 20 min in a humidified chamber. The PBS was removed and the adhering microvessels were washed three times with PBS and fixed with 3% PFA for 30 min. After five wash steps with PBS, microvessels were permeabilized with 0.1% Triton X-100 for 30 min, blocked in blocking buffer (3.1.10) for 1 hour and incubated with

primary antibodies for 2 hours, RT. Microvessels were washed three times with PBS and incubated in secondary antibody 1 hour, RT. Nuclei counterstaining and mounting were performed as described above (3.1.10).

4.2. Results

4.2.1 Test of anti-SNAT5 antibodies in HEK cells heterologously expressing mSNAT5

Since the SNAT5 knockout animals have not yet been generated, we tested anti-SNAT5 antibodies (Ab) using HEK cells exogenously expressing mouse SNAT5 (mSNAT5) (Figure 12). The predicted molecular weight (MW) of the mSNAT5 protein is 55 kDa. The anti-mSNAT5 Ab from Santa Cruz (SC) recognized a band with an apparent MW of 55 kDa in lysates from both transfected and non-transfected cells. However, additionally in transfected cells only, diffuse bands between 43 and 55 kDa were detected (Figure 12A). Staining using an Ab raised against rat SNAT5 (Abcam) resulted in a strong band at ~55 kDa and a faint band at ~50 kDa in both transfected and non-transfected HEK cell lysates. Both anti-mSNAT5 Abs from Everest Biology (EB) 11595 and 11596 recognized multiple bands in transfected as well as non-transfected cell lysates. However, a unique band was detected by EB11595 at ~43 kDa and the band at ~50 kDa was significantly stronger in cells transfected with pLCPX-mSnat5 construct, than in non-transfected or transfected with a vector alone cells (Figure 12A). The EB11596 Ab recognized a similar set of proteins as EB11595 although with an apparent lower affinity. Furthermore, by immunocytochemistry both EB Abs detected apparent plasma membrane proteins in HEK cells transfected with pLCPX-mSNAT5 (Figure 12B).

4. SNAT5 localization in brain endothelial cells

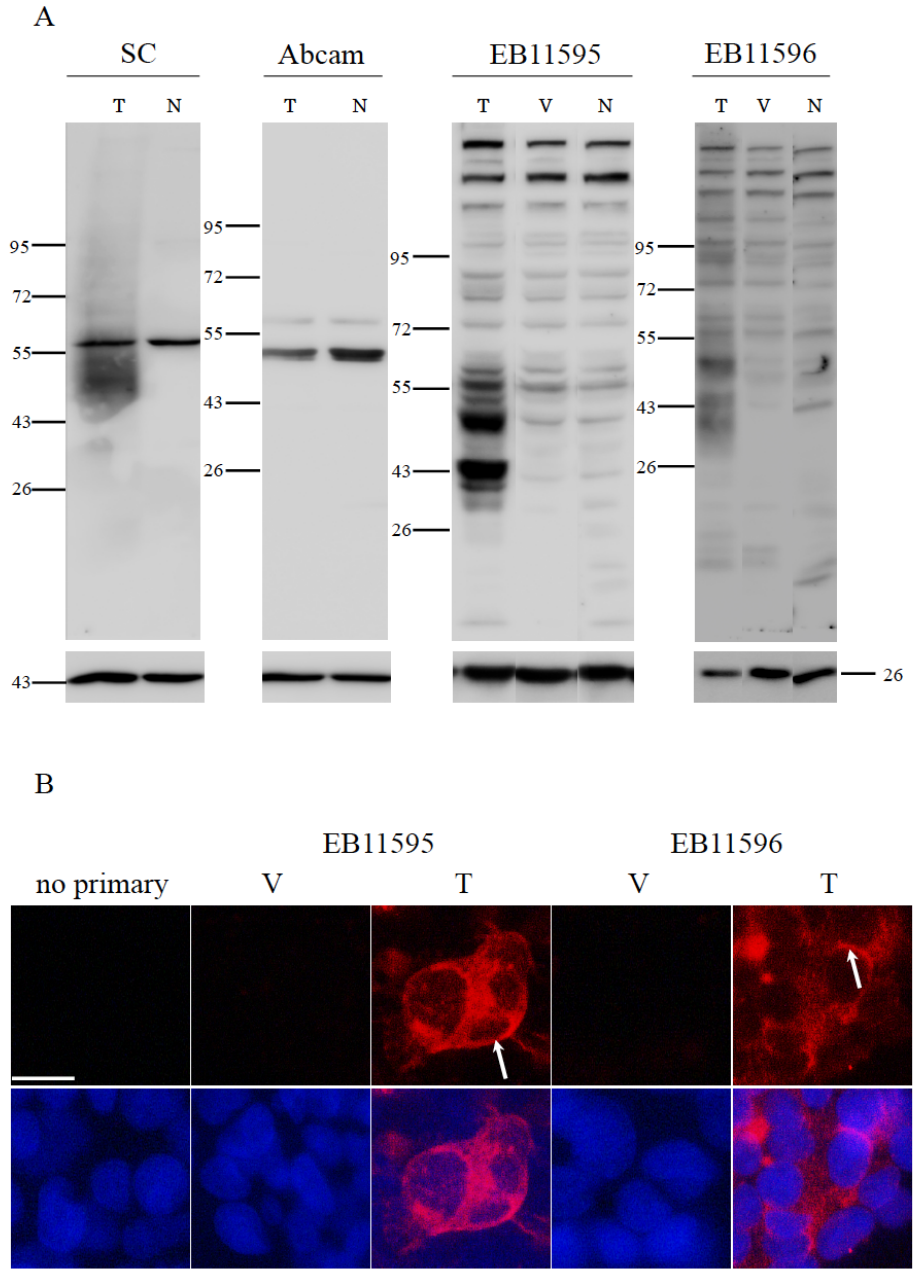

Figure 12. Testing anti-SNAT5 antibodies. Antibodies were tested by (A) western-blotting and (B) immunocytochemistry in HEK cells transfected with pLCPX-mSNAT5. Panel (A) shows representative western blots for lanes: anti-mSNAT5 SC (1:1000), anti-rSNAT5 Abcam (1:1000), anti-mSNAT5 EB 11595 (1:500), anti-mSNAT5 EB 11596 (1:500). 20 ug of cell lysates (72h after transfection) were incubated at 95°C for 5 min in Lämmli buffer with DTT prior to gel-electrophoresis. β - actin (SC, Abcam) or GAPDH (EB11595, EB 11596) were used as loading controls. Anti-mSNAT5 SC and Abcam antibodies were tested on the same gel, while EB 11595 and 11596 on different gels. Panel (B) shows representative immunofluorescence images. For immunocytochemistry cells were fixed 48 h after transfection and stained with anti-mSNAT5 antibodies as follows: (III) EB 11595 1:100 and (IV) EB 11596 1:50. Scale bar is 20 µm. Arrows indicate staining of anti-mSNAT5 Ab.
T – transfected cells, V – cells transfected with vector alone, N – non-transfected HEK cells.

Next the antibodies were tested using HEK cells transfected with mSNAT5-eGFPC1 (Figure 13). The mSNAT5-eGFPC1 product is expressed as fused protein of mSNAT5 with GFP,

therefore the expected apparent MW is ~85 kDa (GFP is 30 kDa). Anti-mSNAT5 SC Ab identified a set of diffuse bands between 55 and 72 kDa with a significant enrichment in the membrane fraction. However this is lower than the predicted MW for the fusion protein (Figure 13A). By immunocytochemistry the SC Ab apparently stained cell plasma membranes and an unidentified cellular compartment, in which the signal partially co-localized with GFP (Figure 13B). Similarly, Abcam anti-rSnat5 Ab detected bands between 55 and 72 kDa, however the signal was weaker in comparison to SC Ab. Conversely, the Abcam Ab did not give a specific signal above background by immunocytochemistry (Figure 13B). The EB11595 Ab recognized a band at ~72 kDa in total lysates and membrane fractions, where the signal was enriched (Figure 13A). By immunocytochemistry, the EB11595 signal was observed at the plasma membrane where it did not co-localize with GFP as well as in an intracellular compartment co-localized with GFP (Figure 13B). Anti-mSnat5 EB11596 detected diffuse bands that were enriched in the membrane fraction at an apparent MW between 55 and 72 kDa. For the same amount of protein lysate and Ab dilution the signal from EB11596 was lower than EB11595 in case of western-blotting, however by immunocytochemistry both antibodies showed similar staining (Figure 13A, B). Additionally all four Abs detected a band at an apparent MW rather greater than ~95 kDa (upper part of the gel) in total cell lysate and membrane fractions, that was also present in HEK cells transfected with peGFP-C1 vector alone.

4. SNAT5 localization in brain endothelial cells

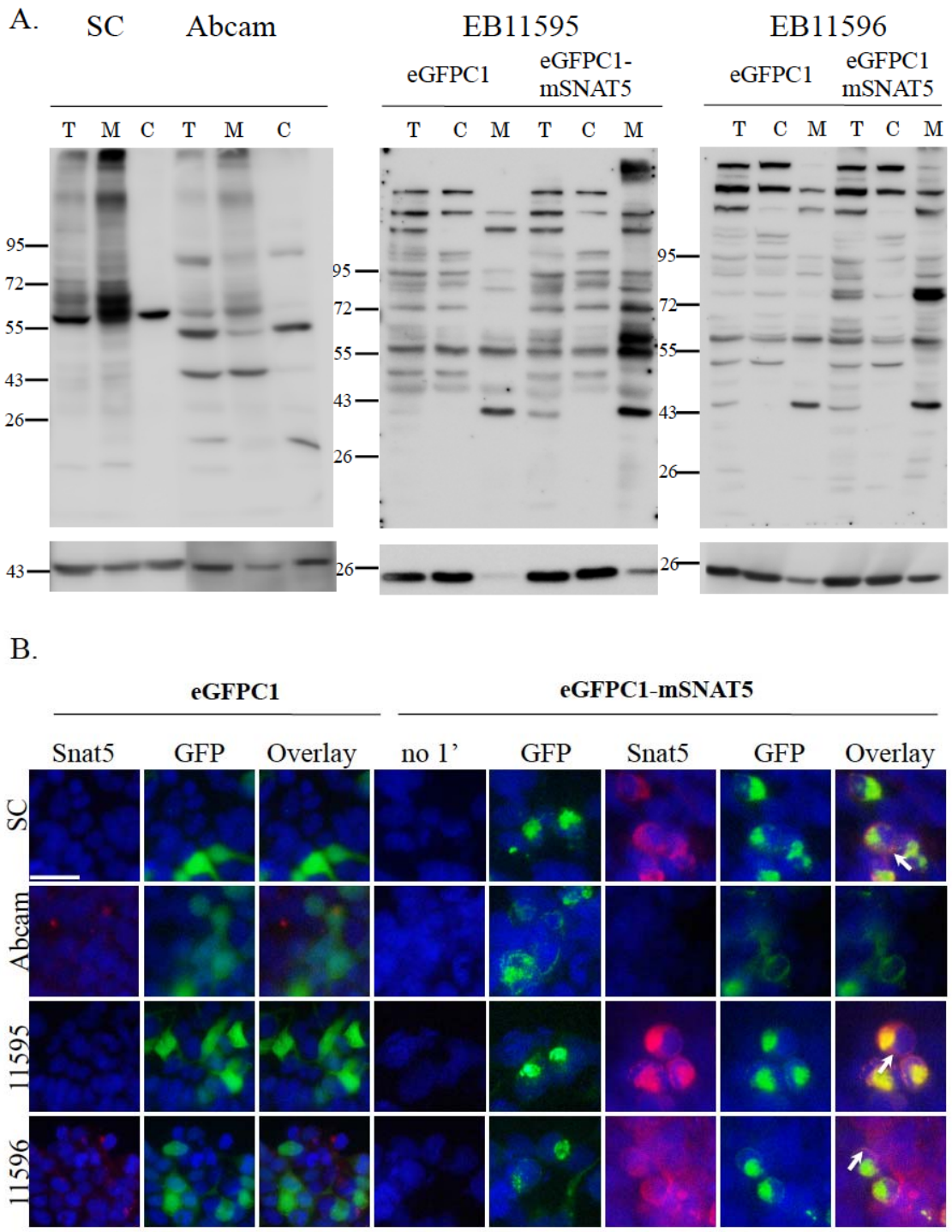

Figure 13. Anti-mSNAT5 antibody validation. Antibodies were tested by (A) western-blotting and (B) immunocytochemistry using HEK cells transfected with eGFPC1 and eGFPC1-mSNAT5. Panel (A) shows representative western blots for lanes: anti-mSNAT5 SC (1:1000), anti-rSNAT5 Abcam (1:1000), anti-mSNAT5 EB 11595 (1:500), anti-mSNAT5 EB 11596 (1:500). 20 ug of cell lysates (72h after transfection) were incubated at 95°C for 5 min in Lämmli buffer with DTT prior to gel-electrophoresis. β - actin (SC, Abcam) or GAPDH (EB 11595, EB 11596) were used as loading controls. T – total cell lysate, C – cytosolic fraction, M – membrane fraction. For immunocytochemistry cells were fixed 48 h after transfection and stained with diluted anti-SNAT5 antibodies as follows: SC 1:200, Abcam 1:200, EB 11595 1:100 and EB 11596 1:50. Scale bar is 20 um. Arrows indicate co-localization in membrane.

4. SNAT5 localization in brain endothelial cells

Next the specificity of the signal detected by anti-mSnat5 SC and EB11595 Abs in the membrane fractions was examined by surface biotinylation of HEK cells expressing mSNAT5-eGFPC1, or pLCPX-mSNAT5, or the corresponding vector alone. The band at ~95 kDa was specifically recognized by anti-mSnat5 SC Ab in the biotinylated fraction of transfected HEK cells (Figure 14A), but not in the same fraction of non-transfected cells. The extent of the surface labeling with biotin was confirmed by incubation with streptavidin-HRP conjugate. To estimate whether biotin accessed only cell surface and did not label cytosolic proteins the blot was incubated with anti-GAPDH Abs. No GAPDH staining was detected in the streptavidin bound fraction in contrast to the total lysate and unbound fractions. The EB11595 Ab recognized a diffuse band in the biotinylated fraction of pLCPX-mSNAT5 transfected cells, but not in the absence of biotin (Figure 14B) or in cells transfected with vector alone. The efficiency of biotinylation procedure and absence of biotin labeling in the cytosolic fraction was tested as described above.

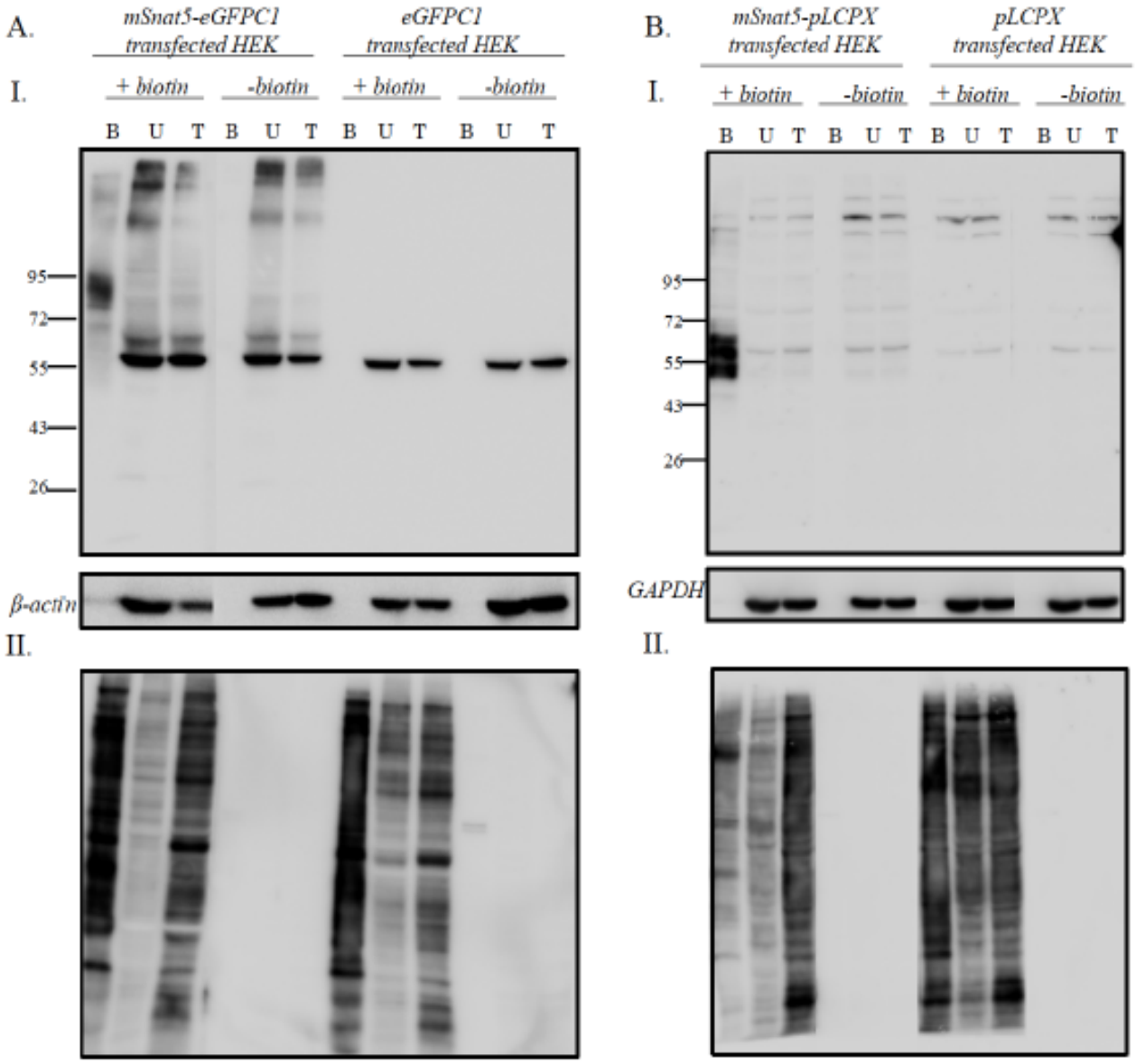

Figure 14. Detection of mSNAT5 by western blot with SC or EB11595 anti-SNAT5 antibodies on SDS-PAGE fractionated lysates from surface biotinylated cells. After incubation with biotin (+ biotin) or with buffer alone (- biotin) transfected cells were lysed and biotinylated proteins pulled-down using neutravidin agarose beads. For SDS-PAGE, 5 µL of total protein lysate (T), 10 µL of unbound proteins (U) and 20 µL of neutravidin-agarose-bound proteins (B). For panel A western blots were probed with: (I) anti-mSNAT5 SC (1:1000), anti-β-actin (intracellular marker) antibodies, and (II) streptavidin-HRP. For panel B blots were probed with (I) anti-mSNAT5 EB11595 (1:500), anti-GAPDH (intracellular marker) antibodies, and (II) streptavidin-HRP.

4.2.2 Application of tested anti-SNAT5 antibodies in brain tissue

The anti-mSNAT5 Abs were tested on brain tissue by western-blotting and immunofluorescence. High levels of *Snat5* mRNA were reported in brain endothelial cells and in pancreas [2, 407]. Therefore, anti-mSNAT5 SC, EB11595 and EB11596 Abs were tested on brain and pancreas tissue lysates (Figure 15ABC).

4. SNAT5 localization in brain endothelial cells

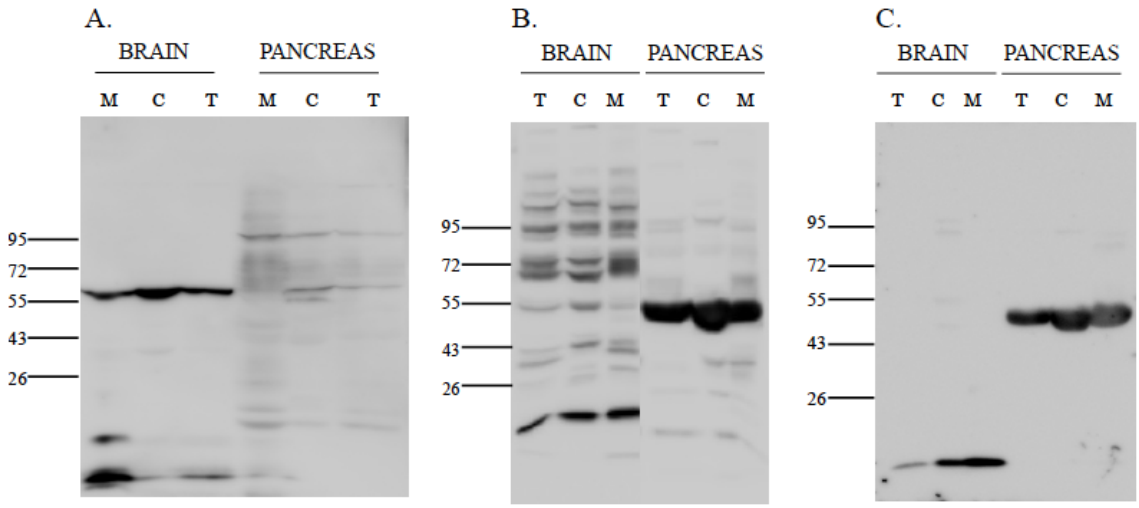

Figure 15. Testing anti-mSNAT5 antibodies on mouse tissue lysates. Representative western blots of SDS-PAGE fractionated mouse lysates from brain (BRAIN), and pancreas (PANCREAS) as follows: membrane (M), cytosolic (C) and total (T) fractions. Membranes were probed with anti-mSNAT5 antibodies as follows in panels: (A) SC anti-mSNAT5 Ab (1:1000), (B) EB11595 anti-mSNAT5 Ab (1:100), and (C) EB11596 anti-mSNAT5 Ab (1:500).

The anti-mSNAT5 SC Ab detected a band at ~55 kDa at a similar intensity in brain total, cytosolic, and membrane lysates. Additionally, a faint most likely non-specific band was detected at an apparent MW of 55 kDa in all pancreatic lysates. This band was suspected to be staining of amylase, which is very highly expressed in pancreas and has an expected MW of ~55kDa. Additionally the SC Ab detected a very faint diffuse banding between 55 and 72 kDa in the pancreas membrane fractions. The EB11595 Ab stained a similar set of diffuse bands in pancreas total lysates that were enriched in the membrane relative to the cytosolic fractions (Figure 15B). However, in the brain samples a 55 kDa band was enriched in cytosolic fraction vs. in total lysates or membrane fractions, and therefore regarded as non-specific. Additionally, EB11595 detected the band at ~72 kDa in the brain membrane fraction, which may be specific staining of SNAT5 however it is difficult to distinguish from a band migrating at nearly the same MW in all brain lysate fractions. Unfortunately, EB11596 recognized an intensely stained 50 kDa band in all pancreas fractions, possibly amylase and, thus, non-specific, while no signal was observed in the brain samples (Figure 15C). By immunofluorescence on brain section multiple thread-like staining with SC antibody, staining in astrocyte like structures with EB11595, and peri-nuclear staining with EB11596 was observed (Figure16 A, B, C).

4. SNAT5 localization in brain endothelial cells

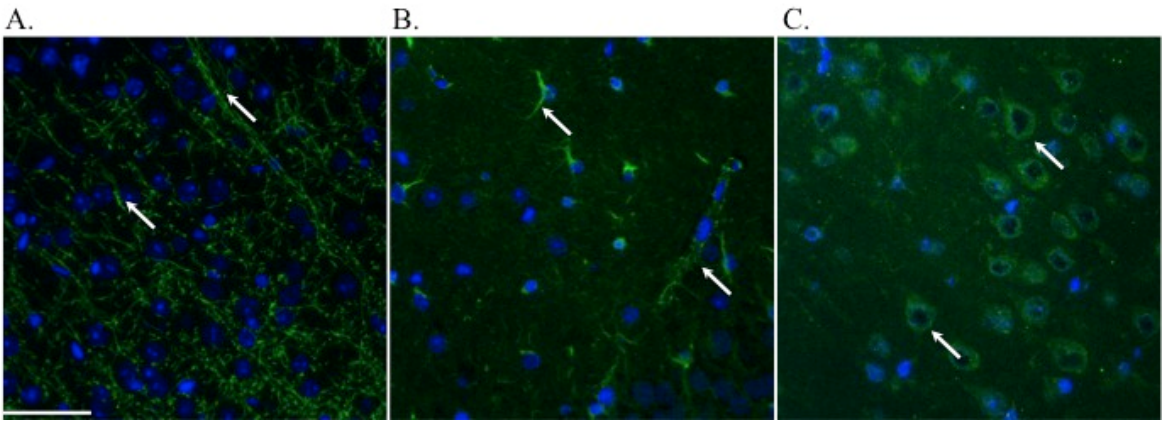

Figure 16. Immunofluorescence staining of paraffin-fixed mouse brain sections with anti-mSNAT5 antibodies. Representative images are shown for anti-SNAT5 (green) staining with (A) Santa Cruz antibody, (B) EB11595, and (C) EB11596, all antiboides were diluted at 1:100, and nuclei are co-labeled (blue), arrows indicate mSNAT5 signal. Scale bar is 50 µm.

Since EB11595 resulted in a possible SNAT5 specific signal, a more detailed analysis of the structures recognized by this antibody *in vivo* was carried out (Figure 17A-R). The EB11595 antibody detected structures in close association with microvessels, but not co-localized with laminin, a marker for microvessels (Figure 17A-I). However, the signal co-localized with astrocyte marker GFAP (Figure 17 J-L). Since *Snat5* mRNA was found in choroid plexus epithelial (CPE) cells, EB11595 was used for immunofluorescence staining of choroid plexus tissue sections. In contrast to the anti-SNAT3 Ab, no specific signal was observed by EB11595 staining of choroid plexus in brain tissue sections (Figure 17 M-O).

4. SNAT5 localization in brain endothelial cells

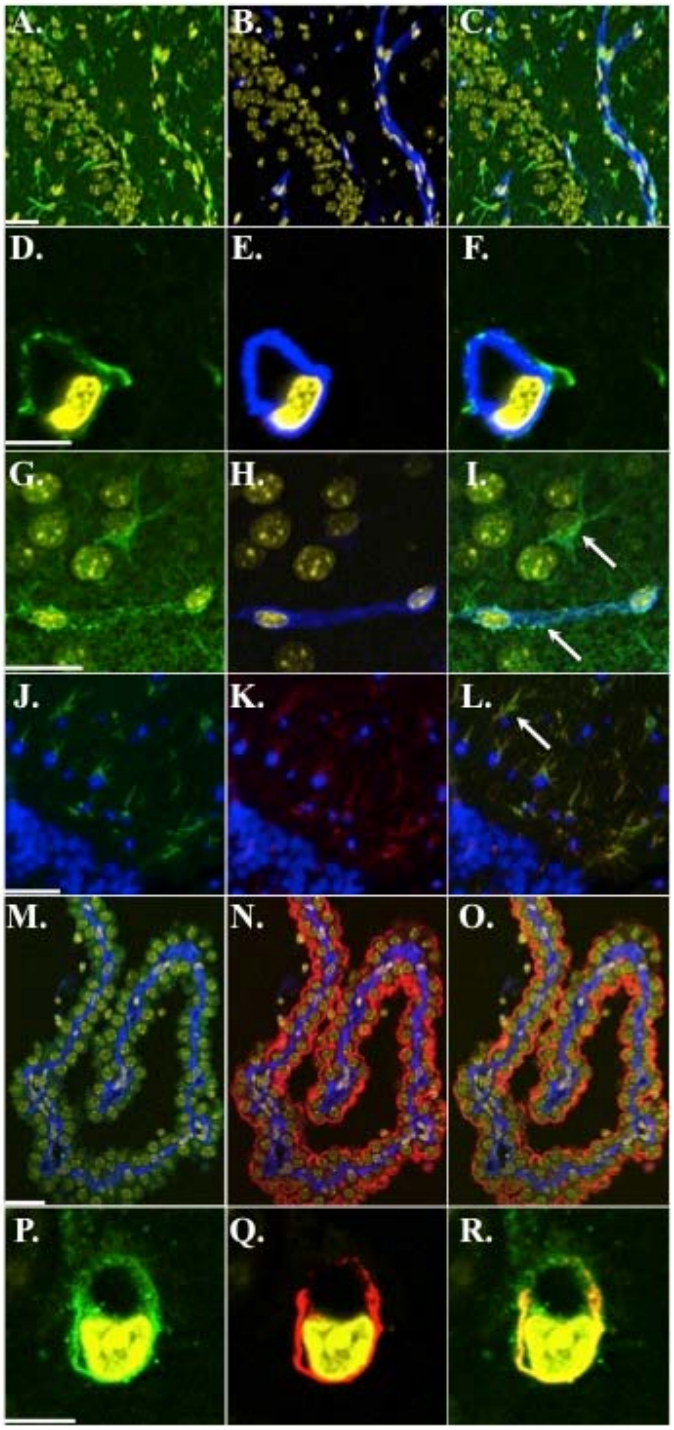

Figure 17. Representative immunofluorescence images of paraffin brain sections. Panels (A–I) are stained with EB11595 anti-mSNAT5 (1:100, green) and anti-laminin (1:200, blue) antibodies. Panels (A-C) low magnification images of a brain section (30 µm scale bar); panels (D-F) capillary cross-section (5 µm scale bar); panels (G-I) longitudinal capillary section (10 µm scale bar); nuclei in yellow. Panels (J–L) are double-stained with anti-mSNAT5 (1:100, green) and anti-GFAP (1:200, red) antibodies (50 µm scale bar), nuclei are stained with DAPI (blue). Panels (M-O) are stained with anti-mSNAT5 (1:200, green), anti-mSNAT3 (1:200, red) and anti-laminin (1:200, blue) antibodies (30 µm scale bar, nuclei (blue)). Panels (P-R) are stained with anti-mSNAT3 (1:200, green) and anti-laminin (1:200, red) antibodies (5 µm scale bar, yellow nuclei). Arrows indicate staining of anti-mSNAT5 EB 11595 Ab.

Previously, anti-mSNAT3 antibodies were shown to be successfully used for immunofluorescence staining with a strong signal to noise using fresh fixed free-floating mouse brain sections, therefore, the anti-mSNAT5 antibodies were tested on fresh fixed vibrotome sections. Staining with neither SC nor EB11596 antibodies resulted in a specific signal under these conditions (data are not shown). However, staining with EB11595 resulted in a similar labeling pattern as previously observed for paraffin-fixed brain sections in structures near to, but not overlapping with microvessel marker staining (Figure18A-F).

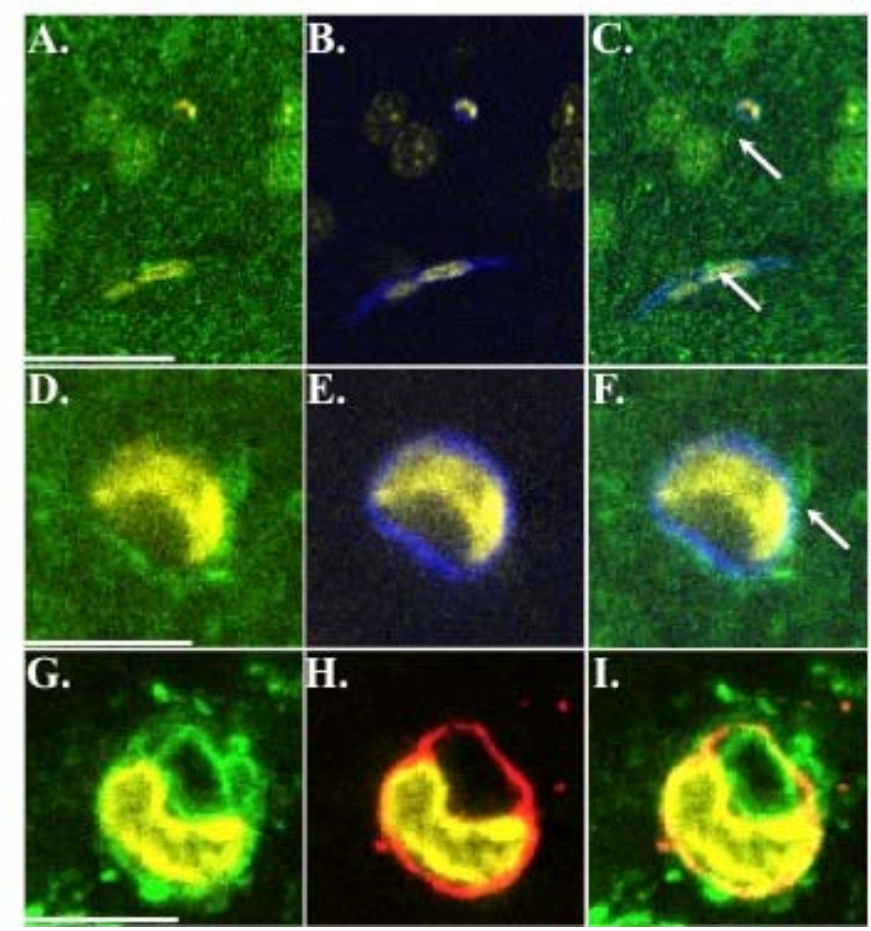

Figure 18. Representative immunofluorescence images of free-floating brain sections. Immunofluorescence was performed with 1:200 dilutions of antibodies as follows: A-F –– anti-mSNAT5 EB 11595 (green) and anti-laminin (blue) antibodies; A-C –– low magnification (30 µm scale bar), D-F –– a capillary cross-section (5 um scale bar); G-I –– staining of anti-mSNAT3 (green) and anti-laminin (red) antibodies (5 um scale bar). Nuclei are shown as yellow. Arrows indicate staining of anti-mSNAT5 EB11595 Ab in the brain sections.

4.2.3 Application of tested anti-SNAT5 antibodies in isolated microvessels

The EB11595 anti-mSNAT5 antibody was further tested on isolated microvessels by western blot and immunofluorescence (Figure 19A-C). As for total brain fractions EB11595 recognized a band at ~72 kDa that was enriched in the membrane fraction. Since the glucose transporter GLUT1 (SLC2A1) is highly expressed in the BBB, the blot was probed with anti-GLUT1

antibodies. An enrichment in GLUT1 (MW~50 kDa) staining was detected in isolated microvessels. Nevertheless, a strong signal for an astrocyte marker GFAP was also detected in the microvessel lysate preparations by western blot. In isolated microvessels EB11595 staining resulted in punctate immunofluorescence signals, while anti-GLUT1 and anti-laminin immunofluorescence resulted in uniformly distributed signals.

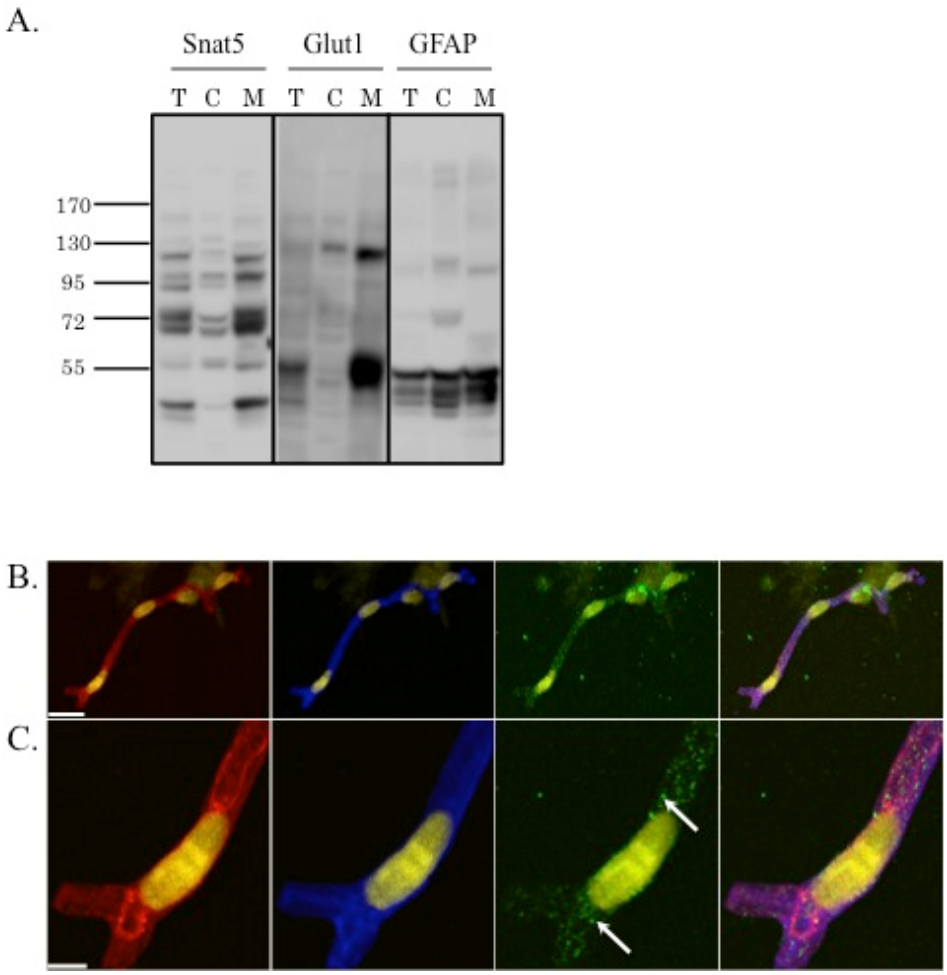

Figure 19. Testing anti-mSNAT5 EB11595 on isolated microvessel preparations. Panel (A) shows representative western blots of microvessel lysates (total lysates (T), cytosolic (C) and membrane (M) fractions) probed with anti-mSNAT5 EB11595 (1:100 dilution), anti-GLUT1 (1:1000) and anti-GFAP (1:500) antibodies. Panels B, C are representative immunofluorescence images of isolated microvessels stained with anti-mSNAT5 EB11595 (1:50, green), anti-GLUT1 (1:200, red) and anti-laminin (1:200). Nuclei are shown in yellow. For (B) 20 µm scale bar; (C) 5 µm scale bar. Arrows indicate punctate EB11595 staining.

4.3. Discussion

Both SNAT3 and SNAT5 transporters are Na^+-dependent pH sensitive Gln transporters. High levels of *Snat5* and *Snat3* mRNAs were reported in freshly isolated highly pure brain endothelial cells. However, a brief *in vitro* culture significantly decreased their expression, suggesting they play an important role *in vivo*, for example, in BBB transendothelial AA transport [2, 370]. Hawkins and colleagues postulated that all Na^+-dependent AATs are localized only on abluminal BEC membranes, however recently SNAT3 expression was identified on both luminal and abluminal membranes [3, 373]. Therefore, SNAT5 localization on the BBB membranes was investigated. Both commercially available as well as in-house produced anti-SNAT5 antibodies were tested for SNAT5 specificity (Table 4). Preliminary tests in HEK cells heterologously expressing mSNAT5 indicated that SC, EB11595, and EB11596 antibodies were potentially good candidates for specific SNAT5 staining. However, by western blot of brain tissue lysates the SC antibody recognized a band of the same intensity in all three brain fractions without any enrichment in the membrane fraction (Figure 15A). Moreover, by immunofluorescence the SC antibody stained unidentified thread-like structures (Figure 16A). The EB11595 antibody detected a diffuse band in brain and microvessels samples between 55 and 72 kDa that was enriched in the membrane fraction (Figure 15B, 19A). However, even considering the single suggested glycosylation site (residue 236, http://www.uniprot.org /uniprot/Q3U1J0) the apparent MW of the band is greater than the expected 55 kDa MW for SNAT5. Anti-mSNAT5 EB11595 antibody also did not stain brain endothelial cells or choroid plexus epithelial cells in brain sections where previously significant mRNA levels were reported. However co-localization of EB11595 staining with anti-GFAP staining was observed (Figure 17J-L), which is in an agreement with previously published SNAT5 expression in the rat brain [279]. In summary, anti-mSNAT5 antibody, EB11595, gave a specific signal in cells heterologously expressing mSNAT5. This antibody also detected SNAT5 expression in astrocytes, but not in microvessels or CP.

Unfortunately, since SNAT5 knockout animals have not yet been generated, EB11595 antibody cannot be validated in *in vivo* and, thus, the specificity is still questionable. Conversely, EB11595 anti-mSNAT5 antibody signal co-localized with the astrocyte marker GFAP. Therefore, the absence of signal for SNAT5 in brain endothelial cells may be explained by several reasons that have either biological or methodological origin. Unfortunately, cases of lack of correlation between mRNA and protein levels are not rare in literature. For instance, no positive correlation between immunohistochemistry and Affymetrix gene expression profile of CD31 was observed in endothelial cells from human prostate isolated by magnetic cells sorting

(MACS) [408]. Generally, a higher mRNA level significantly increases the probability of protein detection [409]. However, the correlation between protein concentration and corresponding mRNA level is reported to be on average 20-40 % [409-411]. The 60% variability can be explained by several factors. For instance, for both mRNAs and proteins the rate of degradation and synthesis are important. On average, for mammals the mRNA production rate is ~two copies per hour, while proteins are synthesized at a rate of ~dozens of molecules per hour. Moreover, the half-life of mRNA (2.6 - 7 hours) is significantly less than the average protein half-life of 46 hours [412, 413]. Additionally, protein abundance is believed to depend on their functions in the cell, for example, structural or housekeeping proteins are considered to be long-lived proteins versus regulatory proteins [409]. Taken together, both synthesis and degradation rates increase the chance of detecting protein expression of a membrane transporter such as SNAT5. However, additionally post-transcriptional regulation impacts protein abundance. For instance, Vogel describes example of an opposite correlation between length of mRNA and protein concentration in yeast [409]. Another example is that in cancer cells highly expressed proteins have shorter 3' untranslated regions (UTR). These UTR regions usually contain micro RNA (miRNA)-binding sites and miRNA are known to mediate translational repression [414, 415]. In addition to biological factors, methodological aspects such as sensitivity and signal to background influence the interpretation of the experimental results. Crosschecking experiments, when the same result is confirmed simultaneously by different techniques or methods, have particular importance. For instance, to confirm anti-mSNAT5 antibody EB11595 specificity, the immunofluorescence signal in brain tissue could be compared with the *in situ* hybridization signal [366]. Moreover, mass spectrometric analysis of the band detected by EB11595 in the brain and microvessel samples can be used for confirmation of this antibody specificity. Unfortunately, the localization of SNAT5 is not yet determined in the brain endothelial cells and further studies are required.

5. Manuscript: "Brain interstitial fluid glutamine homeostasis is controlled by blood-brain barrier SLC7A5/LAT1 amino acid transporter"

This section contains the mentioned above manuscript submitted for publication in the Journal of Cerebral Blood Flow and Metabolism on 27.06.15. My contribution to the manuscript concerns experimental design, performance of all experiments, UPLC AA analysis and data presentation under the supervision of François Verrey and Victoria Makrides.
I wrote the paper with the help of my both supervisors.

Elena Dolgodilina[1], Stefan Imobersteg[2], Endre Laczko[3], Tobias Welt[2], Francois Verrey[1]*, Victoria Makrides[1]*

[1]Institute of Physiology, Zurich Center for Integrative Human Physiology (ZIHP) and NCCR Kidney.CH, University of Zurich, Winterthurerstrasse 190, 8057 Zurich, Switzerland; [2]Division of Psychiatry Research, University of Zurich, Wagistrasse 12, 8952 Schlieren, Switzerland; [3]Functional Genomic Center Zurich (FGCZ), ETH and University of Zurich, Winterthurerstrasse 190, 8057 Zurich, Switzerland.

*Equal contributors

Classification: physiology, neuroscience

Running head: Brain interstitial fluid amino acid homeostasis

Key words: blood brain barrier, cerebrospinal fluid, glial cells, hippocampus, physiology

Corresponding author: Francois Verrey,
Institute of Physiology
Winterthurerstrasse 190,
8057 Zurich, Switzerland
Fax: +41 (0) 44 635 6814
Telephone: +41 (0) 44 635 5044
verrey@access.uzh.ch

Abstract

L-glutamine (Gln) is the most abundant amino acid (AA) in plasma and cerebrospinal fluid (CSF) and a precursor for the main central nervous system excitatory (L-glutamate) and inhibitory (γ-aminobutyric acid (GABA)) neurotransmitters. Concentrations of Gln and 13 other brain interstitial fluid (ISF) AAs were measured in awake, freely-moving mice by hippocampal microdialysis using extrapolation to zero flow rate method. ISF levels for all AAs including Gln were ~5-10 times lower than in CSF. Although the large increase in plasma Gln by intraperitoneal (IP) injection of $^{15}N_2$-labeled Gln (hGln) did not increase total ISF Gln, low levels of hGln were detected in microdialysis samples. Competitive inhibition of system A (SLC38A1&2; SNAT1&2) or system L (SLC7A5&8; LAT1&2) transporters in brain by perfusion with α-(methylamino)-isobutyric acid (MeAIB) or 2-aminobicyclo-(2,2,1)-heptane-2-carboxylic acid (BCH) respectively, was tested. The data showed a significantly greater increase in ISF Gln upon BCH than MeAIB treatment. Furthermore, brain BCH perfusion also strongly increased the influx of hGln into ISF following IP injection consistent with transstimulation of LAT1-mediated transendothelial transport. Taken together the data support the independent homeostatic regulation of AAs in ISF vs. CSF and the role of the blood-brain barrier expressed SLC7A5/LAT1 as a key ISF gatekeeper.

Introduction

The blood-brain barrier (BBB) is an extensive microvascular network controlling entry and exit of substances between the blood and the brain by both physical and metabolic barriers to free exchange. Unlike in the periphery, brain endothelial cells form a tight barrier through expression of contiguous, well-organized tight junctions and lack of transcellular channels and fenestrations. Furthermore, the endothelium exhibits a polarized (luminal vs. abluminal) distribution of proteins including transporters[1-3]. The BBB endothelium in association with pericytes (within a common basement membrane), astrocytic endfeet (with an associated parenchymal basement membrane), and neurons form "the neurovascular unit"[1].

All AAs, whose diverse metabolic and regulatory functions include serving as neurotransmitters and neurotransmitter precursors, are tightly controlled in the central nervous system (CNS). Since testing cerebrospinal fluid (CSF) is less invasive than sampling brain interstitial fluid (ISF), CSF is more thoroughly characterized than ISF. Therefore, CSF is commonly used for diagnostic and drug development as a proxy for ISF. Although, there are known similarities between CSF and ISF, for example, in the ionic composition (i.e. K^+, Ca^{2+}, Na^+, Cl^-), it is unclear

whether this is a valid assumption for many solutes. CSF concentrations for most AAs are ~6 to 10 times lower than in plasma. One exception is the most abundant plasma AA, L-glutamine (Gln), which is nearly as high in CSF as in blood[4]. However, in brain ISF the reported Gln levels vary ~two fold[5, 6]. Gln is a precursor for the major excitatory L-glutamate (Glu) and inhibitory neurotransmitters (γ-aminobutyric acid (GABA))[7]. Furthermore, levels are altered during neuropathologies such as Huntington disease, ischemia, and epilepsy[8-10], and hyperammonemia, or hepatic encephalopathy (HE)[11]. Therefore, Gln concentrations must be efficiently regulated in the ISF.

In general, AA's do not freely diffuse across membranes instead specialized membrane proteins or solute carriers (SLC) transport AAs across membrane barriers. Prior to their molecular identification AA transporters (AAT) were classified as "systems" based on substrate specificity and dependence (or lack of) on Na^+ for activity. Figure 1 illustrates expression of known Gln transporters in the CNS. The Na^+-dependent system A transporters SLC38A1 (SNAT1) and SLC38A2 (SNAT2) expressed by neurons[12, 13] participate in Gln uptake for Glu or GABA synthesis[7], however some other Gln transporters were also found in neurons[14-17]. Astrocytes express a wide range of Gln transporters such as SLC1A5 (ASCT2), SCL38A2 (SNAT2), SCL38A3 (SNAT3), SLC38A5 (SNAT5), SLC7A6 (y^+LAT2), SLC7A5 (LAT1) and SLC7A8 (LAT2)[14, 18-21]. Although in adults ASCT2 and y^+LAT2 levels are minimal[18, 22]. The abundantly expressed Na^+-dependent pH sensitive SNAT3 and SNAT5 are thought to be the main astrocytic transporters for Gln efflux to neurons for the Glu/GABA-Gln cycle[7]. The BBB also expresses several different AAT involved in Gln transport[23]. Due to abundant expression and endothelium membrane localization LAT1 and SNAT3 may perform central roles in the BBB modulated control of brain ISF homeostasis for Gln and other AAs[2, 23].

A central aim of the current study was to accurately measure the ISF AA concentrations. Hippocampal ISF AA content was quantified and AA regulation investigated by *in vivo* microdialysis in freely-moving mice. Here we report a quantitative comparison of AA levels in ISF vs. CSF and plasma. Furthermore, responses to acute peripheral and/or parenchymal challenges support a central role for BBB expressed LAT1 transporters in regulation of Gln homeostasis in the ISF.

Materials and Methods

Animals

All animal experiments were conducted in accordance with the Swiss federal and cantonal law and were performed with the approval of the Swiss Veterinary Council. For all experiments 12-14 week old male C57BL/6J mice (Charles River (Crl), Germany) (22–29 g) were used. Prior to surgeries mice were adapted for one week to food *ad libitum* during the active period (night) and food restriction during the inactive phase (day), with water *ad libitum* at all times.

Microdialysis

Microdialysis materials and chemicals

Microdialysis guide cannulas (CMA 7, P000138,) and probes (CMA 7: 6 kDa MW cut-off, with 1.0 mm (cat. #P000082) or 2.0mm (cat. #P000083) membranes were purchased from CMA Microdialysis AB, Kista, Sweden. Dental acrylic cement (CE 0086) was purchased from Pattern Resin LS, Powder & Liquid, GC America Inc., USA. FEP (fluorinated ethylene propylene) tubing, and tubing adapters were purchased from Microbiotech/se AB (Stockholm, Sweden). Samples were collected in a temperature-controlled fraction collector (EFC-82, Eicom, Dublin, Ireland). Norleucine (NLeu), α-(methylamino)-isobutyric acid (MeAIB), 2-amino-2-norbornanecarboxylic acid (BCH), L-glutamic acid-γ–monohydroxamate (GAH), L-glutamine (Gln), L-valine (Val), sulphosalicylic acid (SSA), and cresyl violet acetate were purchased from Sigma-Aldrich Chemie GmbH (Buchs, Switzerland). $^{15}N_2$ heavy labeled L-glutamine (hGln) and fully labeled L-glutamine $^{13}C_5{}^{15}N_2$, were obtained from Cambridge Isotope Laboratories Inc. (Tewksburry, Masschusetts, USA).

In vitro microdialysis

The relative recovery (RR) and mass transfer coefficient (K_0) were estimated for 1 and 2 mm CMA7 probes *in vitro* (Suppl. Tables 1 and 2). Probes were placed in a solution with 15 standard AAs with and without NLeu. Artificial cerebrospinal fluid (aCSF, composition in mM: NaCl 147; KCl 4.03; $CaCl_2$ 2.52; pH 7.4) or aCSF with 100 µM NLeu was used for perfusion as indicated. For K_0 determination the fractions were collected at four flow rates (0.1, 0.5, 1, and 2 µl/min) with adequate equilibration between flow rate changes. Samples were stored at -80°C for UPLC.

***Intracerebral* microdialysis in awake, freely-moving mice**

Surgery

Mice were deeply anaesthetized by an intraperitoneal (IP) injection (10 µl/g body weight) of fentanyl 50 µg/ml, midazolam 5.0 mg/ml and medetomidin 1 mg/ml in 0.9% sterile saline. Eye cream (Viscotears, Novartis Pharma Schweiz AG, Bern, Switzerland) was applied, and body temperature controlled at 37°C. Using a stereotactic frame guide cannulas were implanted in the hippocampus at AP: −3.1; L: +2.9; V: −2.3[24] and supported by screws and dental acrylic cement. After surgery the anesthetic was antagonized by IP injection of 10 µl/g body weight 0.4 mg/ml naloxon, 0.1 mg/ml flumazenil and 5.0 mg/ml atipamezol in 0.9% sterile saline. For two days post-surgery an analgesic was administered in drinking water (200 µg/50 ml temgesic) and mice fed *ad libitum*. Thereafter and for the duration of microdialysis experiment food restriction was resumed with drinking water *ad libitum*. Food restriction was instituted to preemptively reduce variability in microdialysate AAs. Mice were weighed daily and mice that lost more than 10% body weight were excluded. Additionally, comparisons between 1 µ/min 24 hour microdialysate collection failed to show any significant changes in AAs with or without food restriction (data not shown). Eighteen hours before experimental microdialysate collection, microdialysis probes were inserted and for the first 4-6 hours perfused at 1 µl/min, followed by an overnight perfusion at 0.1 µl/min (Suppl. Fig. 1). During microdialysis mice were subjected to normal 12 h light and dark cycles. They were singly housed in cages equipped with swivels that allowed free movement. Unless otherwise noted, 30 minute samples were collected at 1 µl/min and stored 8-12 hours at +4°C and at -80°C until measurement (Suppl. Fig. 1).

Determination of brain interstitial fluid amino acid concentrations

Amino acid concentrations in brain ISF were determined using an extrapolation of microdialysate concentrations to "zero flow" rate (Flow-rate method)[25]. The extrapolation is based on the inverse relationship between flow rate and the transfer of molecules (mass transfer rate). Relative recovery is a function of flow rate, probe surface area, and the mass transfer coefficient (K_0), due to the chemical and physical properties of the solute and the matrix. The AA concentrations in 30 µl volumes of microdialysates collected at four flow rates (0.1, 0.5, 1, 2 µl/min) were extrapolated to original concentrations (C_0) using the equation:

$$C_0=C_{ISF}-[C_{ISF}\exp(-K_0A/F)] \quad \text{(eqn1)},$$

where C_{ISF} is the concentration in the brain interstitial fluid, K_0 is the average mass transfer coefficient, A is the area of the semipermeable probe membrane (0.75 μm^2 for 1 mm probe) and F is flow rate.

To constrain the solution for C_0, the mass transfer coefficient (K_0) for the non-standard AA NorLeucine, (NLeu) was determined *in vivo* for each mouse[26]. Flow-rate experiments were performed twice: initially with aCSF perfusate, and repeated with aCSF +100 µM NLeu. K_0 for NLeu vs. other AAs of interest was determined *in vitro* and found comparable. NLeu K_0 for each mouse was applied for calculation of C_0 of all other AAs using eqn 1 (Suppl. Fig. 2B).

Microdialysis sampling during intraperitoneal AA injection or/and competitive inhibitors perfusion

For experiments with AA IP injection mice were prepared for microdialysis as described, initially 3-4 control samples were collected (baseline), then vehicle (0.9% sterile NaCl) injected IP and 30 minute samples were collected at 1 µL/min for four hours. Half of the mice received 1.3 g/kg of hGln IP and the other half 240.5 mg/kg Val IP. Samples were collected as before for four hours (Suppl Fig. 1C).

For experiments with perfusion with competitive inhibitors, after baseline samples were collected for two hours, probes were perfused with aCSF + 20 mM methylaminoisobutyric acid (MeAIB) or 20 mM 2-aminobicyclo-(2,2,1)-heptane-2-carboxylic acid (BCH). After a 40-minute equilibration with inhibitor (time until inhibitor has reached the microdialysis probe in the brain and then fraction collector), 30 minute samples were collected for three hours, then aCSF was re-introduced into the probes, equilibrated for 40 minutes and sampling was resumed for 3-4 hours (Suppl Fig 1D).

For simultaneous IP AA administration with inhibitor infusion, baseline samples were collected for two hours, probes equilibrated for 40 min perfusion with aCSF + 20 mM inhibitor. Following inhibitor equilibration, hGln (1.3 g/kg, in 0.9% NaCl) was administrated IP and microdialysate samples were collected for 2 hours. Following cessation of inhibitor perfusion probes were equilibrated with aCSF for 40 min and samples collected for 3 hours (Suppl. Fig 1E).

To calculate the total influx of Gln into the brain from the plasma following IP injection with heavy labeled Gln (hGln) the following calculation was used: (hGln /total Gln in microdialysis sample)/(hGln/total Gln in plasma) = total Gln influx to the brain from plasma.

Organ and tissue collection

Plasma collection

At chosen time points ≈ 20 µl blood samples were collected from tail tip cuts into Na^+-heparinized microhematocrit tubes (Provet AG, Switzerland). Samples were centrifuged

(10000g, 10 min, 4°C) in heparin containing vials (B. Braun Medical AG, Sempach, Switzerland), frozen on dry ice, and stored at −80°C for measurement.

Terminal CSF, plasma, and brain collection

CSF samples were collected prior to terminal perfusion as previously described[27]. Briefly, mice were anaesthetized with IP ketamine (100 mg/kg) and xylazine (10 mg/kg), and an incision made in the skin inferior to the occiput. Under a dissection microscope, the dura mater of the cisterna magna was penetrated and CSF collected into a pulled glass capillary, frozen on dry ice, and stored at -80°C. CSF samples visibly contaminated with blood were discarded.

Blood was drawn by cardiac puncture, transferred to heparin containing tubes, and centrifuged to separate plasma (10000g, 10 min, +4°C). Mice were transcardially perfused with ice-cold PBS (10 mM Na_2HPO_4, 2.5 mM NaH_2PO_4, 150 mM NaCl, 3 mM KCl, pH 7.4), brains harvested and cut into hemispheres. Left hemispheres were incubated in PBS with 4.0% PFA at +4°C overnight, and subsequently paraffin embedded for probe position verification, and right hemispheres were snap-frozen in liquid nitrogen and stored at −80°C.

Amino acid measurements

Ultra Performance Liquid Chromatography (UPLC) amino acid measurements

The analysis of AA concentrations was performed at the Functional Genomic Center Zurich (FGCZ) using the Mass Track Amino Acid Analysis Application Solution by ACQUITY ultra performance liquid chromatography (UPLC; Waters, Milford, USA) according to the manufacturer's protocol. Microdialysis and CSF samples were analyzed without deproteinization, and plasma samples were diluted 1:1 with 10% sulfosalicylic acid (SSA) for deproteinization prior to UPLC.

Mass spectrometry for heavy isotope labeled glutamine quantification

Heavy labeled Gln (hGln) was detected in microdialysis and plasma samples by liquid chromatography mass spectrometry (LC-MS) using a Q Exactive Hybrid Quadrupole-Orbital Trap mass spectrometer (Thermo Scientific, USA) coupled with a nanoAcquity liquid chromatograph (Waters, USA). For quantification 2.5 µM of totally labeled glutamine ($^{13}C_5{}^{15}N_2$) was added as an internal standard (IS) to dialysate samples. After thawing, samples were diluted 5-fold with 50 mM ammonium in acetonitrile - methanol 9:1, vortexed and analyzed immediately. For each independent set of samples, hGln and total Gln calibration curves (10, 5, 2.5, 0.5 µM) containing 2.5 µM IS were measured. Quantification was calculated based on the response factor from calibration curves.

After precipitation with 10% SSA plasma samples were diluted 10 times with borate buffer (500 mM, pH 9), precipitated with methanol 4:1 and analyzed as above. Baseline ratio of hGln/Gln measured by liquid chromatography mass spectrometry (LC-MS) before IP injection was 6.6 ± 2% in plasma and 0.13 ± 0.3% in microdialysates. The higher baseline hGln levels detected in plasma may have been an artifact of the LC-MS analysis since the naturally occurring frequency of the ^{15}N isotope is 0.1-0.5%[28] LC-MS may have over-estimated hGln in plasma but not in microdialysis samples.

Immunohistochemistry

Paraformaldehyde-fixed brains were paraffin embedded (Shandon Xylene Substitute, Thermoscientific), 5 µm coronal sections prepared using a microtome (RM 2235, Leica) and stored at +4°C for staining. Nissl staining was performed for probe position validation. Paraffin sections were deparaffinized (Microm/Histocam AG, Thermoscientific) to 100% ethanol, extensively rinsed in water, and incubated 15 min in warm 2% cresyl violet. Excess cresyl violet was removed, sections dehydrated in 100% ethanol twice, and destained twice with xylene (Shandon Xylene Substitute, Thermoscientific). Nissl stained sections were imaged by a handheld USB digital Firefly GT800 microscope (Belmont, USA).

Statistical Analysis

Sample data were plotted at the collection midpoint and, as indicated, sample time was adjusted for the time required to reach the fraction collector from the probe and reported as "time in the brain" (Suppl. Fig. 1).

Statistical analysis was performed using GraphPad Prism 5.0 (GraphPad Software, USA). Unless otherwise stated between-group comparisons were performed by Students t-test or two-way analysis of variance ANOVA (two independent factors: treatment and time), followed by Dunnett, Bonferroni or Sidak post-test as stated. Statistical significance was accepted at $P < 0.05$ or as indicated. All data are presented as mean ± standard deviation (SD) or mean ± standard error of the mean (SEM).

Results

Measurement of Hippocampal interstitial fluid amino acid levels

Hippocampal ISF AA concentrations (C_0) were extrapolated from microdialysis measurements using a method of extrapolation to "zero flow" (Flow-rate method, Methods, eqn (1))[25]. To reach a unique solution for C_0, the mass transfer coefficient (K_0) for each mouse was determined using

retro-dialysis of a known concentration (100 µM) of the L-leucine analog, Norleucine (NLeu), (Suppl. Fig. 2, Suppl. Tables 1 and 2). *In vitro* experiments verified NLeu K_0 is comparable to K_0 for detected AAs (Suppl. Table 2). To test whether perfusion with aCSF depletes AA in the ISF, samples gathered at 1 µL/min on 3 – 4 sequential days were compared for eight mice from two experiments (Suppl. Fig. 3). Mean levels for 10 detected AAs did not decrease significantly over four days. (Suppl. Fig. 3A-E).

Using the flow-rate protocol brain ISF concentrations (C_0) of 14 standard and 2 non-standard AAs (measured by UPLC) were determined (Table 1). As previously reported, AAs were lower in CSF than in plasma (mean ≈ 11-fold lower)[4]. Although, as expected, Gln level in CSF was nearly as high as in plasma (Table 1). Additionally, AAs were significantly lower in ISF than CSF (mean ≈ 6-fold lower). For example, the branched neutral AA L-valine (Val) was 18 times lower in CSF than plasma and ISF level was a third of CSF concentration. Similarly, ISF Gln was a sixth of CSF value although in CSF it was 86% plasma level. Additionally, L-glutamate (Glu), like Gln was nearly as concentrated in CSF as in plasma (21 ± 4 vs. 37± 7 µM) while in ISF Glu was a sixth the CSF concentration (4.1 ± 0.3 µM). Gln was the most abundant AA in ISF (80 ± 16 µM) with the next most abundant AAs being L-lysine (10.2 ± 3.1 µM) and L-serine (9.8 ± 2.6 µM). Furthermore, taurine (Tau), the highest AA in plasma (735 ± 51 µM), was 9 times lower in CSF (79.5 ± 8.6 µM) and 16 times lower in ISF (4.9 ± 0.9 µM) than CSF (Table 1).

ISF responses to large transient elevations in plasma levels of L-valine vs. L-glutamine

We next tested how acute increases in the plasma concentrations of two LAT1 substrates, Val (Fig. 2A), and Gln (Fig. 2B) affected ISF levels. Mice were injected intraperitonealy (IP) with an amount of each of these AAs corresponding to ~200 times their amount in blood. Within 5 – 10 minutes after IP injection with Val plasma levels significantly increased to 674 ± 259% of the control value (Fig. 2A). Similarly following Gln IP injection, plasma Gln increased to 381± 42% (Fig. 2B). Levels of all other AAs remained stable (data not shown) and IP injection of vehicle alone (0.9% saline) had no effect on Val or Gln levels (Fig. 2A, B). Additionally, following Val IP injection, Val levels in microdialysis samples rose rapidly to 395 ± 175% of baseline (25' post-IP) (Fig. 2A). In contrast there was no significant increase of total Gln in microdialysates at any time after IP with Gln. Rather within one hour of Gln IP injection the non-significant trend was for decreasing ISF Gln levels (Fig. 2B).

To test Gln transendothelial transport from the blood into the brain, Gln labeled with two heavy nitrogens ($^{15}N_2$) (hGln) was used for IP injections. Figure 2B shows total Gln in plasma and

microdialysates measured by UPLC. Additionally, total and labeled Gln in microdialysate and plasma samples collected after hGln IP were analyzed by liquid chromatography mass spectrometry (LC-MS) (Suppl. Fig. 4). Figure 2C shows a time course for percent hGln vs total Gln (hGln/Gln) in plasma and microdialysis samples. After IP injection ~2/3 of total plasma Gln (64 ± 2% baseline) was labeled, while in microdialysates hGln increased to only 3.8 ± 0.9% of total Gln (25' post-IP) (Fig. 2C). Since following IP injection with hGln, 64% of the plasma Gln was labeled therefore, in total 1.6 Gln (labeled and unlabeled) must have been influxed to the brain from the plasma for every hGln recovered by microdialysis (1 / 0.64 = 1.6). This indicates post-IP injection approximately 6% of the Gln in the ISF originated from the plasma (0.04 hGln in ISF / 0.6 hGln in plasma = 0.06 total Gln in ISF was from plasma). In plasma hGln decreased ~10% in the first hour and after 3 hours ~30% of Gln was still labeled. hGln levels in the ISF were stable for one hour before being slowly cleared (Fig. 2C).

Competitive inhibition of system L vs system A transporters in the brain

To test the relative contributions of system A (SNAT1&2) vs. L (LAT1&2) transporters in regulating Gln in ISF, known competitive inhibitors for each transport system type were perfused into the brain through the microdialysis probe. The microdialysate concentrations were normalized to baseline and the time of collection corrected by the time required to reach the fraction collector. Figure 3A and B shows time courses before, during, and after perfusion with 20 mM of the system A (SNAT1/2) inhibitor, methylaminoisobutyric acid (MeAIB) for the system A substrates glycine (Gly) and Gln, and non-substrates, Val and Tau[12, 29]. After 50 minutes of MeAIB perfusion Gly increased 256 ± 90% while Val did not change significantly (105 ± 37%) (Fig. 3A). Whereas Gln levels exhibited unstable behavior, transiently peaking at 80 minutes (219 ± 75%), returning to near baseline at 110 minutes, and rising again at 140 minutes (147 ± 35%) (Fig. 3B). After 140 min of perfusion levels of the osmolyte, taurine (Tau) also doubled (182 ± 48%). Following inhibitor removal all AAs returned to near baseline after 120 minutes of aCSF perfusion.

Figure 3C shows the time course pre-, during, and post-perfusion with 20 mM of the system L inhibitor 2-aminobicyclo-(2,2,1)-heptane-2-carboxylic acid (BCH) for the system L substrates, Val and Gln, and non-substrates, Glu and Tau[30]. Within 50 minutes of BCH treatment levels for Val (515 ± 54%) and Gln (371 ± 27%) rose significantly vs. baseline (Fig. 3C). By 80 minutes of BCH Val plateaued at 579 ± 131% and Gln at 430 ± 134% of baseline (Fig. 3C, D). However, unlike during MeAIB perfusion where Glu did not increase (data not shown), after 170 minutes of BCH treatment Glu significantly increased to 217 ± 102% of baseline. Tau remained stable

throughout the BCH perfusion (Fig. 3C). Removal of BCH by flushing with aCSF fully reversed AAs to baseline within 3 hours (Fig. 3C).

Since the system N transporters (SLC38A3/SNAT3 and SLC38A5/SNAT5) are abundantly expressed in BBB endothelial cells and astrocytes (Fig. 1), a competitive system N inhibitor, glutamate-γ-monohydroxamate (GAH)[31], was tested. Perfusion of 50 mM GAH rapidly elevated Gln to ~300% of baseline levels (at 20'), however as GAH perfusion increased all AAs, a non-specific effect could not be ruled out (Suppl. Fig. 5 A, B). Additionally, both BCH and GAH perfusion increased GABA, which returned to baseline upon inhibitor removal. Since neither inhibitor acts on known GABA transporters (SLC6A1/GAT1 and SLC6A13/GAT3), the data indicate the possible involvement of system L and N transporters in GABA ISF homeostasis (Suppl. Table 3). Finally at no time did any of the competitive inhibitor perfusions produce observable behavioral abnormalities in mice.

Combined system L competitive inhibition and heavy labeled glutamine intraperitoneal injection

Next we tested if the elevated Gln observed during BCH treatment resulted from increased transendothelial transport (by LAT1) or was due to release from another brain cell type expressing system L (eg. astrocyte expressed LAT2). Therefore, BCH perfusion was repeated with hGln IP injection (Fig. 4A, B) and compared to BCH perfusion without IP injection (Fig. 3C, D). Fifty minutes after BCH perfusion of the brain (25' post-hGln IP injection) total Gln increased significantly to 727 ± 238% in animals with hGln IP injection vs. 371 ± 27% for mice treated with BCH alone (Fig. 4A, 3C). The increase in Val after 50 min BCH perfusion and hGln IP injection (25' post-hGln IP injection) was approximately half that with BCH alone (242 ± 161% vs 515 ± 54%, respectively) (Suppl. Fig. 6A). As measured by LC-MS 25' after hGln IP injection (i.e. 50' after of brain perfusion with BCH), 50 ± 19% of the total microdialysate Gln was $^{15}N_2$ labeled, indicating that 83% of the Gln in the ISF came from the plasma (0.53 ISF hGln / 0.64 hGln plasma). Therefore, 600% of the 730% increase in baseline Gln in the ISF came from the plasma (7.3 X 0.83) (Fig. 4B). In contrast, after 50 minutes of MeAIB perfusion + hGln IP injection (25' post-hGln IP injection) no hGln was detected in microdialysis samples and at 80 min MeAIB (55' post-hGln IP) hGln was 0.06 ± 0.007% of total Gln vs 2.5 ± 0.4% in mice receiving hGln IP alone (Suppl. Fig. 6B).

Discussion

Hippocampal interstitial fluid amino acids are significantly lower than in cisterna magna CSF indicating distinct regulation. Here we report results of a quantitative determination of brain ISF AA concentrations in awake, freely-moving mice. Brain concentrations were determined by extrapolation of hippocampal microdialysate concentrations to original ISF values at zero flow rate. Importantly the extrapolation to C_0 was constrained by determination of the mass transfer coefficient K_0 using the non-standard amino acid NLeu. This control was missing from previous studies. Consistent with previous reports steep concentration gradients from plasma to CSF for 16 AA (except Gln as previously reported) were observed. In addition we measured decreased AA concentrations in ISF vs. CSF (Table 1). For example, we measured 80 ±16 µM Gln in ISF. However, in comparison Kanamori and Ross reported 385 µM Gln in striatum of awake rats[5] and Lerma and coworkers measured 190 µM in hippocampus of anaesthetized rats[6]. Although there are many differences between the study protocols used by us and others eg. physiological state (awake vs. anesthetized, fed vs. food restricted), or brain region (striatum vs. hippocampus), or species (mouse vs. rat) tested; the most important factor contributing to the discrepancies may be limitations of the measurement methods.

In general ISF solutes have been measured by either sensor or sampling (either direct or by microdialysis) methods[26]. Sensor detection methods, unfortunately, are only applicable for a few analytes while sampling can be used to broadly screen multiple substances (such as AAs). Direct sampling either involves a "push-pull" method or a very low flow extraction[32, 33]. Microdialysis, while lacking the temporal sensitivity of sensor detection mitigates the tissue damage inflicted by the "push-pull" method of pumping fluid into to the brain to extract samples. Instead fluid is perfused through a semi-permeable microdialysis probe to extract brain solutes[26]. Due to technical limitations most microdialysis studies avoid reporting quantitative data instead normalizing results from experimental manipulations relative to baseline controls. However, two accepted methods for quantification "no-net-flux" and the "extrapolation to zero-flow" (or "Flow-rate") have been developed[26]. The "no-net-flux" method requires a series of perfusions with different concentrations of the substance of interest. The brain concentration is determined as the concentration of the target for which no net exchange occurs during perfusion into the brain. Disadvantages of this method for measuring AAs are each AA concentration must be determined individually, and infusing AAs into the brain may trigger alterations in both brain levels and relative recovery [26]. Our study and both referenced studies used the "Flow-rate" method. The "Flow-rate" method determines C_0 (brain concentration) based on the inverse relationship between flow rate and mass transfer and is applicable to multiple solutes

simultaneously (see Methods eqn (1)). The Flow-rate method algorithm extrapolates a set of microdialysis data to C_0, however, without constraining the mass transfer coefficient, K_0, C_0 does not resolve to a unique solution. Therefore, we, unlike the previously cited groups, used retro-dialysis of a non-natural L-leucine analog, NLeu, to determine K_0 *in vivo* allowing an unequivocal solution to C_0 for ISF AAs[26].

A second commonly raised issue with microdialysis studies is the creation of "an area around the probe in which all solutes capable of crossing the probe membrane are depleted"[26]. For most experiments a perfusate flow rate of 1 µL/min was used, which yielded a relative recovery of ≈ 10 – 20% for 1 mm probes. We examined the possible ISF depletion by comparing relative recovery over the first several days of microdialysis collection at 1 µL/min. Representative results show that mean levels of individual AAs (except proline and alanine) remained stable for all four days of microdialysis (Suppl. Fig. 3A). For most mice mean levels of the sum of the AAs also remained stable or were only modestly changed on day 2 with only one mouse showing an significant change ($p = 0.01$) whereas by day 3 almost half of the mice had somewhat elevated total AA levels ($p= 0.1$) relative to day one (Suppl. Fig. 3B). For Gln levels were generally stable with only one mouse showing a trend to increasing AA levels by the fourth day (Suppl. Fig. 3C). Val levels were somewhat more prone to be elevated on day 2 though none of the differences was staticially significant (Suppl. Fig. 3D). Tau has been suggested to be a marker for ISF osmolality and the generally stable levels suggest no major disturbances in ISF osmotic balance occurred over multiple days of microdialysis for most mice (Suppl. Fig 3E). The slight increases in AAs observed may be due to a trauma layer surrounding the probe causing gliosis (glial activation and proliferation) and/or ischemia (interrupted blood flow)[26]. In our study mice, whose levels were significantly lower or higher relative to mean (>2 SD) were excluded. Additionally, a 2011 study by Jaquin-Gerstl and coworkers found that although dexamethasone significantly reduced gliosis and ischemia, it had only minor effects on dopamine quantitation over several days of microdialysis in comparison to untreated control animals. These data suggest gliosis had a minimal impact on solute recovery during microdialysis[34]. Furthermore, Kennedy and colleagues reported ISF levels for some AAs using a refinement of the direct sampling method. They used 90 µm probes with 1-10 nl/min extraction rates to avoid the need to perfuse fluid into the brain for extraction of samples ("push-pull"). They found somewhat lower values than reported here for striatal ISF from anesthetized rats for Glu (1.8 µM) and Gly (5 µM)[33] vs. 4 and 8 µM, respectively, measured in the current study (Table 1) [33 34 35 35 34 35]. Moreover recently, a low flow "push-pull" study by Slaney and co-authors reported ISF levels of 8.5 µM Glu and 7.2 µM Gly in the midbrain (ventral tegmental area (VTA)) of awake, freely-moving rats[32].

Therefore, our findings of low ISF AA levels are supported by both our carefully controlled study protocol (including the *in vivo* determination of K_0) and the consistent literature reports from direct sampling data available for several AAs.

L-glutamine but not L-valine ISF levels are strongly buffered against large acute plasma increases. Intraperitoneal injection of Val with an amount corresponding to ≈200 times the quantity present in plasma causes a rapid and significant increase in plasma (≈600%) and ISF Val (≈400%) (Fig. 2A). This is consistent with published data in which Val IP injection increased levels ≈4 – 5 fold in brain tissue and ISF, and 8.5 fold in CSF[35] and is expected to be mediated by Lat1, which transports Val with high affinity (Km ~50 μM)[36]. In contrast, hGln IP injection significantly raised Gln levels in plasma (~tripled), but not ISF, and resulted in only ≈4% enrichment of hGln in ISF (Fig. 2BC). Similarly, Bagga and coworkers recently reported that 3 minutes of [U-^{13}C5]-Gln infusion did not increase total cortical Gln and Gln-C4 ^{13}C enrichment was ≈2%[37]. In our experiments the increase of Gln transport was low and transient, which may be in part due to the low affinity of the blood-brain barrier expressed Gln transporters, Lat1 and Snat3 that have Km values on the order of the plasma Gln concentration post-IP injection (1 – 2.3 mM). Additonally Gln transported from plasma may be sequestered in the endothelium and only slowly released abluminally, and/or transported into ISF and subsequently sequestered in the brain by another cell type e.g. astrocytes.

LAT1 transporter regulates ISF influx of plasma Gln. The potential contributions of system A and L transporters in ISF regulation were addressed using brain perfusion with MeAIB or BCH, respectively. Following MeAIB perfusion total ISF Gln is only transiently significantly elevated and then rebounds to near baseline (Fig. 3B). However the system A substrate, Gly, is sustainably increased in ISF (Fig. 3A). Both SNAT1 and SNAT2 transport MeAIB, Gln, and Gly with similar affinities (MeAIB K_m of SNAT1, 1.1 mM, and SNAT2, 0.5 mM; Gln K_m of SNAT1, 0.3 mM, and SNAT2, 1.7 mM; Gly K_m of both SNAT1&2 ~0.5 mM)[12, 38]. Roughly at equilibrium, extraction of MeAIB from the 20 mM perfusate corresponds to 2 – 4 mM, which represents a large excess relative to its K_m (for SNAT1 and SNAT2) and the concentrations of Gln (80 μM) and Gly (8 μM) in the ISF. Therefore, it is consistent with a greater relative competition of Gly than Gln transport. However this does not account for the "ping-ponging" of Gln ISF levels during MeAIB perfusion (Fig. 3B). Gln rebounding to baseline may be due to an unknown compensatory mechanism to restore ISF Gln (but not Gly) homeostasis. Figure 1 shows that Gln is transported by a number of highly expressed AATs in the neurovascular unit including LAT1, SNAT1&2, and SNAT3&5, of which LAT1 and SNAT3 selectively transport Gln and not Gly [12, 31, 39]. Finally, IP injection of Gln in combination with BCH results in a

significant increase of total ISF Gln from no net increase in the absence of BCH, to ~400% for treatment with BCH alone, to over ~700% baseline levels for IP injection in combination with BCH treatment (Fig. 4A). Further, BCH in the presence of increased circulating peripheral hGln dramatically stimulates net Gln transendothelial transport from the plasma to the ISF approximately 100-fold, ie. total Gln influx increased from ≈6% (IP injection without BCH perfusion) to ≈600% (IP injection with BCH perfusion) (Fig. 4B). Since, SNAT3 does not bind BCH, the data indicate LAT1 can mediate large changes in Gln influx from the plasma. This strong effect of BCH may be accomplished by driving the transendothelial transport of Gln from the blood into the ISF via transstimulation of LAT1 exchanger expressed in endothelial cell membranes. Indeed, he high BCH concentration in ISF could transstimulate Gln transport from the endothelial cells into the ISF. And BCH thereby accumulating in the endothelial cells would in turn transstimulate the uptake of Gln from the blood into endothelial cells. This hypothesis is consistent with a key role for the endothelial BBB expressed LAT1 in regulating Gln ISF homeostasis.

Disclosures/Conflict of Interest.

The authors have no conflict of interest.

Acknowledgements

The authors would like to thank and acknowledge the contributions of the Functional Genomics Center Zurich, in general, and Dr. Peter Hunziker specifically for invaluable technical support for the UPLC amino acid analysis. This work has been supported by the SNF grant 31-130471/1 and a grant from Ajinomoto (2010-2012).

Supplementary information is available at the Journal of Cerebral Blood Flow & Metabolism website – www.nature.com/jcbfm

References

1. Abbott NJ, Ronnback L, Hansson E. Astrocyte-endothelial interactions at the blood-brain barrier. *Nat Rev Neurosci* 2006; 7(1)**:** 41-53.

2. Ruderisch N, Virgintino D, Makrides V, Verrey F. Differential axial localization along the mouse brain vascular tree of luminal sodium-dependent glutamine transporters Snat1 and Snat3. *Journal of cerebral blood flow and metabolism : official journal of the International Society of Cerebral Blood Flow and Metabolism* 2011; 31(7)**:** 1637-47.

3. Sanchez del Pino MM, Peterson DR, Hawkins RA. Neutral amino acid transport characterization of isolated luminal and abluminal membranes of the blood-brain barrier. *The Journal of biological chemistry* 1995; 270(25)**:** 14913-8.

4. McGale EHF, Pye IF, Stonier C, Hutchinson EC, Aber GM. STUDIES OF THE INTER-RELATIONSHIP BETWEEN CEREBROSPINAL FLUID AND PLASMA AMINO ACID CONCENTRATIONS IN NORMAL INDIVIDUALS. *Journal of neurochemistry* 1977; 29(2)**:** 291-297.

5. Kanamori K, Ross BD. Quantitative determination of extracellular glutamine concentration in rat brain, and its elevation in vivo by system A transport inhibitor, alpha-(methylamino)isobutyrate. *Journal of neurochemistry* 2004; 90(1)**:** 203-10.

6. Lerma J, Herranz AS, Herreras O, Abraira V, del Rio RM. In vivo determination of extracellular concentration of amino acids in the rat hippocampus. A method based on brain dialysis and computerized analysis. *Brain research* 1986; 384(1)**:** 145-155.

7. Bak LK, Schousboe A, Waagepetersen HS. The glutamate/GABA-glutamine cycle: aspects of transport, neurotransmitter homeostasis and ammonia transfer. *Journal of neurochemistry* 2006; 98(3)**:** 641-53.

8. Bacci A, Sancini G, Verderio C, Armano S, Pravettoni E, Fesce R *et al.* Block of glutamate-glutamine cycle between astrocytes and neurons inhibits epileptiform activity in hippocampus. *Journal of neurophysiology* 2002; 88(5)**:** 2302-10.

9. Behrens PF, Franz P, Woodman B, Lindenberg KS, Landwehrmeyer GB. Impaired glutamate transport and glutamate-glutamine cycling: downstream effects of the Huntington mutation. *Brain : a journal of neurology* 2002; 125(Pt 8)**:** 1908-22.

10. Berthet C, Lei H, Gruetter R, Hirt L. Early predictive biomarkers for lesion after transient cerebral ischemia. *Stroke; a journal of cerebral circulation* 2011; 42(3)**:** 799-805.

11. Brusilow SW, Koehler RC, Traystman RJ, Cooper AJ. Astrocyte glutamine synthetase: importance in hyperammonemic syndromes and potential target for therapy. *Neurotherapeutics : the journal of the American Society for Experimental NeuroTherapeutics* 2010; 7(4)**:** 452-70.

12. Mackenzie B, Schafer MK, Erickson JD, Hediger MA, Weihe E, Varoqui H. Functional properties and cellular distribution of the system A glutamine transporter SNAT1 support

specialized roles in central neurons. *The Journal of biological chemistry* 2003; 278(26)**:** 23720-30.

13. Gonzalez-Gonzalez IM, Cubelos B, Gimenez C, Zafra F. Immunohistochemical localization of the amino acid transporter SNAT2 in the rat brain. *Neuroscience* 2005; 130(1)**:** 61-73.

14. Braun D, Kinne A, Brauer AU, Sapin R, Klein MO, Kohrle J *et al.* Developmental and cell type-specific expression of thyroid hormone transporters in the mouse brain and in primary brain cells. *Glia* 2011; 59(3)**:** 463-71.

15. Hagglund MG, Roshanbin S, Lofqvist E, Hellsten SV, Nilsson VC, Todkar A *et al.* B(0)AT2 (SLC6A15) is localized to neurons and astrocytes, and is involved in mediating the effect of leucine in the brain. *PloS one* 2013; 8(3)**:** e58651.

16. Hagglund MG, Sreedharan S, Nilsson VC, Shaik JH, Almkvist IM, Backlin S *et al.* Identification of SLC38A7 (SNAT7) protein as a glutamine transporter expressed in neurons. *The Journal of biological chemistry* 2011; 286(23)**:** 20500-11.

17. Bae SY, Xu Q, Hutchinson D, Colton CA. Y+ and y+ L arginine transporters in neuronal cells expressing tyrosine hydroxylase. *Biochimica et biophysica acta* 2005; 1745(1)**:** 65-73.

18. Deitmer JW, Bröer A, Bröer S. Glutamine efflux from astrocytes is mediated by multiple pathways. *Journal of neurochemistry* 2003; 87(1)**:** 127-135.

19. Boulland JL, Rafiki A, Levy LM, Storm-Mathisen J, Chaudhry FA. Highly differential expression of SN1, a bidirectional glutamine transporter, in astroglia and endothelium in the developing rat brain. *Glia* 2003; 41(3)**:** 260-75.

20. Cubelos B, Gonzalez-Gonzalez IM, Gimenez C, Zafra F. Amino acid transporter SNAT5 localizes to glial cells in the rat brain. *Glia* 2005; 49(2)**:** 230-44.

21. Tanaka K, Yamamoto A, Fujita T. Functional expression and adaptive regulation of Na+ -dependent neutral amino acid transporter SNAT2/ATA2 in normal human astrocytes under amino acid starved condition. *Neuroscience letters* 2005; 378(2)**:** 70-5.

22. Gliddon CM, Shao Z, LeMaistre JL, Anderson CM. Cellular distribution of the neutral amino acid transporter subtype ASCT2 in mouse brain. *Journal of neurochemistry* 2009; 108(2)**:** 372-83.

23. Lyck R, Ruderisch N, Moll AG, Steiner O, Cohen CD, Engelhardt B *et al.* Culture-induced changes in blood-brain barrier transcriptome: implications for amino-acid transporters in vivo. *Journal of cerebral blood flow and metabolism : official journal of the International Society of Cerebral Blood Flow and Metabolism* 2009; 29(9)**:** 1491-502.

24. Paxinos G. The mouse brain in stereotaxic coordinates. In: Franklin KBJ, Franklin KBJ, (eds). 2nd ed. ed. San Diego :: Academic Press, 2001.

25. Jacobson I, Sandberg M, Hamberger A. Mass transfer in brain dialysis devices--a new method for the estimation of extracellular amino acids concentration. *Journal of neuroscience methods* 1985; 15(3)**:** 263-8.

26. Chefer VI, Thompson AC, Zapata A, Shippenberg TS. Overview of brain microdialysis. *Current protocols in neuroscience / editorial board, Jacqueline N. Crawley ... [et al.]* 2009; Chapter 7**:** Unit7 1.

27. Liu L, Duff K. A technique for serial collection of cerebrospinal fluid from the cisterna magna in mouse. *Journal of visualized experiments : JoVE* 2008; (21).

28. Berglund M, Wieser Michael E. Isotopic compositions of the elements 2009 (IUPAC Technical Report). In: *Pure and Applied Chemistry*, 2011. p 397.

29. Christensen HN, Oxender DL, Liang M, Vatz KA. The use of N-methylation to direct route of mediated transport of amino acids. *The Journal of biological chemistry* 1965; 240(9)**:** 3609-16.

30. Christensen HN, Handlogten ME, Lam I, Tager HS, Zand R. A bicyclic amino acid to improve discriminations among transport systems. *The Journal of biological chemistry* 1969; 244(6)**:** 1510-20.

31. Baird FE, Beattie KJ, Hyde AR, Ganapathy V, Rennie MJ, Taylor PM. Bidirectional substrate fluxes through the system N (SNAT5) glutamine transporter may determine net glutamine flux in rat liver. *The Journal of physiology* 2004; 559(Pt 2)**:** 367-81.

32. Slaney TR, Mabrouk OS, Porter-Stransky KA, Aragona BJ, Kennedy RT. Chemical gradients within brain extracellular space measured using low flow push-pull perfusion sampling in vivo. *ACS chemical neuroscience* 2013; 4(2)**:** 321-9.

33. Kennedy RT, Thompson JE, Vickroy TW. In vivo monitoring of amino acids by direct sampling of brain extracellular fluid at ultralow flow rates and capillary electrophoresis. *Journal of neuroscience methods* 2002; 114(1)**:** 39-49.

34. Jaquins-Gerstl A, Shu Z, Zhang J, Liu Y, Weber SG, Michael AC. Effect of dexamethasone on gliosis, ischemia, and dopamine extraction during microdialysis sampling in brain tissue. *Analytical chemistry* 2011; 83(20)**:** 7662-7.

35. Bongiovanni R, Kirkbride B, Newbould E, Durkalski V, Jaskiw GE. Relationships between large neutral amino acid levels in plasma, cerebrospinal fluid, brain microdialysate and brain tissue in the rat. *Brain research* 2010; 1334**:** 45-57.

36. Yanagida O, Kanai Y, Chairoungdua A, Kim DK, Segawa H, Nii T *et al.* Human L-type amino acid transporter 1 (LAT1): characterization of function and expression in tumor cell lines. *Biochimica et biophysica acta* 2001; 1514(2)**:** 291-302.

37. Bagga P, Behar KL, Mason GF, De Feyter HM, Rothman DL, Patel AB. Characterization of cerebral glutamine uptake from blood in the mouse brain: implications for metabolic modeling of 13C NMR data. *Journal of cerebral blood flow and metabolism : official*

journal of the International Society of Cerebral Blood Flow and Metabolism 2014; 34(10)**:** 1666-72.

38. Yao D, Mackenzie B, Ming H, Varoqui H, Zhu H, Hediger MA *et al.* A novel system A isoform mediating Na+/neutral amino acid cotransport. *The Journal of biological chemistry* 2000; 275(30)**:** 22790-7.

39. Rossier G, Meier C, Bauch C, Summa V, Sordat B, Verrey F *et al.* LAT2, a new basolateral 4F2hc/CD98-associated amino acid transporter of kidney and intestine. *The Journal of biological chemistry* 1999; 274(49)**:** 34948-54.

40. Hawkins RA, O'Kane RL, Simpson IA, Vina JR. Structure of the blood-brain barrier and its role in the transport of amino acids. *The Journal of nutrition* 2006; 136(1 Suppl)**:** 218s-26s.

Titles and legends to figures

Figure 1. Diagram of glutamine transporters expressed in neurovascular unit cells. The abbreviations used for the transporters are: ASCT2 (SLC1A5), B^0AT2 (SLC6A14), LAT1 (SLC7A5), y^+LAT2 (SLC7A6), y^+LAT2 (SLC7A7), LAT2 (SLC7A8), SNAT1 (SCL38A1), SNAT2 (SLC38A2), SNAT3 (SCL38A3), SNAT5 (SLC38A5). Expression levels are indicated by box borders with thick borders = high, thin solid borders = moderate, and thin dotted borders = low expression. BCH-sensitive system L transporters are represented by grey boxes and the system A transporters sensitive to MeAIB by dotted boxes. The data are based on *in vivo* and *in vitro* studies [2, 3, 12-23, 40].

Figure 2. Plasma and brain interstitial fluid amino acid responses to intraperitoneal injection of L-valine or L-glutamine.

The amount of each amino acid (AA) injected intraperitoneal (IP) in mg/kg body weight corresponds to ≈200 times total measured amount in plasma (concentration ^{x} blood volume). **A.** Impact of L-valine (Val) IP injection (240 mg/kg Val or 0.9% NaCl vehicle (veh)) on plasma and interstitial fluid (ISF) Val concentration (mean ± SD from 4 animals). **B.** Impact of heavy labeled L-glutamine (hGln) IP injection (1.37 g/kg of $^{15}N_2$ labeled Gln (hGln) vs. 0.9% NaCl vehicle (veh)) on plasma and ISF hGln concentration (mean ± SD from 4 animals). **C.** Ratio of hGln to total Gln (hGln/Gln) in plasma and ISF, as measured by liquid chromatography mass spectrometry (LC-MS). Data are presented as mean ± SEM for microdialysates from 3 independent experiments (n=10 total mice) and mean ± SD for plasma from 1 experiment (n=4). For all experiments, baseline samples are indicated by solid lines and arrows indicate the time of AA IP injection. Statistical analysis was performed by two-way Anova with Dunnets post-test and statisticaly significant changes relative to baseline are indicated as: #### = $p<0.0001$ and ## = $p<0.01$; ∗∗∗∗ = $p< 0.0001$ and ∗∗ = $p<0.01$.

Figure 3. Impact of brain perfusion of system A and L competitive inhibitors on amino acids in brain microdialysates. Competitive inhibitors (20 mM) were introduced in the brain by perfusion via the microdialysis probe (as indicated by the grey area) for 3 hours. For each panel the indicated amino acid responses in ISF are plotted normalized to baseline values vs time in brain (adjusted for the time samples take to reach fraction collector). In panel **A,** Glycine (Gly), L-valine (Val) and in panel **B,** L-glutamine (Gln), taurine (Tau) responses as a result of 20 mM methylaminoisobutyric acid (MeAIB) brain perfusion. Data are mean ± SD from 3 animals. **C.** Val, Gln, L-glutamate (Glu) and Tau concentrations as a result of brain perfusion of 20 mM 2-aminobicyclo-(2,2,1)-heptane-2-carboxylic acid (BCH). Data are means ± SD from 4 animals. **D.**

Gln levels in ISF normalized to the mean baseline values prior to MeAIB or BCH perfusion, respectively, and compared to Gln levels at 50 and 80 minutes of perfusion with the indicated inhibitor. For all panels, baseline samples are indicated by the solid line. Perfusate equilibration without sample collection is indicated by the break in the X axis (time in brain). Inhibitor presence in perfusate is indicated by the shaded area of the graph and underlined X axis region. Statistical comparisons were performed by two-way Anova with Dunnets post-test for the comparision of values obtained with inhibitor versus baseline (**A, B, C**) and with Bonferroni post-test for the comparison of values obtained with different inhibitors and with baseline (**D**). Tracked amino acids are indicated in the individual panel keys. Statistical significance for all panels are: ∗∗∗∗ = p< 0.0001, ∗∗∗ = p<0.001, ∗∗ = p<0.01, and ∗ = p<0.1; #### = p< 0.0001, ## = p<0.01 and # = p<0.1; $$$$ = p< 0.0001 and $ = p<0.1.

Figure 4. Interstitial fluid total and labeled L-glutamine concentrations following brain perfusion with BCH without or with labeled hGln intraperitoneal injection.

A. ISF Gln levels are plotted relative to baseline for samples collected before, during, and after 20 mM (2-aminobicyclo-(2,2,1)-heptane-2-carboxylic acid (BCH) brain perfusion alone (data from Fig. 3B) or in combination with hGln intraperitoneal (IP) injection. Data are mean percent relative to baseline ± SD from 4 animals (BCH + IP). See panel for key. Vertical arrow indicates the time of hGln IP injection. Data were compared by two-way Anova with Sidak post-test. Statistical significance indicated as ∗∗∗ = p<0.001 for comparison of treatments with each other. **B.** Labeled Gln (hGln) as percent (%) of total Gln (hGln/Gln) in microdialysate samples. Samples were collected 25 minutes post hGln IP injection in the absence (data from Fig. 3C) or in the presence of BCH perfusion (at 50' of BCH perfusion, corresponding to 25' post-IP injection of hGln) (panel A). Data were compared with unpaired t-test and statistical significance indicated as ∗∗∗∗ = p<0.0001.

Figure 1

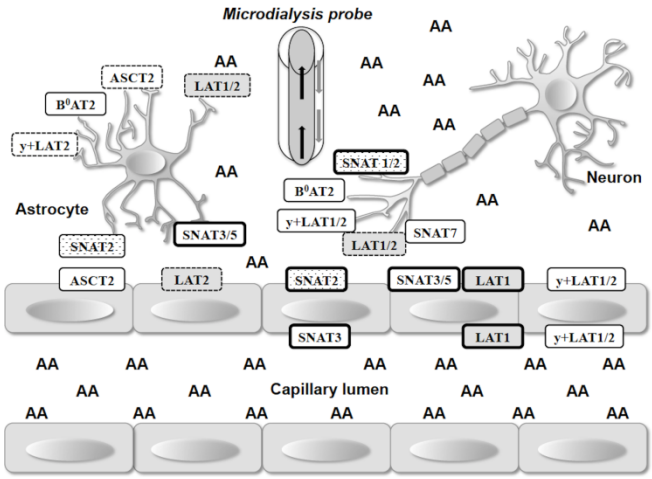
Microdialysis probe
AA
ASCT2
LAT1/2
B⁰AT2
y+LAT2
Astrocyte
SNAT3/5
SNAT2
ASCT2
LAT2
SNAT2
SNAT3
SNAT 1/2
B⁰AT2
y+LAT1/2
LAT1/2
SNAT7
SNAT3/5
LAT1
y+LAT1/2
LAT1
y+LAT1/2
Neuron
Capillary lumen

Table 1. Mouse brain interstitial fluid, cerebrospinal fluid, and plasma amino acid concentrations and ratios.

	[1]Concentration (µM ± SEM)			Ratio	
Amino acid	**[2]ISF**	**[3]CSF**	**Plasma**	**ISF/plasma**	**CSF/plasma**
		Nitrogen rich			
Glutamine (Gln)	80 ±16[3]	517 ± 20	598 ± 29	0.13	0.86
Asparagine (Asn)	1.4 ± 0.4	8.2 ± 2.4	68 ± 17	0.02	0.12
		Straight chain			
Alanine (Ala)	9.3 ± 1.4	57 ± 0.7	408 ± 24	0.02	0.14
Serine (Ser)	9.8 ± 2.6	37 ± 2.3	109 ± 6.5	0.09	0.34
Glycine (Gly)	7.8 ± 1.2	34 ± 7.9	246 ± 11	0.03	0.14
Proline (Pro)	1.8 ± 0.2	4.2 ± 0.7	60 ± 1.7	0.03	0.07
Threonine (Thr)	3.5 ± 1.0	22 ± 2.3	113 ± 6.4	0.03	0.19
		Branched chain			
Valine (Val)	2.9 ± 0.7	9.4 ± 1.0	173 ± 11	0.02	0.05
Leucine (Leu)	1.5±0.1	6.6 ± 0.2	127 ± 11	0.01	0.05
		Aromatic			
Tyrosine (Tyr)	0.7 ± 0.1	7.2 ± 1.2	54 ± 6.1	0.01	0.13
		Basic			
Histidine[*] (His)	1.2 ± 0.2	8.9 ± 0.7	59 ± 3.6	0.02	0.15
Lysine (Lys)	10 ± 3.1	46 ± 0.9	321 ± 35	0.03	0.14
Arginine (Arg)	3.2 ± 0.7	18 ± 2.3	103 ± 9.5	0.03	0.17
		Acidic			
Glutamate (Glu)	4.1±0.3	21.3±4.0	37.3±6.7	0.11	0.49
		Non-proteinogenic			
Taurine (Tau)	4.9 ± 0.9	80 ± 8.6	735 ± 51	0.01	0.11
Ornithine (Orn)	0.9 ± 0.2	3.4 ± 0.5	53 ± 8.1	0.02	0.06

[1]Values are given as mean micromolar (µM) concentration ± standard error (SEM.) of n mice from x independent experiments: Plasma, n=40, x=5; CSF, n=17, x=3; ISF, n=12, x=4; [2]CSF, cerebrospinal fluid; [3]ISF, interstitial fluid;

Figure 2

A

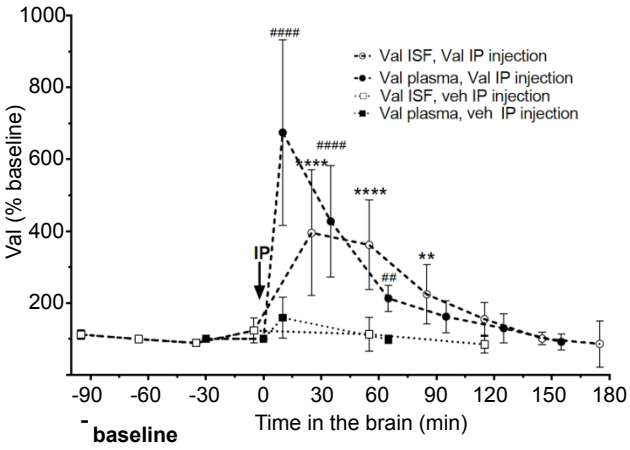
Val (% baseline)
Time in the brain (min)
Val ISF, Val IP injection
Val plasma, Val IP injection
Val ISF, veh IP injection
Val plasma, veh IP injection
IP
baseline

B

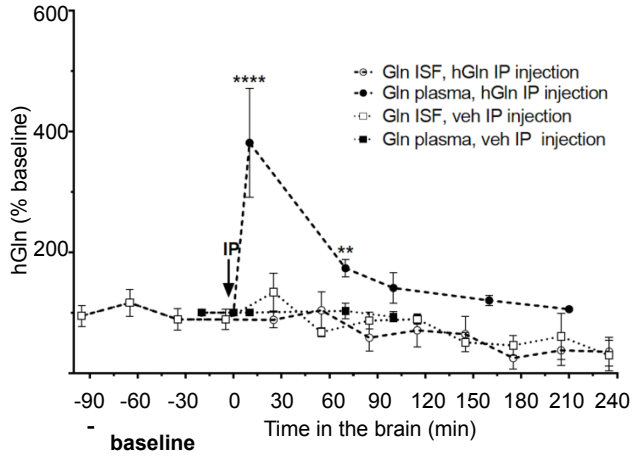
hGln (% baseline)
Time in the brain (min)
Gln ISF, hGln IP injection
Gln plasma, hGln IP injection
Gln ISF, veh IP injection
Gln plasma, veh IP injection
IP
baseline

C

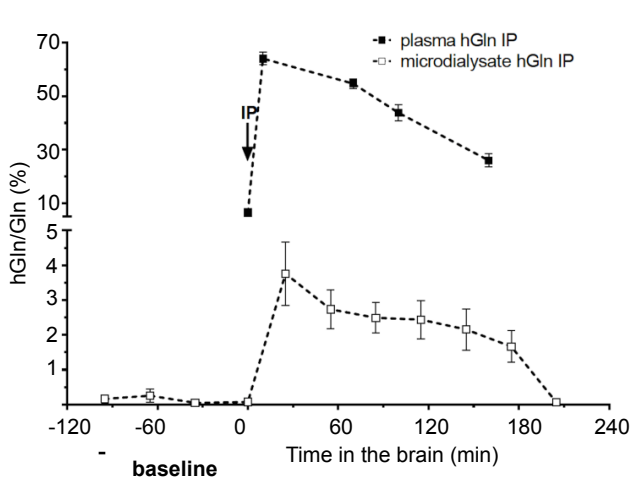
hGln/Gln (%)
Time in the brain (min)
plasma hGln IP
microdialysate hGln IP
IP
baseline

Figure 3

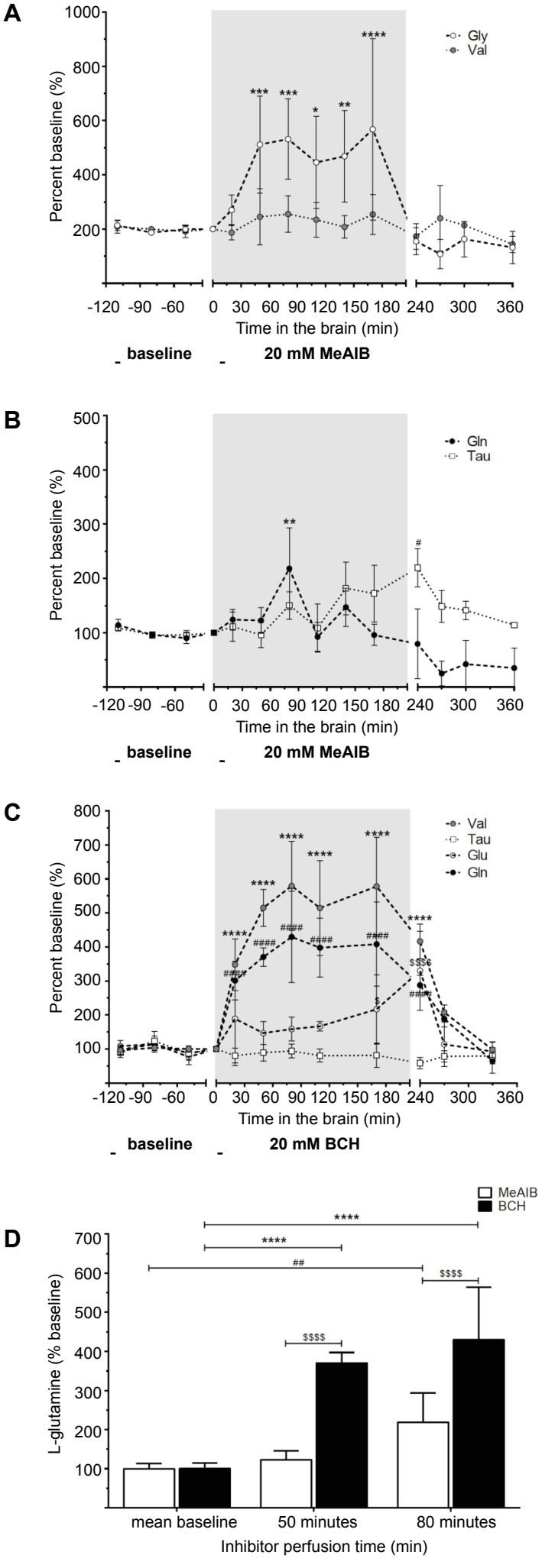
A
Percent baseline (%)
Gly
Val
Time in the brain (min)
baseline
20 mM MeAIB
B
Percent baseline (%)
Gln
Tau
Time in the brain (min)
baseline
20 mM MeAIB
C
Percent baseline (%)
Val
Tau
Glu
Gln
Time in the brain (min)
baseline
20 mM BCH
D
MeAIB
BCH
L-glutamine (% baseline)
mean baseline
50 minutes
80 minutes
Inhibitor perfusion time (min)

Figure 4

A

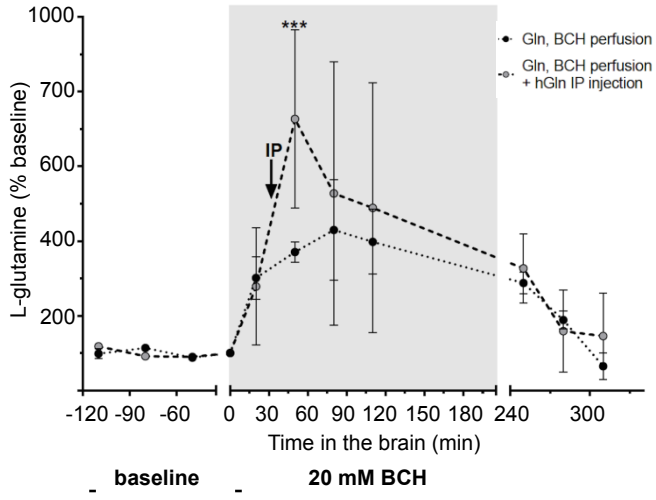
1000
700
600
400
200
L-glutamine (% baseline)
***
IP
Gln, BCH perfusion
Gln, BCH perfusion
+ hGln IP injection
-120 -90 -60 0 30 60 90 120 150 180 240 300
Time in the brain (min)
baseline
20 mM BCH

B

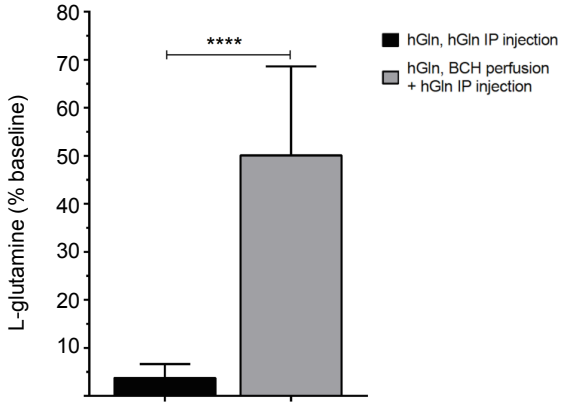
80
70
60
50
40
30
20
10
L-glutamine (% baseline)
****
hGln, hGln IP injection
hGln, BCH perfusion
+ hGln IP injection

5. Manuscript

A

B

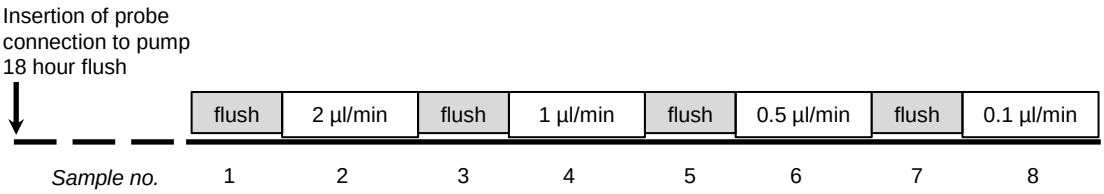

C

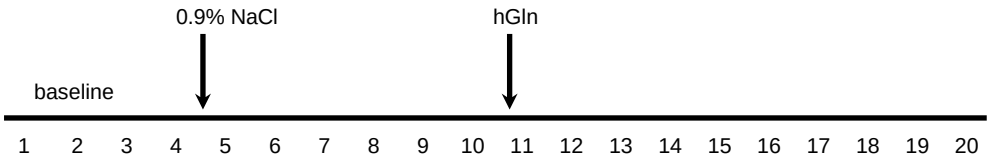

D

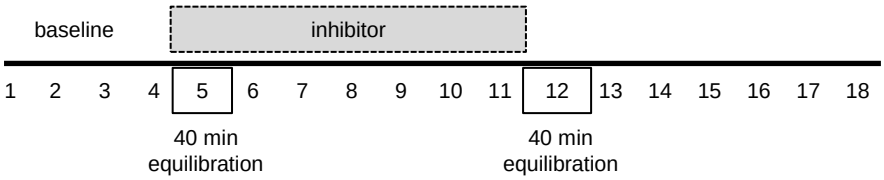

E

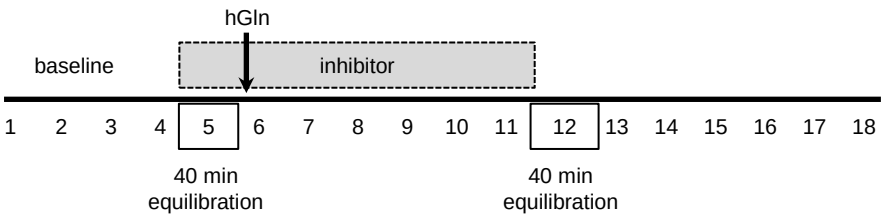

Supplementary Figure 1. In vivo microdialysis experimental protocols. A. Diagram of the *in vivo* microdialysis tubing set-up. Starting from the syringe pump containing the perfusion buffer there are three pieces of FEP tubing (numbered 1-3) with corresponding lengths of 30, 70 and 100 cm. I indicates the microdialysis probe inlet FEP tubing (10 cm length), O is the probe FEP outlet (15 cm length), V is the valve, FC is the fraction collector. The respective volumes are: 1) the FEP tubing volume 1.2 µl/10 cm, 2) the probe inlet and outlets are each 3.6 µl, 3) the probe shaft is 1 µl, and 4) the probe membrane is 0.045 µl. The volumes were used to calculate the "time in brain" or the time each sample reaching the fraction collector was in the brain. For each experiment the sample mid-point of the "time in brain" was graphed. **B-E** show the microdialysis schedules used for: **B)** flow-rate, **C)** intraperitoneal (IP) AA injection (Val or hGln), **D)** brain perfusion with competitive inhibitors (BCH or MeAIB), and **E)** combined perfusion with competitive inhibitors (BCH or MeAIB) and hGln IP injection experiments. For each scheme the sample number is indicated. For the flow-rate studies (B) the flush (grey box) indicates the equilibration period at the subsequent perfusion flow rate. For the inhibitor perfusions there was a 40 minute equilibration prior to- and following perfusion with inhibitor to allow the first sample either with or without inhibitor (respectively) to reach the fraction collector. For all experiments 30 µl samples were collected. For C-E the sample perfusion rate was 1 µl/min and the collection time was 30 min per sample.

A

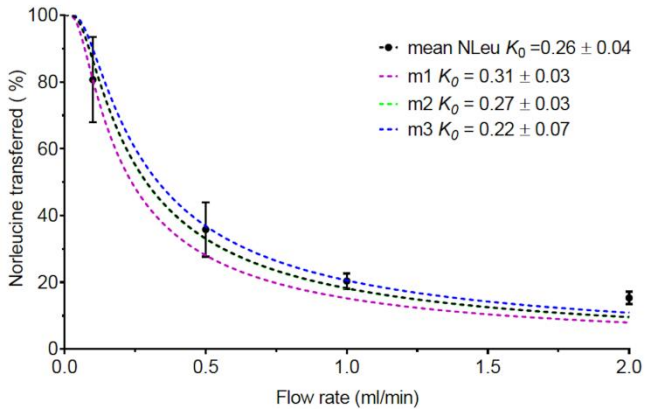

B

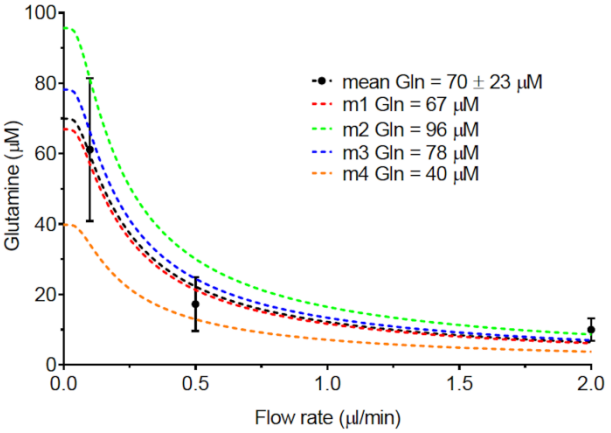

C

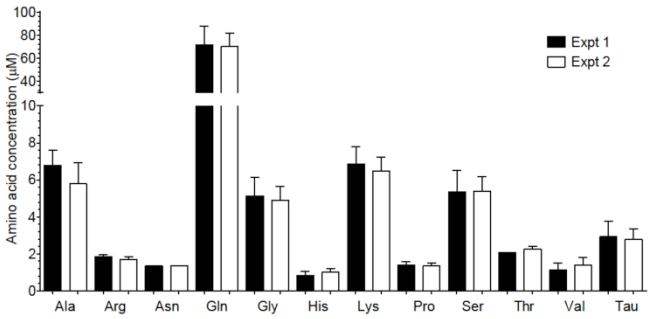

Supplementary Figure 2. Calculation of brain interstitial fluid amino acid concentrations by extrapolation to zero flow (Flow-rate) method. To calculate the brain interstitial fluid amino acid concentrations the mass transfer coefficients (K_0) for individual mice were experimentally determined. The *in vivo* K_0 were determined using retrodialysis of 100 µM (C_{PER}) of the non-standard amino acid Norleucine (NLeu) at 0.1, 0.5, 1, and 2 µl/min. Percent Nleu transferred (C_L) from microdialysate samples was quantified and values fit with the equation $C_L=C_{PER}-[C_{PER}\exp(-K_0A/F)]$, where A is probe area, and F is flow rate. **A.** shows representative flow rate results for individual mice from a single experimental determination of NLeu K_0 for three mice. Both the mean (± SD) for the loss of NLeu and the extrapolation curves for individual mice are shown as indicated. **B.** shows a representative experimental Gln concentration determination for four mice based on eqn 1 with constraint to experimentally determined NLeu K_0 values for each mouse. Both the mean (± SD) Gln microdialysate concentrations and the extrapolations for the individual mice are shown. **C.** shows a comparison of AA mean µM ± SD concentrations determined from two independent experiments using individually measured *in vivo* K_0 values, n = 3 – 8 (depending on AA) animals.

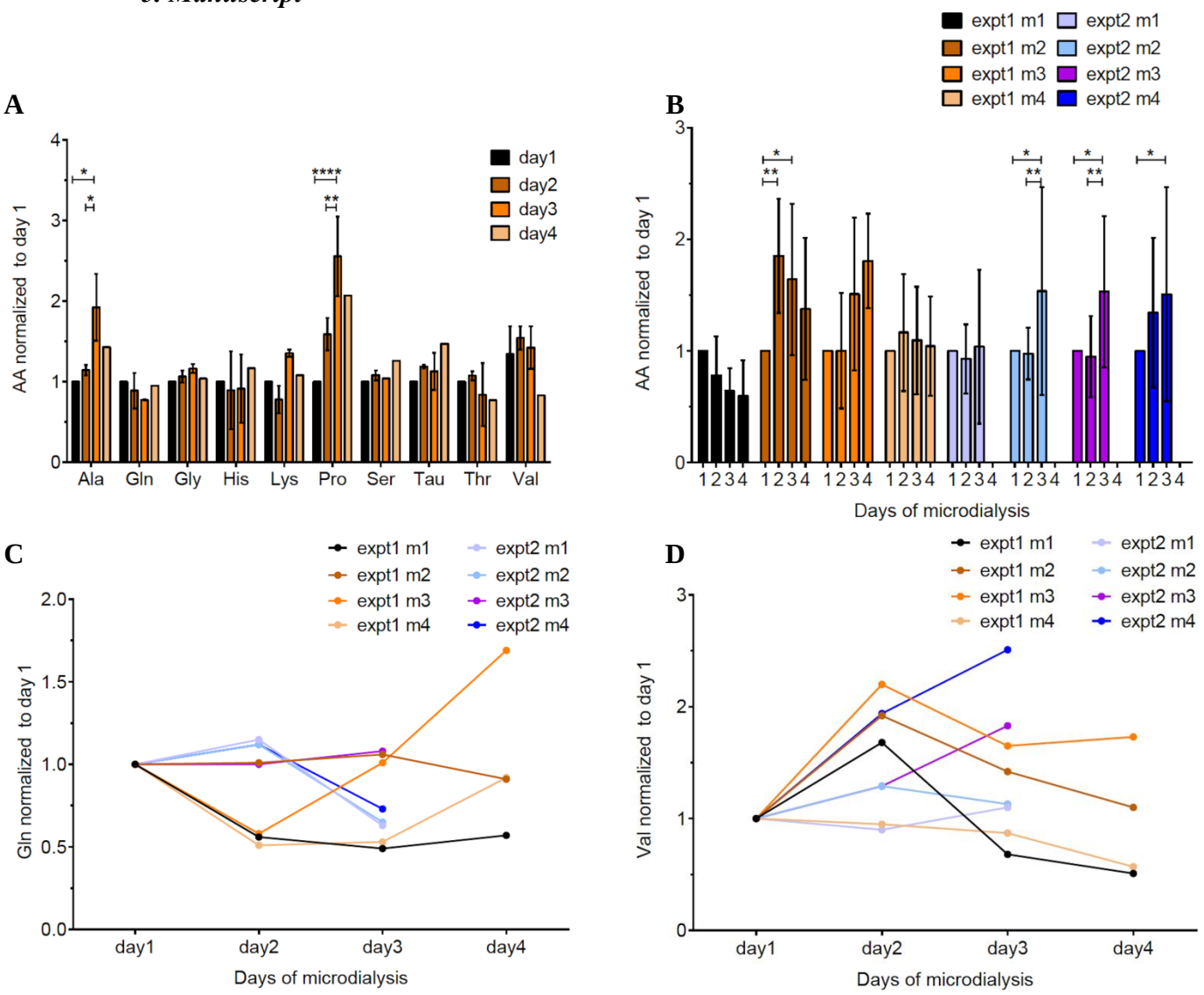

Supplementary Figure 3. Comparison of amino acid levels in microdialysis samples. Amino acid levels in 1 µl/min samples collected from eight mice during three or four (depending on the experiment) consecutive days were normalized to day 1 levels for comparison. **A**. Levels of each AA on days 2-4 were normalized to day 1 and presented are means ± SEM for 8 mice from two independent experiments. **B**. Concentration of each measured AA was normalized to the corresponding level on the day 1 individually, these values were summed up for each mouse on each day and plotted on the graph. Data presented as mean (± SD), when several 1 ul/min fractions were collected on the same day. Panels **C, D, E** show the normalized (to day 1) levels of Gln **(C),** Val **(D)** and Tau **(E)** in microdialysis samples for eight mice. n=4 for each of two independent experiments. Levels of individual AAs normalized to day 1 on 3-4 consecutive days of mD experiment were compared between each other (A) as well as the total AAs concentration normalized to day 1 for each mouse was compared within days 2-4 of mD (B). Statistical analysis was performed using two-way Anova with Tukeys post-test (A, B). Statistical significance are **** = $p<0.0001$, **= $p<0.01$, * = $p<0.1$.

A

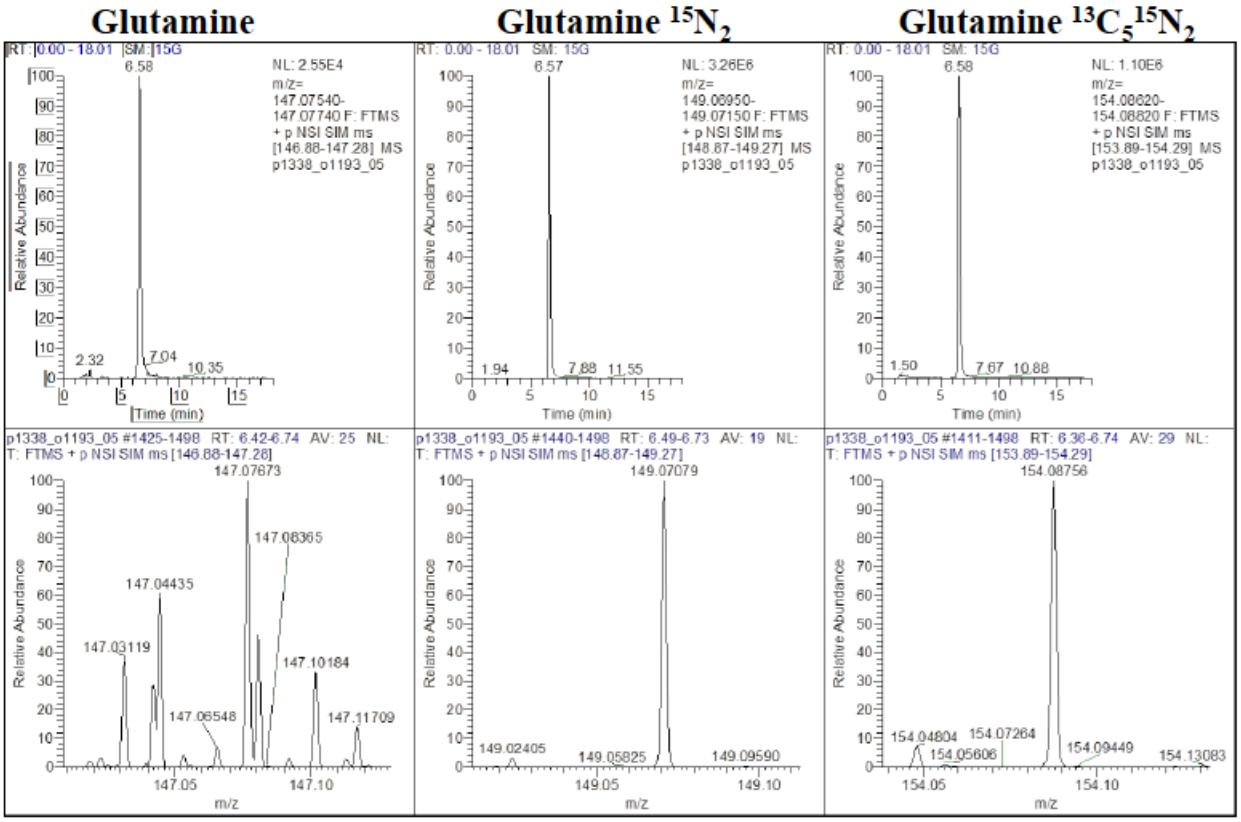

B

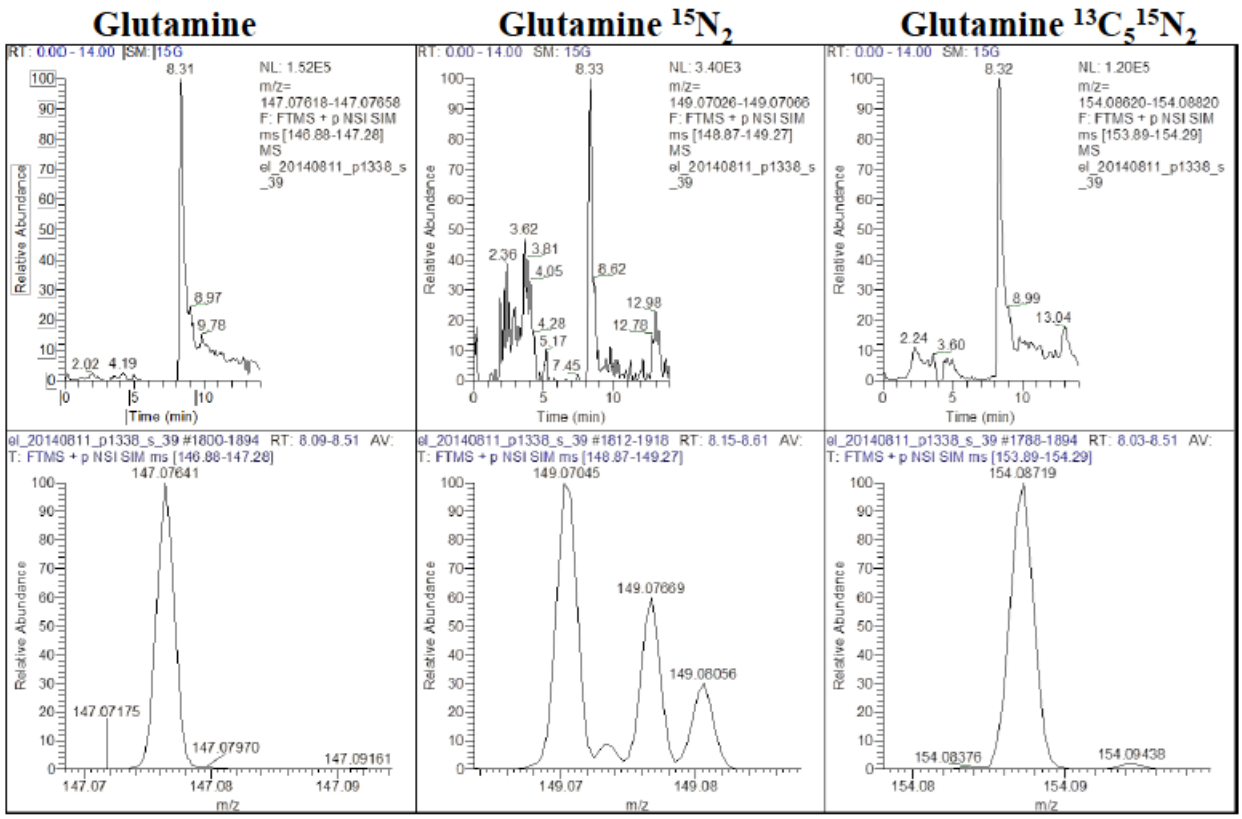

Supplementary Figure 4. Representative liquid chromatographs and mass spectra of glutamine and heavy labeled glutamine isotopes $^{15}N_2$ and $^{13}C_5{}^{15}N_2$. For each sample, the representative liquid chromatographs (upper panel) and mass spectra (lower panel) of glutamine and the $^{15}N_2$ and $^{13}C_5{}^{15}N_2$ heavy labeled glutamine isotopes are shown. **A.** analysis of a representative plasma sample collected following $^{15}N_2$-Gln intraperitoneal (IP) injection and with $^{13}C_5{}^{15}N_2$-Gln added as an internal control are shown. **B.** analysis of a microdialysate sample collected after $^{15}N_2$-Gln IP injection and with $^{13}C_5{}^{15}N_2$-Gln added as an internal control

A

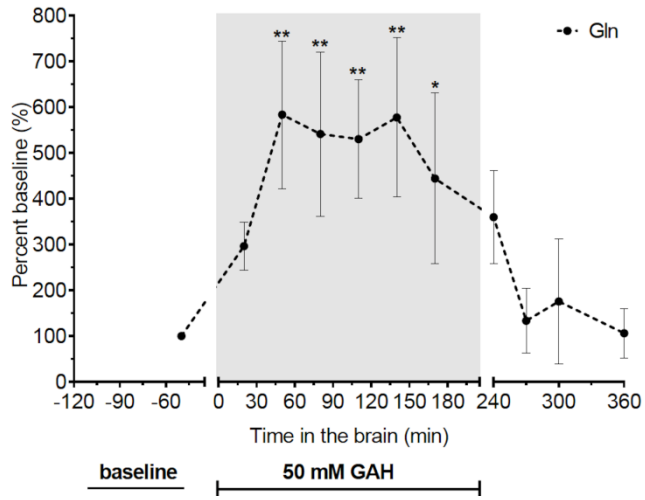

B

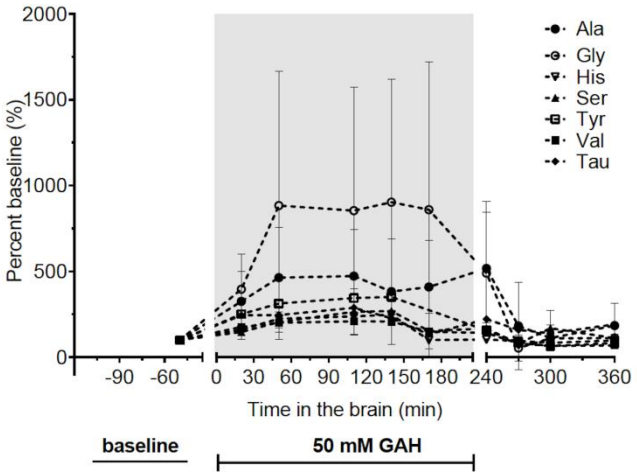

Supplementary Figure 5. Impact of brain perfusion with a system N competitive inhibitor on amino acid levels in microdialysates. The effect of competitive inhibition of system N transporters was tested using brain perfusion with 50 mM L-glutamic acid-γ–monohydroxamate (GAH) for 3 hours. For each panel the indicated amino acid responses in ISF collected at 1 µl/min and normalized to baseline vs time in brain (adjusted for the time for samples to reach the fraction collector) are shown. **A**. L-glutamine (Gln) mean ± SD responses before, during and after brain perfusion with GAH. Statistical comparisons was performed by two-way Anova with Dunnets post-test and statistically significant differences to baseline are indicated: **= $p<0.01$, and *= $p<0.1$. **B.** Percent baseline for Ala (L-alanine), Gly (Glycine), His (L-histidine), Ser (L-serine), Tyr (L-tyrosine), Val (L-valine) and Tau (Taurine). For both panels, data are from three animals from one experiment. Baseline samples are indicated by the label and solid line. Perfusate equilibration without sample collection is indicated by the break in the X axis (time in brain). GAH perfusion is indicated by underlined X axis region with label, and the shaded area of the graph.

A

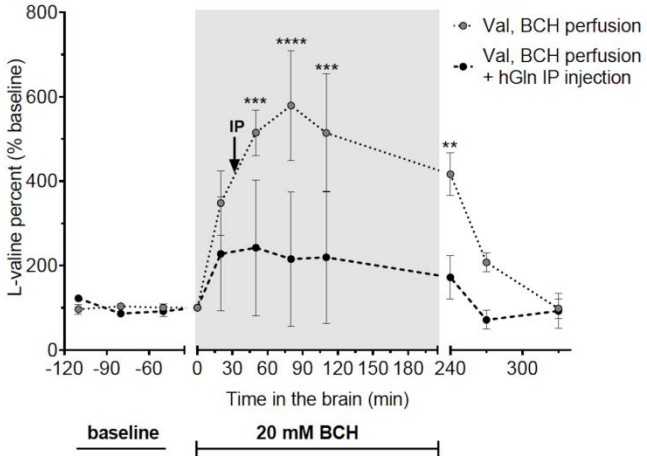

B

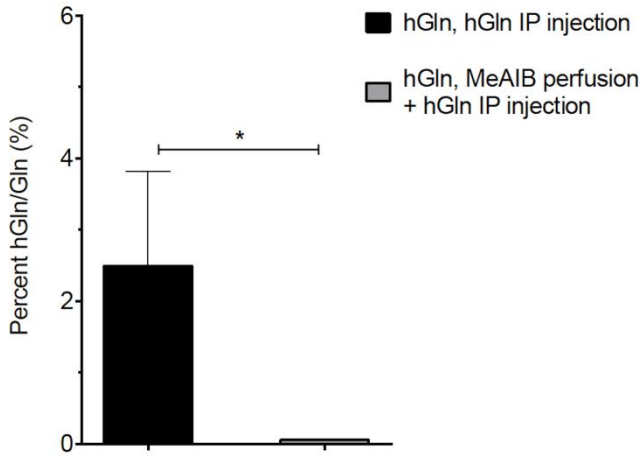

Supplementary Figure 6. Interstitial fluid total amino acid concentrations following brain perfusion with inhibitor without or with labeled hGln intraperitoneal injection. A. ISF Val levels relative to baseline for samples collected before, during, and after 20 mM (2-aminobicyclo-(2,2,1)-heptane-2-carboxylic acid (BCH) perfusion either alone (n = 4 animals) or in combination with hGln intraperitoneal (IP) injection (n = 4 animals). Data are mean percent ± SD. See panel for key. Comparison was performed between two types of treatment by two-way Anova test with Sidak post-test. **B.** Labeled Gln (detected by LC-MS) as percent (%) of total Gln (hGln/Gln) in microdialysate samples at 30 minutes post-IP alone (data from Fig. 3C) vs. IP + MeAIB (α-(methylamino)-isobutyric acid) perfusion (at 55' of MeAIB perfusion, corresponding to 30' post-IP). Data are mean ± SEM (IP alone, n = 10 animals in total, from three independent experiments; IP + MeAIB, n = 2 animals). Comparison was performed by un-paired two-sided t-test.
For both panels, statistical significance is given as **** = $p<0.0001$, *** = $p<0.001$, **= $p<0.01$, * = $p<0.1$.

	Mean relative recovery (% ± SD)	
	Probe length, mm	
Amino acid	**1 mm**	**2 mm**
arginine	8.4 ± 1.1	21 ± 3.5
asparagine	8.8 ± 1.2	25 ± 2.1
glutamine	12 ± 1.5	28 ± 5.0
glycine	13 ± 2.1	33 ± 2.8
histidine	8.0 ± 1.3	20 ± 0.7
isoleucine	9.3 ± 1.2	21 ± 2.1
leucine	8.9 ± 1.1	21 ± 2.1
lysine	8.6 ± 0.9	20 ± 2.1
methionine	8.1 ± 1.7	22 ± 3.5
phenylalanine	7.8 ± 1.0	26 ± 2.8
proline	11 ± 1.6	28 ± 3.5
serine	11 ± 1.6	23 ± 2.8
threonine	10 ± 1.3	19 ± 2.1
tryptophan	7.4 ± 1.0	20 ± 2.1
valine	10 ± 1.3	27 ± 2.1

Supplementary Table 1. ***The in vitro*** **microdialysis relative recovery of amino acids.** The *in vitro* relative recoveries from microdialysis of 100 µM amino acids at 1 µl/min flow rates were determined for CMA 7 probes (1 and 2 mm lengths). Data are expressed as mean percent (n=2 for each of two independent experiments).

Amino acid	Mean K_0 ± SD
norleucine	0.16 ± 0.04
arginine	0.13 ± 0.02
asparagine	0.17 ± 0.04
glutamine	0.17 ± 0.08
glycine	0.15 ± 0.02
histidine	0.23 ± 0.06
isoleucine	0.12 ± 0.03
leucine	0.14 ± 0.03
lysine	0.14 ± 0.03
methionine	0.14 ± 0.03
phenylalanine	0.15 ± 0.03
proline	0.18 ± 0.04
serine	0.19 ± 0.04
threonine	0.16 ± 0.03
tryptophan	0.13 ± 0.03
valine	0.15 ± 0.03

Supplementary Table 2. *In vitro* microdialysis amino acid mass transfer coefficients (K_0) of CMA 7 probes. *In vitro* amino acid mass transfer coefficients (K_0) of CMA 7 probes (2 mm) were calculated by the Flow-rate method using perfusion flow rates of 0.2, 0.5, 1, and 2 µl/min and an initial concentration of 100 µM per amino acid. Data are expressed as mean K_0 ± SD. Data is for n=2 from one experiment.

	GABA, mean µM ± SD	
Time (min)	**20 mM BCH**	**50 mM GAH**
-30	n.d.	n.d.
30	1.2 ± 0.3	5.6 ± 1.5
60	2.0 ± 0.1	15 ± 3.0
90	1.9 ± 0.2	14 ± 4.0
120	1.8 ± 0.02	15 ± 1.8
150	2.0 ± 0.3	18 ± 4.1
180	0.8 ± 0.2	14 ± 6.2
260	0.05 ± 0.06	5.8 ± 0.8
290	n.d.	n.d.

Supplementary Table 3. Concentrations of the inhibitory neurotransmitter, GABA, in microdialysis samples from brain perfusions with BCH or GAH competitive inhibitors. GABA concentrations (µM) in microdialysis samples collected pre-, during, and post- brain perfusion with 20 mM BCH or 50 mM GAH at perfusion rates of 1 µl/min. Time of perfusion with inhibitor is indicated by bold font and grey shading. Data is for n = 4 (BCH) or n = 3 (GAH) mice for one experiment per inhibitor. BCH (2-amino-bicyclo-(2,2,1)-heptane-2-carboxylic acid), GABA (γ-amino butyric acid), GAH (2-aminobicyclo-(2,2,1)-heptane-2-carboxylic acid).

6. Discussion and outlook

In this work existence of an AA concentration gradient between CSF and the brain ISF was demonstrated. Next we focused on investigation of responses in AA levels in the brain ISF to different challenges in order to study the roles of AATs in homeostasis. The transendothelial transport of glutamine and valine across the BBB after bolus IP administration was shown. For valine, a rapid statistically significant comparable response in both plasma and the brain ISF was observed. However, the acute increase in Gln plasma concentrations did not result in elevation of Gln in the ISF. Using hGln the presence of this isotope in mD samples collected after IP injection was demonstrated. Moreover, inhibition of system A and system L *in vivo* via perfusion into the brain of the competitive inhibitors MeAIB and BCH, respectively, resulted in elevation of Gln in the brain ISF. However, the response was more significant and stable for BCH than for MeAIB application, yielding 4.3 vs 2.2 fold increases, correspondingly. Furthermore, by simultaneous administration of system L inhibitor with bolus IP injection of hGln increased Gln influx from periphery into the brain ISF was observed. Taken together, these data support significant role for system L in the *in vivo* regulation of Gln in the brain ISF. System L includes LAT1, LAT2, LAT3, and LAT4 transporters, among which LAT1 expression is the highest in the BBB vs other tissues. Thus, based on expression data from different cells in the CNS and localization on both BBB membranes LAT1 might be a key player in Gln homeostasis for the brain ISF. Unfortunately, the attempt to localize SNAT5 in the BBB was inconclusive and this aspect of the project highlighted some limitations of antibody-based methods. A clarification of the role of other Gln transporters expressed in the BBB, in particular of the system N transporters SNAT3 and SNAT5, as well as their function in other cells in the brain (astrocytes, neurons) is necessary for understanding homeostatic regulation not only in the brain ISF, but also in the brain in general.

be truncated [441]. We consider that this model will allow investigation of the role of SNAT3 expressed in the BBB and in astrocytes for regulation of Gln homeostasis in the brain ISF.

First of all, the efficiency of SNAT3 gene abolishment in the BEC cells must be characterized, since this process is tamoxifen-dose and age dependent [441]. Next, the generated model can be characterized in terms of AA levels in the brain ISF and efficiency of transendothelial Gln transport as compared to wild-type animals. In addition, transport of AAs such as glycine and histidine across the BBB can be tested. These AA are lower affinity substrates for SNAT3 than SNAT5 and if SNAT3 is eliminated from the BBB, then the detection of elevation of these AA levels in the brain ISF would be indirect evidence of SNAT5 function in the BBB. Moreover, our preliminary *in vivo* test of L-glutamic acid-γ-monohydroxamate (GAH) resulted in the significant elevation of Gln in the brain ISF. Previously, this AA analog was shown to inhibit Gln transport in oocytes expressing SNAT5 [352]. Therefore, we assume that comparative analysis of changes in Gln level in the brain ISF under application GAH in wild-type versus SNAT3fl//fl VeCadCreERT2+//-animals might provide information about the relative importance of SNAT3 and SNAT5 in this regulation.

Since SNAT3 is abundantly expressed not only in the BBB, but also in astrocytes we decided in parallel to generate a mouse model, in which SNAT3 expression is eliminated in astrocytes. Thus, we crossed available SNAT3 floxed animals with FVB,129-TG(GFAP-CreER)Fki generated in the lab of Frank Kirchhoff and kindly provided for our research by Prof. Isabelle Mansuy. Interestingly, a correlation between elevation of K^+ and Glu in the brain interstitial fluid resulting from concussive brain injury has been shown [442]. However, no data were provided for Gln concentration under the same conditions. SNAT3 transporter expressed in astrocytes is considered to be an important player in glutamate/GABA-glutamine cycle. Temporal elevation of K^+ via mD probe during the experiment causes neuronal depolarization and increase of neuronal activity and as a result release of Glu from glutamatergic neurons. Excess of Glu has to be taken up by astrocytes and transformed into Gln that is then thought to be released via SNAT3 and SNAT5 transporters and consumed by neurons for Glu synthesis [273]. Therefore, we consider that the described experiments performed in our SNAT3fl//fl GFAP-CreER +//- knockout animal model may be essential for the investigation of changes in ISF neurotransmitters (Glu, GABA) as well as other AAs (Gln).

We consider that the comparative analysis of the two mouse models that lack SNAT3 expression in the BBB or in astrocytes will help clarify the role of this AAT for Gln homeostasis in brain ISF.

6.1. Discussion

6.1.1 Methods of ISF measurements

Brain ISF is the direct microenvironment for the cells in the brain and is mainly produced by the BBB. It has an estimated volume of only ~18-20% of total brain volume [109]. Its small volume and distribution throughout the brain is an obstacle for gaining information about its qualitive and quantitative content. Several methods have been developed for measuring the chemical content of the brain ISF *in vivo* and applied in neurobiology, physiology and pharmacology. One of the first developed methods was a cortical cup technique, when a small cylindric cup was fixed to an exposed cortical surface of an anesthetized animal [416]. This technique allowed measurement of the release of acetylcholine, AAs, and nucleosides. However it's application was restricted to the cortex. A similar approach is used in the push-pull method that is based on the implantation of a cannula in the brain and subsequent simultaneous delivery (push) and removal (pull) of perfusion fluid [416]. Thus, in this case substances diffuse between brain ISF and perfusion fluid. This method was successfully used for studies of neurotransmitters, peptides, and proteins. However, one of the most important limitations of the technique is the requirement for equilibrium between delivered and extracted volumes of fluid, otherwise it might lead to severe lesions. Moreover, initially relatively high rates of perfusion were used. As a result, for a while this method was mainly replaced by other techniques. However, the design of a capillary push-pull cannula with a tip diameter of ~200 μm and the use of low flow rates reduced tissue damage. It has regained use due to its high spatial resolution [417-419]. A third method is an *in vivo* voltammetric technique, when a small electrode is implanted in brain tissue, and the voltammetric curve corresponds to the chemical detected at the surface of the electrode [420]. This technique gives high temporal (time of detection depends on substance diffusion and the response time of electrode) and spatial resolution (the size of targeted area corresponds the electrode diameter 10-20 μm) [421]. However, an essential disadvantage of the method is the limited number of individually detectable chemicals and generally only one compound can be detected by each microelectrode. Additionally, different compounds that are electrolyzed at similar potentials result in the same responses and cannot be distinguished. For example, the fast-scan cyclic voltammograms of dopamine and norepinephrine are identical [421]. Today microdialysis (mD) is a well-established technique widely used in neuroscience research and drug development. However, as any of already mentioned methods it has benefits and limitations. This technique has such important advantages as minimal invasiveness and continuous sampling from brain ISF [422]. Microdialysis is a good tool for qualitative

determination of relative changes in substance levels as a result of experimental manipulations. Additionally the semipermeable probe membrane allows application of compounds of interest into the brain tissue. However, one of the main limitations of mD is a low temporal and spatial resolution [422]. The longer mD samples are collected, the higher concentration of brain solutes in the recovered dialysates. However, long collection periods also decrease detection of rapid changes, for instance, neurotransmitter release. Another important issue is that the probe-specific relative recovery of different solutes impacts the estimation of solute concentration in the brain ISF. Nevertheless, methods for quantification (extrapolation to zero flow rate (or flow-rate method), no-net-flux, retrodialysis, etc.) have been developed [423].

6.1.2 Concentration gradient for amino acids between ISF and CSF

Taking into account the advantages and disadvantages of currently used methods for quantification of substances in the brain ISF, mD was chosen for determination of AA levels in the brain ISF. The extrapolation to zero flow rate method with retro-dialysis of a non-natural AA for determination of the corresponding mass transfer coefficient was used to calculate a unique value for initial brain AA concentrations. To our knowledge this work is the first demonstration of concentration gradients between ISF and CSF for 14 standard and 2 non-standard AAs. Moreover, we confirmed Gln to be the most abundant AA in the brain ISF as previously reported [171, 172]. We found that the concentration difference for Gln between plasma and CSF is 1.15 times, while between CSF and ISF it is 6.4. The literature reports similar concentration differences for glucose: glucose is 1.5 times more concentrated in plasma than CSF, and ~ 5 times lower in ISF than CSF [173-175, 177]. The CSF is mainly produced by the choroid plexus epithelium (CPE) with ~25% contribution from ISF [110-112], while the brain ISF is considered to be primarily formed by the BBB [136]. Since ependymal cells of ventricle walls do not form TJ complexes, ISF and CSF might exchange relatively freely in the ventricles. However, concentration differences between the ISF and CSF could result from the greater surface of the BBB compared to BCSF (~15-25 m^2 vs 0.021 m^2 for humans) and the nearly 10 times slower production of ISF than CSF [29, 113, 144, 424].

6.1.3 Can concentration gradients be formed between ISF in different brain regions?

Since the brain ISF exhibits bulk flow, no gradients are believed to exist between different brain regions [136]. The perivascular circulation route from CSF into the brain along arteries penetrating the outer brain surface and then back out from the brain tissue along large-caliber

draining veins has been shown to be an important "clearance route" [148-151, 153, 418]. However, all experiments that described the perivascular route involved usage of radiolabeled tracers not naturally found in the brain, for example horseradish peroxidase (HRP). Therefore the importance of this pathway for equilibration of naturally occurring solutes such as sugars, AA, nucleosides, etc., in ISF between different brain regions is not clear. For instance, Kanamori observed no statistically significant difference in Gln levels in mD samples collected from the somatosensory cortex, hippocampus, and thalamus [172]. In contrast, glucose levels determined by *in vivo* microdialysis by several groups varied 2 – 6 fold between striatum, hippocampus, and cortex [167-169, 173, 174, 176, 177]. Additionally there is evidence for heterogeneous distribution of enzymes, including receptors, and transporters for neurotransmitters in the brain that might be the basis for its functional heterogeneity. For instance, transporters for the inhibitory neurotransmitter, glycine, such as GlyT1, and GlyT2, and for GABA, i.e. GAT1, and GAT3 are relatively equally expressed in cortical neurons [425]. However, hippocampal neurons preferentially express GlyT1, GlyT2, and GAT1, and in thalamus Glyt2 is highly expressed [425]. Another important example of heterogeneity is regional distribution in the brain of ionotropic $GABA_A$ receptors ($GABA_AR$) subunits. To date 19 subunits have been identified, these receptors are heteropentamers and generally consist of two α, two β and a variable fifth subunit (γ, δ, ε, θ, or π) [426]. The six known isoforms for α subunits have distinct distributions in the brain: α2 expression is high in the cortex, striatum, and hippocampus, and lower in the hypothalamus, thalamus, and cerebellum. In contrast, the α3 subunit is primarily expressed in the cortex, olfactory bulb, and thalamus [426]. Therefore, neurons as well as astrocytes and endothelial cells can significantly influence the content of the brain ISF depending on the particular protein expression patterns occurring in different brain regions. A recent study comparing ISF neurotransmitter concentrations in the ventral tegmental area (VTA; enriched with dopamine (DA) neurons) and red nucleus (RN) that are separated by a distance of only ~ 200 μm [427] using low flow push-pull sampling demonstrated significant differences in DA levels [162]. A similar, but non-significant trend was found for glutamate [162]. This approach could be used to investigate metabolite concentrations in ISF from different brain regions. Generally, the methods used (mD, push-pull low sampling) for this type of studies require a high spatial resolution.

6.1.4 Cells actively regulate ISF content

On the one hand, brain endothelial cells control flux of substances in to and out of the brain and, therefore, regulate ISF qualitive and quantitative content. On the other hand, neurons, as

electrically excitable cells, along with glial (astrocytes, oligodendrocytes) and microglial cells consume various compounds and produce metabolites and as a result change ISF content. Simultaneously cells closely interact with each other in the brain and, consequently, such complex interactions also regulate the concentration of compounds in ISF. For instance, during increased neuronal activity neurotransmitter concentrations, as well as, glucose and lactate in the brain ISF vary highly. Currently several contradictory theories have been suggested to explain events occurring during increased neuronal activity [428]. According to the most accepted astrocyte-to-neuron lactate shuttle (ANLS) hypothesis glycolysis is increased in astrocytes and the produced lactate is transported from astrocytes into neurons for further oxidation [95]. This model relates excitatory neurotransmission of Glu, the glutamate-glutamine cycle and astrocyte-neuron metabolic coupling. In this case glutamatergic activation leads to Glu increase in ISF, which is taken up by neurons and astrocytes. Glu transport occurs in Na^+-dependent manner and increased intracellular Na^+ concentration activates Na^+/K^+ pump. As a result, consumption of ATP increases due to its utilization for conversion glutamate into glutamine and for pumping Na^+ out of the cell. In this case glycolysis is suggested to be the source for an increased ATP demand and consequently lactate is produced, which is then released and used by neurons as energy source [428]. Alternatively, another theory that explains events taking place during neuronal activity and changes in lactate levels in the brain ISF has been suggested by Simpson based on expression pattern in different brain cells of glucose transporters and their kinetic parameters [429]. The neuron to astrocyte lactate shuttle (NALS) model suggests that during increased activity neurons demand high levels of energy and consequently glucose uptake via a high affinity glucose transporter GLUT3 increases [429, 430]. As a result, glucose levels decrease in the ISF, glycolysis is upregulated in neurons and lactate released by neurons to the ISF. Increased lactate level in ISF is suggested to be normalized by active consumption of lactate by astrocytes and transport of lactate across the BBB into blood [428]. Thus, NALS model suggests that lactate flux between neurons and astrocytes depends on neuronal status [429]. The reversibility of lactate transport between neurons and astrocytes has already been described by Cerdán and depends on relative values of cytocolic and mitochondrial redox states in neurons and astrocytes [431]. Interestingly, it has been shown that upon neuronal activation glucose transport increases via the BBB. This increased transport might be aimed to provide glucose for neurons and normalize ISF glucose levels. This phenomenon was named as neurobarrier coupling [97]. Taken together, these examples demonstrate the direct and strong impact of metabolism occurring in different cells in the brain on the brain ISF.

6.1.5 Glutamine origin in the ISF and its regulation

Generally, enzymes and transporters can be regarded as key molecular regulators of Gln concentrations in brain ISF. This can be illustrated by the glutamate/GABA-glutamine cycle [273]. Glu levels are tightly controlled in the CNS since its high levels are neurotoxic [234]. After Glu release in synaptic cleft it binds to neuronal neurotransmitter receptors, while excess of Glu is taken up by transporters expressed mainly in astrocytes. Next glutamate is converted by glutamine synthetase (GS) into glutamine [273]. Glutamine is transported from astrocytes mainly via SNAT3 and SNAT5 into the brain ISF [279] [275-278, 280], where it is taken up by neurons via SNAT1, SNAT2, and possibly SNAT7 for Glu synthesis [283, 350, 351, 366, 432]. Thus, here we already observe the close cooperation between receptors, transporters, and metabolic enzymes expressed in two cell types in Gln regulation. The picture is becoming more complicated, when other cell types such as BEC as well as Gln from the blood stream are considered. Interestingly, GS plays an important role during hyperammonemia, since it catalyzes the reaction between ammonia from the blood and glutamate to form Gln [322]. Experiments with a known GS inhibitor L-methionine-S,R-sulfoximine (MSO) significantly reduced the newly synthesized glutamine from (^{13}N) labeled ammonia, in comparison to control animals that did not receive the inhibitor [322]. There are eleven transporters expressed in the brain, which can potentially play an important role in Gln homeostasis regulation. However, as usual for AATs none of them transports Gln exclusively. Moreover, the same AAT can be expressed in different brain cell types. Therefore, investigation of the roles of various Gln transporters in brain ISF homeostasis is challenging. First, in order to understand the role of a particular AAT in brain ISF Gln regulation it is important to know the relative AAT expression in various brain cell types. Moreover, for the BEC the membrane localization pattern (both membranes, or luminal, or abluminal only) must be investigated (Table 3). Next, the functional impact of different AAT systems has to be studied.

In our studies we used two approaches to challenge the homeostatic conditions in the brain ISF. Since Gln is actively produced in astrocytes as a part of glutamate/GABA-glutamine cycle it is important to know how much Gln is produced in the brain and how much originates from plasma. We investigated transendothelial transport of AAs by acute elevation in peripheral circulation. This approach gives the opportunity to answer the question whether the transport of particular chemical is possible across the BBB into ISF *in vivo* and simultaneously to determine concentration in plasma and ISF. For example, intravenous infusion of (U-13C5) Gln in mice resulted in 11.8% enrichment of labeled Gln in brain lysates corresponding to plasma Gln concentrations greater than 1.1 mM [433]. Extrapolation to physiological plasma Gln levels

(~600 μM) yields 7%, including intra- and extracellular glutamine. Interestingly, in our experiments $^{15}N_2$ Gln IP resulted in ~4% of labeled Gln in the brain ISF. Nevertheless, this method has two possible disadvantages. First of all, elevated levels are strongly different from physiological conditions and observed transport under extreme conditions might not occur under normal conditions. Second of all, acute manner of administration gives the possibility to observe changes for a relatively short period of time. As an alternative method to acute elevation an intravenous infusion can be used, since in this case transport under "steady state" conditions can be investigated. Moreover, Gln levels are known to be elevated in plasma during hyperammonemia. Consequently, this condition can be imitated by intravenous infusion of Gln alone (such as in the study by Bagga and coworkers) and the possibility of transport across the BBB under this pathological condition can be examined [433]. Nevertheless, the mentioned approach has one major disadvantage of the necessity for animals being anesthetized during the whole procedure.

Some AAT systems are known to be competitively inhibited by non-natural AA analogs, for example, MeAIB (system A inhibitor) or BCH (system L inhibitor). Perfusion of these competitive inhibitors into the brain might provide a general idea about the relative importance of one or another AAT system for the regulation of AA homeostasis. In our study I demonstrated a significantly stronger impact on Gln levels in the brain ISF using BCH vs. MeAIB administration via the mD probe. Since these inhibitors are applied *in vivo* it is important to note that they might have an impact on cell metabolism. For example, BCH activates glutamate hydrogenase and as a result decreases intracellular Glu levels [434, 435]. Thus, inhibitors might additionally affect not only levels of the AA of interest, but also other AAs therefore adequate controls must be chosen. Also since the inhibitor is applied to a complex system for a relatively long period of time it might cause initial changes in AA levels, which might lead to subsequent changes in other AAs. Therefore, it might not be possible to distinguish the primary events from the secondary effects. The observed elevated Gln in case of competitive inhibition might come from periphery (blood) or from intracellular pools (cells in the brain). In order to answer this question about Gln source, BCH was administrated to the brain ISF with simultaneous IP injection of $^{15}N_2$ Gln. As a result a large increase in labeled Gln in the brain ISF was observed. Accordingly, we assumed that BCH applied in the brain ISF transstimulated system L expressed in the BBB and caused the plasma Gln influx into the brain. In summary, described functional approaches give the opportunity to distinguish the AAT system involved in Gln concentration regulation, but do not allow identification of the AAT on the molecular level.

6.1.6 Methods for SNAT5 localization in the BBB

Polarized expression of different transporter systems is a key basis for the BBB function as a transport barrier between blood and brain. Studies of AAT localization in the BBB have significance not only for understanding of their physiological roles, but also for potential applications in drug delivery to the CNS. Membrane fractionation can be used for enrichment of luminal and abluminal membranes in the lower and higher-density layers, respectively [436]. Kinetic studies using fractionated BBB membrane vesicles have been used in the investigation of the transport properties of luminal and abluminal membranes and, thus, for the identification of transporter systems [139, 372]. Based on this approach, for example, system L was shown to be distributed on both membranes, while system A was found to be restricted to abluminal membranes. However, this assay did not provide the molecular identity of transporters and moreover separation of luminal and abluminal fractions might have been not complete. Application of antibody-based methods such as immunofluorescence and western-blotting of biotin labeled luminal membranes resulted in identification of SNAT3 on both BBB membranes [3]. Nonetheless, the main limitation of antibody-based approaches is the availability of specific antibodies. Unfortunately, I faced this problem during my attempts to localize SNAT5 expression in BBB membranes, since none of the anti-mSNAT5 antibodies tested recognized SNAT5 in microvessels. Development of new non-antibody dependent methods for localization of transporters on the BBB membranes represents an important area of study. For example, recently a method based on combination of membrane fractionation with liquid chromatography-mass spectrometry (LC-MS/MS) was applied for localization of some transporters in luminal and abluminal BBB membranes [437]. In order to overcome the problem of cross-contamination luminal and abluminal membranes the authors suggested using a correction based on the absolute amounts of marker proteins specifically localized in luminal or abluminal membranes. Based on the fractional analysis of this study together with previous immunohistochemical and functional studies the authors suggested using MDR1 (multidrug resistance protein 1, or permeability glycoprotein 1, Pgp, or ATP-binding cassette sub-family B member 1 (ABCB1)) as a luminal membrane marker, and SNAT2 as an abluminal membrane marker. Interestingly, during preparation of different fractions from the BBB the authors did not detect SNAT1 in agreement with data previously published from our lab [3]. Based on this approach the ABC transporters, ABCG2 (or BCRP), and SLC transporters, such as the glucose transporter GLUT1 (SLC2A1), and organic anion transporter OATP3A1 (SLCO3A1) are shown to be luminal-dominant transporters, while ABCA1 and the long chain fatty acid transporter, FATP1 (SLC27A1) have abluminal-dominant localization. At the same time the authors suggested that

the ACB subfamily C transporter (ABCC5 or MRP5) and the monocarboxylate transporter, MCT1 (SLC16A1), as well as the Na^+/K^+ ATPase have a similar distribution on the two membranes. Nevertheless, there are two disadvantages of this method. First, a significant amount of material is required, that is why in the described study porcine brains were used. Second, isolated microvessels can be contaminated with astrocytes, pericytes, and neurons.

6.2. Outlook

6.2.1 Investigation of the role of SNAT3 expressed in the BBB and glial cells in the brain ISF glutamine homeostasis

During the Gln transendothelial transport study at 5 min post-IP injection, plasma Gln was elevated to ~ 2.3 mM. Both LAT1 and SNAT3, which transport Gln with low affinity at respective K_m values of 1.6 and 0.9 mM, could be involved in BBB transendothelial Gln transport (Table 3). This suggestion is also supported by high levels of expression of mRNA of both transporters in the BBB and the localization of both transporters on luminal and abluminal membranes. Moreover, competitive inhibition by BCH *in vivo* during brain perfusion significantly increases Gln in the ISF confirming the role of system L in Gln ISF homeostasis. Based on the literature about LAT1 and LAT2 expression in different CNS cells, we suggest that the observed effect on Gln ISF level is mainly due to BBB expressed LAT1. Indeed, system L transporters are obligatory exchangers and transport is driven by AA gradients generated by Na^+-dependent system A and N transporters [438]. Thus, the next steps in the investigation of Gln homeostasis in the brain ISF must focus on understanding the roles of BBB expressed LAT1 and SNAT3. To perform these studies *in vivo* knockout SNAT3 and/or LAT1 models must be used. Unfortunately, the constitutive knockout mouse models for these two transporters have lethal phenotypes. Abolishing LAT1 resulted in death during embryonic development, while SNAT3 loss caused death at post-natal ~18 – 21 days [439, 440]. To overcome the severe consequences of the constitutive SNAT3 knockout an endothelial and astrocyte targeted inducible knock-outs of SNAT3 were bred. This was accomplished by creating a floxed SNAT3 mouse strain from an ES cell clone (EPD0351_2_A12) generated by the Wellcome Trust Sanger Institute and bred by the KOMP Repository (WWW.KOMP.org) and the Mouse Biology Program (www.mousebiology.org) at the University of California Davis. Next we crossed floxed SNAT3 with VeCadCreERT2 mice kindly provided by Dr. Luisa Iruela-Arispe. In this case Cre-recombinase expressed under VE-Cadherin promoter will be activated in all endothelial cells including the BBB by tamoxifen administration, and as a result of recombination *Snat3* gene will

be truncated [441]. We consider that this model will allow investigation of the role of SNAT3 expressed in the BBB and in astrocytes for regulation of Gln homeostasis in the brain ISF.

First of all, the efficiency of SNAT3 gene abolishment in the BEC cells must be characterized, since this process is tamoxifen-dose and age dependent [441]. Next, the generated model can be characterized in terms of AA levels in the brain ISF and efficiency of transendothelial Gln transport as compared to wild-type animals. In addition, transport of AAs such as glycine and histidine across the BBB can be tested. These AA are lower affinity substrates for SNAT3 than SNAT5 and if SNAT3 is eliminated from the BBB, then the detection of elevation of these AA levels in the brain ISF would be indirect evidence of SNAT5 function in the BBB. Moreover, our preliminary *in vivo* test of L-glutamic acid-γ-monohydroxamate (GAH) resulted in the significant elevation of Gln in the brain ISF. Previously, this AA analog was shown to inhibit Gln transport in oocytes expressing SNAT5 [352]. Therefore, we assume that comparative analysis of changes in Gln level in the brain ISF under application GAH in wild-type versus SNAT3fl//fl VeCadCreERT2+//-animals might provide information about the relative importance of SNAT3 and SNAT5 in this regulation.

Since SNAT3 is abundantly expressed not only in the BBB, but also in astrocytes we decided in parallel to generate a mouse model, in which SNAT3 expression is eliminated in astrocytes. Thus, we crossed available SNAT3 floxed animals with FVB,129-TG(GFAP-CreER)Fki generated in the lab of Frank Kirchhoff and kindly provided for our research by Prof. Isabelle Mansuy. Interestingly, a correlation between elevation of K^+ and Glu in the brain interstitial fluid resulting from concussive brain injury has been shown [442]. However, no data were provided for Gln concentration under the same conditions. SNAT3 transporter expressed in astrocytes is considered to be an important player in glutamate/GABA-glutamine cycle. Temporal elevation of K^+ via mD probe during the experiment causes neuronal depolarization and increase of neuronal activity and as a result release of Glu from glutamatergic neurons. Excess of Glu has to be taken up by astrocytes and transformed into Gln that is then thought to be released via SNAT3 and SNAT5 transporters and consumed by neurons for Glu synthesis [273]. Therefore, we consider that the described experiments performed in our SNAT3fl//fl GFAP-CreER +//- knockout animal model may be essential for the investigation of changes in ISF neurotransmitters (Glu, GABA) as well as other AAs (Gln).

We consider that the comparative analysis of the two mouse models that lack SNAT3 expression in the BBB or in astrocytes will help clarify the role of this AAT for Gln homeostasis in brain ISF.

7. References

1. McGale, E.H.F., et al., *STUDIES OF THE INTER-RELATIONSHIP BETWEEN CEREBROSPINAL FLUID AND PLASMA AMINO ACID CONCENTRATIONS IN NORMAL INDIVIDUALS.* Journal of Neurochemistry, 1977. 29(2): p. 291-297.
2. Lyck, R., et al., *Culture-induced changes in blood-brain barrier transcriptome: implications for amino-acid transporters in vivo.* J Cereb Blood Flow Metab, 2009. 29(9): p. 1491-502.
3. Ruderisch, N., et al., *Differential axial localization along the mouse brain vascular tree of luminal sodium-dependent glutamine transporters Snat1 and Snat3.* J Cereb Blood Flow Metab, 2011. 31(7): p. 1637-47.
4. Pelvig, D.P., et al., *Neocortical glial cell numbers in human brains.* Neurobiol Aging, 2008. 29(11): p. 1754-62.
5. Charles, N., *Diffusion and related transport mechanisms in brain tissue.* Reports on Progress in Physics, 2001. 64(7): p. 815.
6. Aiello, L.C. and P. Wheeler, *The Expensive-Tissue Hypothesis: The Brain and the Digestive System in Human and Primate Evolution.* Current Anthropology, 1995. 36(2): p. 199-221.
7. Abbott, N.J., *Dynamics of CNS Barriers: Evolution, Differentiation, and Modulation.* Cellular and Molecular Neurobiology, 2005. 25(1): p. 5-23.
8. Abbott, N.J., et al., *Structure and function of the blood-brain barrier.* Neurobiol Dis, 2010. 37(1): p. 13-25.
9. Saunders, N.R., S.A. Liddelow, and K.M. Dziegielewska, *Barrier mechanisms in the developing brain.* Front Pharmacol, 2012. 3: p. 46.
10. Neuwelt, E.A., et al., *Engaging neuroscience to advance translational research in brain barrier biology.* Nat Rev Neurosci, 2011. 12(3): p. 169-82.
11. Segal, M., *The Choroid Plexuses and the Barriers Between the Blood and the Cerebrospinal Fluid.* Cellular and Molecular Neurobiology, 2000. 20(2): p. 183-196.
12. Hawkins, B.T. and T.P. Davis, *The blood-brain barrier/neurovascular unit in health and disease.* Pharmacol Rev, 2005. 57(2): p. 173-85.
13. Redzic, Z., *Molecular biology of the blood-brain and the blood-cerebrospinal fluid barriers: similarities and differences.* Fluids Barriers CNS, 2011. 8(1): p. 3.
14. Abbott, N.J., L. Ronnback, and E. Hansson, *Astrocyte-endothelial interactions at the blood-brain barrier.* Nat Rev Neurosci, 2006. 7(1): p. 41-53.
15. Gonzalez-Mariscal, L., et al., *Tight junction proteins.* Prog Biophys Mol Biol, 2003. 81(1): p. 1-44.
16. Andreeva, A.Y., et al., *Assembly of tight junction is regulated by the antagonism of conventional and novel protein kinase C isoforms.* Int J Biochem Cell Biol, 2006. 38(2): p. 222-33.
17. Nitta, T., et al., *Size-selective loosening of the blood-brain barrier in claudin-5-deficient mice.* J Cell Biol, 2003. 161(3): p. 653-60.
18. Matter, K. and M.S. Balda, *Holey barrier: claudins and the regulation of brain endothelial permeability.* J Cell Biol, 2003. 161(3): p. 459-60.
19. Van Itallie, C.M. and J.M. Anderson, *The role of claudins in determining paracellular charge selectivity.* Proc Am Thorac Soc, 2004. 1(1): p. 38-41.
20. Wolburg, H., et al., *Agrin, aquaporin-4, and astrocyte polarity as an important feature of the blood-brain barrier.* Neuroscientist, 2009. 15(2): p. 180-93.
21. Wolburg, H., et al., *Claudin-1, claudin-2 and claudin-11 are present in tight junctions of choroid plexus epithelium of the mouse.* Neurosci Lett, 2001. 307(2): p. 77-80.

22. Bazzoni, G., et al., *Homophilic interaction of junctional adhesion molecule.* J Biol Chem, 2000. 275(40): p. 30970-6.
23. Bazzoni, G. and E. Dejana, *Endothelial cell-to-cell junctions: molecular organization and role in vascular homeostasis.* Physiol Rev, 2004. 84(3): p. 869-901.
24. Taddei, A., et al., *Endothelial adherens junctions control tight junctions by VE-cadherin-mediated upregulation of claudin-5.* Nat Cell Biol, 2008. 10(8): p. 923-34.
25. Liebner, S., et al., *Wnt/beta-catenin signaling controls development of the blood-brain barrier.* J Cell Biol, 2008. 183(3): p. 409-17.
26. Catala, M., *Embryonic and fetal development of structures associated with the cerebro-spinal fluid in man and other species. Part I: The ventricular system, meninges and choroid plexuses.* Arch Anat Cytol Pathol, 1998. 46(3): p. 153-69.
27. Johansson, P.A., *The choroid plexuses and their impact on developmental neurogenesis.* Front Neurosci, 2014. 8: p. 340.
28. Wolburg, H. and W. Paulus, *Choroid plexus: biology and pathology.* Acta Neuropathol, 2010. 119(1): p. 75-88.
29. Zlokovic, B.V., *Neurovascular mechanisms of Alzheimer's neurodegeneration.* Trends Neurosci, 2005. 28(4): p. 202-8.
30. Engelhardt, B., *Development of the blood-brain barrier.* Cell Tissue Res, 2003. 314(1): p. 119-29.
31. Butt, A.M., H.C. Jones, and N.J. Abbott, *Electrical resistance across the blood-brain barrier in anaesthetized rats: a developmental study.* The Journal of Physiology, 1990. 429: p. 47-62.
32. Saunders, N.R., G.W. Knott, and K.M. Dziegielewska, *Barriers in the immature brain.* Cell Mol Neurobiol, 2000. 20(1): p. 29-40.
33. Bauer, H.C. and H. Bauer, *Neural induction of the blood-brain barrier: still an enigma.* Cell Mol Neurobiol, 2000. 20(1): p. 13-28.
34. Haseloff, R.F., et al., *In search of the astrocytic factor(s) modulating blood-brain barrier functions in brain capillary endothelial cells in vitro.* Cell Mol Neurobiol, 2005. 25(1): p. 25-39.
35. Obermeier, B., R. Daneman, and R.M. Ransohoff, *Development, maintenance and disruption of the blood-brain barrier.* Nat Med, 2013. 19(12): p. 1584-1596.
36. Crone, C. and S.P. Olesen, *Electrical resistance of brain microvascular endothelium.* Brain Res, 1982. 241(1): p. 49-55.
37. Nag, S. *The Blood-Brain and Other Neural Barriers Reviews and Protocols*. 2010;
38. Oldendorf, W.H. and W.J. Brown, *Greater number of capillary endothelial cell mitochondria in brain than in muscle.* Proc Soc Exp Biol Med, 1975. 149(3): p. 736-8.
39. Oldendorf, W.H., M.E. Cornford, and W.J. Brown, *The large apparent work capability of the blood-brain barrier: a study of the mitochondrial content of capillary endothelial cells in brain and other tissues of the rat.* Ann Neurol, 1977. 1(5): p. 409-17.
40. Nag, S., D.M. Robertson, and H.B. Dinsdale, *Quantitative estimate of pinocytosis in experimental acute hypertension.* Acta Neuropathol, 1979. 46(1-2): p. 107-16.
41. Connell, C.J. and K.L. Mercer, *Freeze-fracture appearance of the capillary endothelium in the cerebral cortex of mouse brain.* Am J Anat, 1974. 140(4): p. 595-9.
42. Vidu, R., et al., *Nanostructures: a platform for brain repair and augmentation.* Front Syst Neurosci, 2014. 8: p. 91.
43. Chen, Y. and L. Liu, *Modern methods for delivery of drugs across the blood–brain barrier.* Advanced Drug Delivery Reviews, 2012. 64(7): p. 640-665.
44. Avdeef, A., *Physicochemical profiling (solubility, permeability and charge state).* Curr Top Med Chem, 2001. 1(4): p. 277-351.

45. Lipinski, C.A., et al., *Experimental and computational approaches to estimate solubility and permeability in drug discovery and development settings.* Adv Drug Deliv Rev, 2001. 46(1-3): p. 3-26.
46. Dahlin, A., et al., *Expression profiling of the solute carrier gene family in the mouse brain.* J Pharmacol Exp Ther, 2009. 329(2): p. 558-70.
47. Daneman, R., et al., *The Mouse Blood-Brain Barrier Transcriptome: A New Resource for Understanding the Development and Function of Brain Endothelial Cells.* PLoS ONE, 2010. 5(10): p. e13741.
48. Rip, J., G.J. Schenk, and A.G. de Boer, *Differential receptor-mediated drug targeting to the diseased brain.* Expert Opin Drug Deliv, 2009. 6(3): p. 227-37.
49. Drin, G., et al., *Studies on the internalization mechanism of cationic cell-penetrating peptides.* J Biol Chem, 2003. 278(33): p. 31192-201.
50. Herve, F., N. Ghinea, and J.M. Scherrmann, *CNS delivery via adsorptive transcytosis.* Aaps j, 2008. 10(3): p. 455-72.
51. Wolburg, H., K. Wolburg-Buchholz, and B. Engelhardt, *Diapedesis of mononuclear cells across cerebral venules during experimental autoimmune encephalomyelitis leaves tight junctions intact.* Acta Neuropathol, 2005. 109(2): p. 181-90.
52. Bolton, S.J., D.C. Anthony, and V.H. Perry, *Loss of the tight junction proteins occludin and zonula occludens-1 from cerebral vascular endothelium during neutrophil-induced blood-brain barrier breakdown in vivo.* Neuroscience, 1998. 86(4): p. 1245-57.
53. Konsman, J.P., B. Drukarch, and A.M. Van Dam, *(Peri)vascular production and action of pro-inflammatory cytokines in brain pathology.* Clin Sci (Lond), 2007. 112(1): p. 1-25.
54. Ueno, M., *Mechanisms of the penetration of blood-borne substances into the brain.* Curr Neuropharmacol, 2009. 7(2): p. 142-9.
55. Wong, A.D., et al., *The blood-brain barrier: an engineering perspective.* Front Neuroeng, 2013. 6: p. 7.
56. Engelhardt, B. and L. Sorokin, *The blood-brain and the blood-cerebrospinal fluid barriers: function and dysfunction.* Semin Immunopathol, 2009. 31(4): p. 497-511.
57. Vahedi, K., et al., *COL4A1 mutation in a patient with sporadic, recurrent intracerebral hemorrhage.* Stroke, 2007. 38(5): p. 1461-4.
58. Gould, D.B., et al., *Mutations in Col4a1 cause perinatal cerebral hemorrhage and porencephaly.* Science, 2005. 308(5725): p. 1167-71.
59. Hamilton, N.B., D. Attwell, and C.N. Hall, *Pericyte-mediated regulation of capillary diameter: a component of neurovascular coupling in health and disease.* Front Neuroenergetics, 2010. 2.
60. Dalkara, T., Y. Gursoy-Ozdemir, and M. Yemisci, *Brain microvascular pericytes in health and disease.* Acta Neuropathol, 2011. 122(1): p. 1-9.
61. Daneman, R., et al., *Pericytes are required for blood-brain barrier integrity during embryogenesis.* Nature, 2010. 468(7323): p. 562-6.
62. Oberheim, N.A., et al., *Astrocytic complexity distinguishes the human brain.* Trends Neurosci, 2006. 29(10): p. 547-53.
63. Abbott, N.J., N.J. Lane, and M. Bundgaard, *The Blood-Brain Interface in Invertebratesa.* Annals of the New York Academy of Sciences, 1986. 481(1): p. 20-42.
64. Abbott, N.J., *Comparative Physiology of the Blood-Brain Barrier*, in *Physiology and Pharmacology of the Blood-Brain Barrier*, M.B. Bradbury, Editor. 1992, Springer Berlin Heidelberg. p. 371-396.
65. Volterra, A. and J. Meldolesi, *Astrocytes, from brain glue to communication elements: the revolution continues.* Nat Rev Neurosci, 2005. 6(8): p. 626-40.
66. Pellerin, L., et al., *Evidence supporting the existence of an activity-dependent astrocyte-neuron lactate shuttle.* Dev Neurosci, 1998. 20(4-5): p. 291-9.

67. Ullian, E.M., et al., *Control of Synapse Number by Glia.* Science, 2001. 291(5504): p. 657-661.
68. Fiacco, T.A., C. Agulhon, and K.D. McCarthy, *Sorting out astrocyte physiology from pharmacology.* Annu Rev Pharmacol Toxicol, 2009. 49: p. 151-74.
69. Lee, S.-W., et al., *SSeCKS regulates angiogenesis and tight junction formation in blood-brain barrier.* Nat Med, 2003. 9(7): p. 900-906.
70. Freeman, M.R., *Specification and Morphogenesis of Astrocytes.* Science, 2010. 330(6005): p. 774-778.
71. Halassa, M.M. and P.G. Haydon, *Integrated brain circuits: astrocytic networks modulate neuronal activity and behavior.* Annu Rev Physiol, 2010. 72: p. 335-55.
72. Beck, D.W., et al., *Glial cells influence polarity of the blood-brain barrier.* J Neuropathol Exp Neurol, 1984. 43(3): p. 219-24.
73. Raub, T.J., S.L. Kuentzel, and G.A. Sawada, *Permeability of bovine brain microvessel endothelial cells in vitro: barrier tightening by a factor released from astroglioma cells.* Exp Cell Res, 1992. 199(2): p. 330-40.
74. Tao-Cheng, J.H., Z. Nagy, and M.W. Brightman, *Tight junctions of brain endothelium in vitro are enhanced by astroglia.* J Neurosci, 1987. 7(10): p. 3293-9.
75. Dehouck, B., et al., *Upregulation of the low density lipoprotein receptor at the blood-brain barrier: intercommunications between brain capillary endothelial cells and astrocytes.* J Cell Biol, 1994. 126(2): p. 465-73.
76. Gaillard, P.J., et al., *Establishment and functional characterization of an in vitro model of the blood-brain barrier, comprising a co-culture of brain capillary endothelial cells and astrocytes.* Eur J Pharm Sci, 2001. 12(3): p. 215-22.
77. Arthur, F.E., R.R. Shivers, and P.D. Bowman, *Astrocyte-mediated induction of tight junctions in brain capillary endothelium: an efficient in vitro model.* Brain Res, 1987. 433(1): p. 155-9.
78. Maxwell, K., J.A. Berliner, and P.A. Cancilla, *Induction of gamma-glutamyl transpeptidase in cultured cerebral endothelial cells by a product released by astrocytes.* Brain Res, 1987. 410(2): p. 309-14.
79. Prat, A., et al., *Glial cell influence on the human blood-brain barrier.* Glia, 2001. 36(2): p. 145-55.
80. Tran, N.D., et al., *Transforming growth factor-beta mediates astrocyte-specific regulation of brain endothelial anticoagulant factors.* Stroke, 1999. 30(8): p. 1671-8.
81. Sobue, K., et al., *Induction of blood-brain barrier properties in immortalized bovine brain endothelial cells by astrocytic factors.* Neurosci Res, 1999. 35(2): p. 155-64.
82. Sun, D., C. Lytle, and M.E. O'Donnell, *IL-6 secreted by astroglial cells regulates Na-K-Cl cotransport in brain microvessel endothelial cells.* Am J Physiol, 1997. 272(6 Pt 1): p. C1829-35.
83. Stanimirovic, D.B., R. Ball, and J.P. Durkin, *Evidence for the role of protein kinase C in astrocyte-induced proliferation of rat cerebromicrovascular endothelial cells.* Neurosci Lett, 1995. 197(3): p. 219-22.
84. Saijo, K. and C.K. Glass, *Microglial cell origin and phenotypes in health and disease.* Nat Rev Immunol, 2011. 11(11): p. 775-787.
85. Fantin, A., et al., *Tissue macrophages act as cellular chaperones for vascular anastomosis downstream of VEGF-mediated endothelial tip cell induction.* Blood, 2010. 116(5): p. 829-40.
86. Tammela, T., et al., *VEGFR-3 controls tip to stalk conversion at vessel fusion sites by reinforcing Notch signalling.* Nat Cell Biol, 2011. 13(10): p. 1202-13.
87. Kreutzberg, G.W., *Microglia: a sensor for pathological events in the CNS.* Trends Neurosci, 1996. 19(8): p. 312-8.

88. Fonseca, A.C.C.D., et al., *The impact of microglial activation on blood-brain barrier in brain diseases.* Frontiers in Cellular Neuroscience, 2014. 8.
89. Schlageter, K.E., et al., *Microvessel organization and structure in experimental brain tumors: microvessel populations with distinctive structural and functional properties.* Microvasc Res, 1999. 58(3): p. 312-28.
90. Harder, D.R., et al., *Functional hyperemia in the brain: hypothesis for astrocyte-derived vasodilator metabolites.* Stroke, 1998. 29(1): p. 229-34.
91. Lou, H.C., L. Edvinsson, and E.T. MacKenzie, *The concept of coupling blood flow to brain function: revision required?* Ann Neurol, 1987. 22(3): p. 289-97.
92. Villringer, A. and U. Dirnagl, *Coupling of brain activity and cerebral blood flow: basis of functional neuroimaging.* Cerebrovasc Brain Metab Rev, 1995. 7(3): p. 240-76.
93. Zonta, M., et al., *Neuron-to-astrocyte signaling is central to the dynamic control of brain microcirculation.* Nat Neurosci, 2003. 6(1): p. 43-50.
94. Tsacopoulos, M. and P.J. Magistretti, *Metabolic coupling between glia and neurons.* J Neurosci, 1996. 16(3): p. 877-85.
95. Pellerin, L., *Lactate as a pivotal element in neuron-glia metabolic cooperation.* Neurochem Int, 2003. 43(4-5): p. 331-8.
96. Fillenz, M., et al., *The role of astrocytes and noradrenaline in neuronal glucose metabolism.* Acta Physiol Scand, 1999. 167(4): p. 275-84.
97. Leybaert, L., *Neurobarrier coupling in the brain: a partner of neurovascular and neurometabolic coupling?* J Cereb Blood Flow Metab, 2005. 25(1): p. 2-16.
98. Cornford, E.M., E.V. Nguyen, and E.M. Landaw, *Acute upregulation of blood-brain barrier glucose transporter activity in seizures.* Am J Physiol Heart Circ Physiol, 2000. 279(3): p. H1346-54.
99. Gronlund, K.M., et al., *Chronic seizures increase glucose transporter abundance in rat brain.* J Neuropathol Exp Neurol, 1996. 55(7): p. 832-40.
100. Farrell, C.L. and W.M. Pardridge, *Blood-brain barrier glucose transporter is asymmetrically distributed on brain capillary endothelial lumenal and ablumenal membranes: an electron microscopic immunogold study.* Proceedings of the National Academy of Sciences of the United States of America, 1991. 88(13): p. 5779-5783.
101. Pardridge, W.M., *Introduction to the Blood-Brain Barrier: Methodology, Biology and Pathology*. 2006: Cambridge University Press.
102. Braet, K., et al., *Astrocyte-endothelial cell calcium signals conveyed by two signalling pathways.* Eur J Neurosci, 2001. 13(1): p. 79-91.
103. Leybaert, L., et al., *Inositol-trisphosphate-dependent intercellular calcium signaling in and between astrocytes and endothelial cells.* Glia, 1998. 24(4): p. 398-407.
104. McKinley Michael J., C.I.J., Oldfield Brian J, *Circumventricular organs*, in *The Human Nervous System*, P.G. Mai Juergen K, Editor. 2012, Elsevier USA. p. 594-617.
105. Johnson, A.K. and P.M. Gross, *Sensory circumventricular organs and brain homeostatic pathways.* Faseb j, 1993. 7(8): p. 678-86.
106. Cottrell, G.T. and A.V. Ferguson, *Sensory circumventricular organs: central roles in integrated autonomic regulation.* Regul Pept, 2004. 117(1): p. 11-23.
107. Fry, M. and A.V. Ferguson, *The sensory circumventricular organs: brain targets for circulating signals controlling ingestive behavior.* Physiol Behav, 2007. 91(4): p. 413-23.
108. Ganong, W.F., *Circumventricular organs: definition and role in the regulation of endocrine and autonomic function.* Clin Exp Pharmacol Physiol, 2000. 27(5-6): p. 422-7.
109. Huynh, G.H., D.F. Deen, and F.C. Szoka, Jr., *Barriers to carrier mediated drug and gene delivery to brain tumors.* J Control Release, 2006. 110(2): p. 236-59.
110. Johanson, C.E., et al., *Multiplicity of cerebrospinal fluid functions: New challenges in health and disease.* Cerebrospinal Fluid Res, 2008. 5: p. 10.

111. Edsbagge, M., et al., *Spinal CSF absorption in healthy individuals.* Am J Physiol Regul Integr Comp Physiol, 2004. 287(6): p. R1450-5.
112. Perez-Figares, J.M., A.J. Jimenez, and E.M. Rodriguez, *Subcommissural organ, cerebrospinal fluid circulation, and hydrocephalus.* Microsc Res Tech, 2001. 52(5): p. 591-607.
113. Rudick, R.A., D.K. Zirretta, and R.M. Herndon, *Clearance of albumin from mouse subarachnoid space: a measure of CSF bulk flow.* J Neurosci Methods, 1982. 6(3): p. 253-9.
114. Pollay, M., F.A. Stevens, and P.A. Roberts, *Alteration in Choroid-Plexus Blood Flow and Cerebrospinal- Fluid Formation by Increased Ventricular Pressure*, in *Neurobiology of Cerebrospinal Fluid 2*, J. Wood, Editor. 1983, Springer US. p. 687-695.
115. Swetloff, A. and P. Ferretti, *Changes in E2F5 intracellular localization in mouse and human choroid plexus epithelium with development.* Int J Dev Biol, 2005. 49(7): p. 859-65.
116. Johanson, C.E., D.J. Reed, and D.M. Woodbury, *Active transport of sodium and potassium by the choroid plexus of the rat.* The Journal of Physiology, 1974. 241(2): p. 359-372.
117. Praetorius, J., *Water and solute secretion by the choroid plexus.* Pflugers Arch, 2007. 454(1): p. 1-18.
118. Praetorius, J., L.N. Nejsum, and S. Nielsen, *A SCL4A10 gene product maps selectively to the basolateral plasma membrane of choroid plexus epithelial cells.* Am J Physiol Cell Physiol, 2004. 286(3): p. C601-10.
119. Johanson, C.E., Z. Parandoosh, and M.L. Dyas, *Maturational differences in acetazolamide-altered pH and HCO3 of choroid plexus, cerebrospinal fluid, and brain.* Am J Physiol, 1992. 262(5 Pt 2): p. R909-14.
120. Johanson, C.E., Z. Parandoosh, and Q.R. Smith, *Cl-HCO3 exchange in choroid plexus: analysis by the DMO method for cell pH.* Am J Physiol, 1985. 249(4 Pt 2): p. F478-84.
121. Zlokovic, B.V., et al., *Differential expression of Na,K-ATPase alpha and beta subunit isoforms at the blood-brain barrier and the choroid plexus.* J Biol Chem, 1993. 268(11): p. 8019-25.
122. Keep, R.F., J. Xiang, and A.L. Betz, *Potassium cotransport at the rat choroid plexus.* Am J Physiol, 1994. 267(6 Pt 1): p. C1616-22.
123. Brown, P.D., et al., *Molecular Mechanisms of Cerebrospinal Fluid Production.* Neuroscience, 2004. 129(4): p. 957-970.
124. Johanson, C.E., *Differential effects of acetazolamide, benzolamide and systemic acidosis on hydrogen and bicarbonate gradients across the apical and basolateral membranes of the choroid plexus.* J Pharmacol Exp Ther, 1984. 231(3): p. 502-11.
125. Johanson, C.E., D.J. Reed, and D.M. Woodbury, *Developmental studies of the compartmentalization of water and electrolytes in the choroid plexus of the neonatal rat brain.* Brain Res, 1976. 116(1): p. 35-48.
126. Smith, Q.R. and C.E. Johanson, *Active transport of chloride by lateral ventricle choroid plexus of the rat.* Am J Physiol, 1985. 249(4 Pt 2): p. F470-7.
127. Bondy, C., et al., *Developmental gene expression and tissue distribution of the CHIP28 water-channel protein.* Proceedings of the National Academy of Sciences of the United States of America, 1993. 90(10): p. 4500-4504.
128. Davson, H. and M.B. Segal, *Physiology of the CSF and Blood-Brain Barriers*. 1995: Taylor & Francis.
129. Johnston, M., et al., *Subarachnoid injection of Microfil reveals connections between cerebrospinal fluid and nasal lymphatics in the non-human primate.* Neuropathol Appl Neurobiol, 2005. 31(6): p. 632-40.
130. Koh, L., et al., *Development of cerebrospinal fluid absorption sites in the pig and rat: connections between the subarachnoid space and lymphatic vessels in the olfactory turbinates.* Anat Embryol (Berl), 2006. 211(4): p. 335-44.

131. Zakharov, A., et al., *Integrating the roles of extracranial lymphatics and intracranial veins in cerebrospinal fluid absorption in sheep.* Microvasc Res, 2004. 67(1): p. 96-104.
132. Boulton, M., et al., *Contribution of extracranial lymphatics and arachnoid villi to the clearance of a CSF tracer in the rat.* Am J Physiol, 1999. 276(3 Pt 2): p. R818-23.
133. Johnston, M., et al., *Evidence of connections between cerebrospinal fluid and nasal lymphatic vessels in humans, non-human primates and other mammalian species.* Cerebrospinal Fluid Res, 2004. 1(1): p. 2.
134. Mollanji, R., et al., *Comparison of cerebrospinal fluid transport in fetal and adult sheep.* Am J Physiol Regul Integr Comp Physiol, 2001. 281(4): p. R1215-23.
135. Upton, M.L. and R.O. Weller, *The morphology of cerebrospinal fluid drainage pathways in human arachnoid granulations.* J Neurosurg, 1985. 63(6): p. 867-75.
136. Abbott, N.J., *Evidence for bulk flow of brain interstitial fluid: significance for physiology and pathology.* Neurochem Int, 2004. 45(4): p. 545-52.
137. O'Donnell, M.E., et al., *Estradiol reduces activity of the blood-brain barrier Na-K-Cl cotransporter and decreases edema formation in permanent middle cerebral artery occlusion.* J Cereb Blood Flow Metab, 2006. 26(10): p. 1234-49.
138. Vorbrodt, A.W., *Ultrastructural cytochemistry of blood-brain barrier endothelia.* Prog Histochem Cytochem, 1988. 18(3): p. 1-99.
139. Sanchez del Pino, M.M., R.A. Hawkins, and D.R. Peterson, *Biochemical discrimination between luminal and abluminal enzyme and transport activities of the blood-brain barrier.* J Biol Chem, 1995. 270(25): p. 14907-12.
140. Millar, I.D. and P.D. Brown, *NBCe2 exhibits a 3 HCO3(-):1 Na+ stoichiometry in mouse choroid plexus epithelial cells.* Biochem Biophys Res Commun, 2008. 373(4): p. 550-4.
141. Taylor, C.J., et al., *Transporters involved in regulation of intracellular pH in primary cultured rat brain endothelial cells.* J Physiol, 2006. 576(Pt 3): p. 769-85.
142. Nicola, P.A., et al., *Transport activities involved in intracellular pH recovery following acid and alkali challenges in rat brain microvascular endothelial cells.* Pflugers Arch, 2008. 456(5): p. 801-12.
143. Vigne, P., A. Lopez Farre, and C. Frelin, *Na(+)-K(+)-Cl- cotransporter of brain capillary endothelial cells. Properties and regulation by endothelins, hyperosmolar solutions, calyculin A, and interleukin-1.* J Biol Chem, 1994. 269(31): p. 19925-30.
144. Cserr, H.F., et al., *Efflux of radiolabeled polyethylene glycols and albumin from rat brain.* Am J Physiol, 1981. 240(4): p. F319-28.
145. Szentistvanyi, I., et al., *Drainage of interstitial fluid from different regions of rat brain.* Am J Physiol, 1984. 246(6 Pt 2): p. F835-44.
146. Geer, C.P. and S.A. Grossman, *Interstitial fluid flow along white matter tracts: a potentially important mechanism for the dissemination of primary brain tumors.* J Neurooncol, 1997. 32(3): p. 193-201.
147. Konsman, J.P., V. Tridon, and R. Dantzer, *Diffusion and action of intracerebroventricularly injected interleukin-1 in the CNS.* Neuroscience, 2000. 101(4): p. 957-67.
148. Rennels, M.L., et al., *Evidence for a 'paravascular' fluid circulation in the mammalian central nervous system, provided by the rapid distribution of tracer protein throughout the brain from the subarachnoid space.* Brain Res, 1985. 326(1): p. 47-63.
149. Rennels, M.L., O.R. Blaumanis, and P.A. Grady, *Rapid solute transport throughout the brain via paravascular fluid pathways.* Adv Neurol, 1990. 52: p. 431-9.
150. Proescholdt, M.G., et al., *Studies of cerebrospinal fluid flow and penetration into brain following lateral ventricle and cisterna magna injections of the tracer [14C]inulin in rat.* Neuroscience, 2000. 95(2): p. 577-92.

151. Weller, R.O., S. Kida, and E.T. Zhang, *Pathways of fluid drainage from the brain--morphological aspects and immunological significance in rat and man.* Brain Pathol, 1992. 2(4): p. 277-84.
152. Zhang, E.T., et al., *Directional and compartmentalised drainage of interstitial fluid and cerebrospinal fluid from the rat brain.* Acta Neuropathol, 1992. 83(3): p. 233-9.
153. Iliff, J.J., et al., *A paravascular pathway facilitates CSF flow through the brain parenchyma and the clearance of interstitial solutes, including amyloid beta.* Sci Transl Med, 2012. 4(147): p. 147ra111.
154. Hadaczek, P., et al., *The "perivascular pump" driven by arterial pulsation is a powerful mechanism for the distribution of therapeutic molecules within the brain.* Mol Ther, 2006. 14(1): p. 69-78.
155. Schley, D., et al., *Mechanisms to explain the reverse perivascular transport of solutes out of the brain.* J Theor Biol, 2006. 238(4): p. 962-74.
156. Nedergaard, M., *Garbage Truck of the Brain.* Science (New York, N.Y.), 2013. 340(6140): p. 1529-1530.
157. Nicholson, C. and E. Sykova, *Extracellular space structure revealed by diffusion analysis.* Trends Neurosci, 1998. 21(5): p. 207-15.
158. Sykova, E., *Extrasynaptic volume transmission and diffusion parameters of the extracellular space.* Neuroscience, 2004. 129(4): p. 861-76.
159. Sykova, E. and L. Vargova, *Extrasynaptic transmission and the diffusion parameters of the extracellular space.* Neurochem Int, 2008. 52(1-2): p. 5-13.
160. Cserr, H.F., *Physiology of the choroid plexus.* Physiol Rev, 1971. 51(2): p. 273-311.
161. Groothuis, D.R., et al., *Efflux of drugs and solutes from brain: the interactive roles of diffusional transcapillary transport, bulk flow and capillary transporters.* J Cereb Blood Flow Metab, 2007. 27(1): p. 43-56.
162. Slaney, T.R., et al., *Chemical Gradients within Brain Extracellular Space Measured using Low Flow Push–Pull Perfusion Sampling in Vivo.* ACS Chemical Neuroscience, 2013. 4(2): p. 321-329.
163. Irani, D.N., *CHAPTER 10 - Properties and Composition of Normal Cerebrospinal Fluid*, in *Cerebrospinal Fluid in Clinical Practice*, D.N. Irani, Editor. 2009, W.B. Saunders: Philadelphia. p. 69-89.
164. Boron, W.F. and E.L. Boulpaep, *Medical Physiology, 2e Updated Edition: with STUDENT CONSULT Online Access*. 2012: Elsevier Health Sciences.
165. Lund-Andersen, H. and L. Hertz, *Effects of potassium and of glutamate on swelling and on sodium and potassium content in brain-cortex slices from adult rats.* Experimental Brain Research, 1970. 11(2): p. 199-212.
166. Bourke, R.S. and K.M. Nelson, *FURTHER STUDIES ON THE K+-DEPENDENT SWELLING OF PRIMATE CEREBRAL CORTEX IN VIVO: THE ENZYMATIC BASIS OF THE K+-DEPENDENT TRANSPORT OF CHLORIDE.* Journal of Neurochemistry, 1972. 19(3): p. 663-685.
167. Lowry, J.P., et al., *Continuous monitoring of extracellular glucose concentrations in the striatum of freely moving rats with an implanted glucose biosensor.* J Neurochem, 1998. 70(1): p. 391-6.
168. Fellows, L.K., M.G. Boutelle, and M. Fillenz, *Extracellular brain glucose levels reflect local neuronal activity: a microdialysis study in awake, freely moving rats.* J Neurochem, 1992. 59(6): p. 2141-7.
169. Fray, A.E., M. Boutelle, and M. Fillenz, *Extracellular glucose turnover in the striatum of unanaesthetized rats measured by quantitative microdialysis.* J Physiol, 1997. 504 (Pt 3): p. 721-6.

170. Abi-Saab, W.M., et al., *Striking differences in glucose and lactate levels between brain extracellular fluid and plasma in conscious human subjects: effects of hyperglycemia and hypoglycemia.* J Cereb Blood Flow Metab, 2002. 22(3): p. 271-9.
171. Lerma, J., et al., *In vivo determination of extracellular concentration of amino acids in the rat hippocampus. A method based on brain dialysis and computerized analysis.* Brain Research, 1986. 384(1): p. 145-155.
172. Kanamori, K. and B.D. Ross, *Quantitative determination of extracellular glutamine concentration in rat brain, and its elevation in vivo by system A transport inhibitor, alpha-(methylamino)isobutyrate.* J Neurochem, 2004. 90(1): p. 203-10.
173. de Vries, M.G., et al., *Extracellular glucose in rat ventromedial hypothalamus during acute and recurrent hypoglycemia.* Diabetes, 2003. 52(11): p. 2767-73.
174. Silver, I.A. and M. Erecinska, *Extracellular glucose concentration in mammalian brain: continuous monitoring of changes during increased neuronal activity and upon limitation in oxygen supply in normo-, hypo-, and hyperglycemic animals.* J Neurosci, 1994. 14(8): p. 5068-76.
175. Steffens, A.B., et al., *Penetration of peripheral glucose and insulin into cerebrospinal fluid in rats.* Am J Physiol, 1988. 255(2 Pt 2): p. R200-4.
176. Ronne-Engstrom, E., et al., *Influence of perfusate glucose concentration on dialysate lactate, pyruvate, aspartate, and glutamate levels under basal and hypoxic conditions: a microdialysis study in rat brain.* J Neurochem, 1995. 65(1): p. 257-62.
177. McNay, E.C. and P.E. Gold, *Extracellular glucose concentrations in the rat hippocampus measured by zero-net-flux: effects of microdialysis flow rate, strain, and age.* J Neurochem, 1999. 72(2): p. 785-90.
178. Begley, D.J., A. Reichel, and A. Ermisch, *Simple high-performance liquid chromatographic analysis of free primary amino acid concentrations in rat plasma and cisternal cerebrospinal fluid.* J Chromatogr B Biomed Appl, 1994. 657(1): p. 185-91.
179. Miele, M., et al., *The determination of the extracellular concentration of brain glutamate using quantitative microdialysis.* Brain Res, 1996. 707(1): p. 131-3.
180. Osborne, P.G., et al., *Determination of striatal extracellular gamma-aminobutyric acid in non-hibernating and hibernating arctic ground squirrels using quantitative microdialysis.* Brain Res, 1999. 839(1): p. 1-6.
181. Xi, Z.X., et al., *GABA transmission in the nucleus accumbens is altered after withdrawal from repeated cocaine.* J Neurosci, 2003. 23(8): p. 3498-505.
182. Wagner, I. and H. Musso, *New Naturally Occurring Amino Acids.* Angewandte Chemie International Edition in English, 1983. 22(11): p. 816-828.
183. Lehninger, A., D. Nelson, and M. Cox, *Lehninger Principles of Biochemistry*. 2008: W. H. Freeman.
184. Freitas, R.A., *Nanomedicine*. Vol. Chapter 3.1. 1999: Landes Bioscience.
185. World Health Organization, F.a.A.O.o.t.U.N., United Nations University, *Protein and amino acid requirements in human nutrition. Report of a joint FAO/WHO/UNU expert consultation (WHO Technical Report Series 935)*. 2007. p. 265.
186. Wu, G., *Amino acids: metabolism, functions, and nutrition.* Amino Acids, 2009. 37(1): p. 1-17.
187. Tapiero, H., et al., *II. Glutamine and glutamate.* Biomed Pharmacother, 2002. 56(9): p. 446-57.
188. Brosnan, J.T., *Glutamate, at the interface between amino acid and carbohydrate metabolism.* J Nutr, 2000. 130(4S Suppl): p. 988s-90s.
189. Felig, P., et al., *Alanine: key role in gluconeogenesis.* Science, 1970. 167(3920): p. 1003-4.

190. Wise, D.R. and C.B. Thompson, *Glutamine addiction: a new therapeutic target in cancer.* Trends Biochem Sci, 2010. 35(8): p. 427-33.
191. House, J.D., B.N. Hall, and J.T. Brosnan, *Threonine metabolism in isolated rat hepatocytes.* Am J Physiol Endocrinol Metab, 2001. 281(6): p. E1300-7.
192. Newsholme, P., et al., *Glutamine and glutamate as vital metabolites.* Braz J Med Biol Res, 2003. 36(2): p. 153-63.
193. Curi, R., et al., *Molecular mechanisms of glutamine action.* J Cell Physiol, 2005. 204(2): p. 392-401.
194. Morris, S.M., Jr., *Regulation of enzymes of the urea cycle and arginine metabolism.* Annu Rev Nutr, 2002. 22: p. 87-105.
195. Wallner, S., et al., *The alpha-amino group of L-arginine mediates its antioxidant effect.* Eur J Clin Invest, 2001. 31(2): p. 98-102.
196. Lawler, J.M., et al., *Direct antioxidant properties of creatine.* Biochem Biophys Res Commun, 2002. 290(1): p. 47-52.
197. Machlin, L.J. and A. Bendich, *Free radical tissue damage: protective role of antioxidant nutrients.* Faseb j, 1987. 1(6): p. 441-5.
198. Bellon, G., et al., *Glutamine increases collagen gene transcription in cultured human fibroblasts.* Biochim Biophys Acta, 1995. 1268(3): p. 311-23.
199. Brasse-Lagnel, C., et al., *Glutamine stimulates argininosuccinate synthetase gene expression through cytosolic O-glycosylation of Sp1 in Caco-2 cells.* J Biol Chem, 2003. 278(52): p. 52504-10.
200. Huang, Y.F., Y. Wang, and M. Watford, *Glutamine directly downregulates glutamine synthetase protein levels in mouse C2C12 skeletal muscle myotubes.* J Nutr, 2007. 137(6): p. 1357-62.
201. Jobgen, W., et al., *High fat feeding and dietary L-arginine supplementation differentially regulate gene expression in rat white adipose tissue.* Amino Acids, 2009. 37(1): p. 187-98.
202. Leong, H.X., et al., *Short-term arginine deprivation results in large-scale modulation of hepatic gene expression in both normal and tumor cells: microarray bioinformatic analysis.* Nutrition & Metabolism, 2006. 3: p. 37-37.
203. Wang, J., et al., *Gene expression is altered in piglet small intestine by weaning and dietary glutamine supplementation.* J Nutr, 2008. 138(6): p. 1025-32.
204. Escobar, J., et al., *Physiological rise in plasma leucine stimulates muscle protein synthesis in neonatal pigs by enhancing translation initiation factor activation.* Am J Physiol Endocrinol Metab, 2005. 288(5): p. E914-21.
205. Escobar, J., et al., *Regulation of cardiac and skeletal muscle protein synthesis by individual branched-chain amino acids in neonatal pigs.* Am J Physiol Endocrinol Metab, 2006. 290(4): p. E612-21.
206. Meijer, A.J. and P.F. Dubbelhuis, *Amino acid signalling and the integration of metabolism.* Biochem Biophys Res Commun, 2004. 313(2): p. 397-403.
207. Yao, K., et al., *Dietary arginine supplementation increases mTOR signaling activity in skeletal muscle of neonatal pigs.* J Nutr, 2008. 138(5): p. 867-72.
208. Meijer, A.J., *Amino acids as regulators and components of nonproteinogenic pathways.* J Nutr, 2003. 133(6 Suppl 1): p. 2057s-2062s.
209. Moncada, S. and E.A. Higgs, *Molecular mechanisms and therapeutic strategies related to nitric oxide.* Faseb j, 1995. 9(13): p. 1319-30.
210. Palmer, R.M., D.S. Ashton, and S. Moncada, *Vascular endothelial cells synthesize nitric oxide from L-arginine.* Nature, 1988. 333(6174): p. 664-6.
211. Wu, G. and S.M. Morris, Jr., *Arginine metabolism: nitric oxide and beyond.* Biochem J, 1998. 336 (Pt 1): p. 1-17.

212. Curtis, D.R. and G.A. Johnston, *Amino acid transmitters in the mammalian central nervous system.* Ergeb Physiol, 1974. 69(0): p. 97-188.
213. Curtis, D.R., L. Hosli, and G.A. Johnston, *Inhibition of spinal neurons by glycine.* Nature, 1967. 215(5109): p. 1502-3.
214. Bowery, N.G. and T.G. Smart, *GABA and glycine as neurotransmitters: a brief history.* Br J Pharmacol, 2006. 147 Suppl 1: p. S109-19.
215. Johnson, J.W. and P. Ascher, *Glycine potentiates the NMDA response in cultured mouse brain neurons.* Nature, 1987. 325(6104): p. 529-531.
216. Zafra, F., C. Aragon, and C. Gimenez, *Molecular biology of glycinergic neurotransmission.* Mol Neurobiol, 1997. 14(3): p. 117-42.
217. Oda, M., et al., *Direct correlation between ischemic injury and extracellular glycine concentration in mice with genetically altered activities of the glycine cleavage multienzyme system.* Stroke, 2007. 38(7): p. 2157-64.
218. Sakata, Y., et al., *Structure and expression of the glycine cleavage system in rat central nervous system.* Brain Res Mol Brain Res, 2001. 94(1-2): p. 119-30.
219. Sato, K., et al., *Glycine cleavage system in astrocytes.* Brain Res, 1991. 567(1): p. 64-70.
220. Kojima-ishii, K., et al., *Model mice for mild-form glycine encephalopathy: behavioral and biochemical characterizations and efficacy of antagonists for the glycine binding site of N-methyl D-aspartate receptor.* Pediatr Res, 2008. 64(3): p. 228-33.
221. Jimenez-Jimenez, F.J., et al., *Cerebrospinal fluid biochemical studies in patients with Parkinson's disease: toward a potential search for biomarkers for this disease.* Front Cell Neurosci, 2014. 8: p. 369.
222. DeFelipe, J., *Neocortical neuronal diversity: chemical heterogeneity revealed by colocalization studies of classic neurotransmitters, neuropeptides, calcium-binding proteins, and cell surface molecules.* Cereb Cortex, 1993. 3(4): p. 273-89.
223. Ribak CE, Y.X.-X., *GABA neurons in the neocortex*, in *GABA in the Nervous System: The View at Fifty Years*, O.R. Martin DL, Editor. 2000, Lippincott Williams & Wilkins: Philadelphia, PA. p. 357-368.
224. Petroff, O.A., *GABA and glutamate in the human brain.* Neuroscientist, 2002. 8(6): p. 562-73.
225. Watanabe, M., et al., *GABA and GABA Receptors in the Central Nervous System and Other Organs*, in *International Review of Cytology*, W.J. Kwang, Editor. 2002, Academic Press. p. 1-47.
226. Conti, F., A. Minelli, and M. Melone, *GABA transporters in the mammalian cerebral cortex: localization, development and pathological implications.* Brain Res Brain Res Rev, 2004. 45(3): p. 196-212.
227. During, M.J., K.M. Ryder, and D.D. Spencer, *Hippocampal GABA transporter function in temporal-lobe epilepsy.* Nature, 1995. 376(6536): p. 174-7.
228. Wood, J.H., et al., *Low cerebrospinal fluid gamma-aminobutyric acid content in seizure patients.* Neurology, 1979. 29(9 Pt 1): p. 1203-8.
229. Curtis, D.R., J.W. Phillis, and J.C. Watkins, *The chemical excitation of spinal neurones by certain acidic amino acids.* The Journal of Physiology, 1960. 150(3): p. 656-682.
230. Brodal, P., *The Central Nervous System*. 2010: Oxford University Press.
231. Puri, B. and I. Treasaden, *Psychiatry: An evidence-based text*. 2009: Taylor & Francis.
232. McKenna, M.C., et al., *Aspartate aminotransferase in synaptic and nonsynaptic mitochondria: differential effect of compounds that influence transient hetero-enzyme complex (metabolon) formation.* Neurochem Int, 2006. 48(6-7): p. 629-36.
233. Zhou, Y. and N.C. Danbolt, *Glutamate as a neurotransmitter in the healthy brain.* Journal of Neural Transmission, 2014. 121(8): p. 799-817.

234. Choi, D.W., *Glutamate neurotoxicity and diseases of the nervous system.* Neuron, 1988. 1(8): p. 623-34.
235. Arriza, J.L., et al., *Excitatory amino acid transporter 5, a retinal glutamate transporter coupled to a chloride conductance.* Proceedings of the National Academy of Sciences of the United States of America, 1997. 94(8): p. 4155-4160.
236. Fairman, W.A., et al., *An excitatory amino-acid transporter with properties of a ligand-gated chloride channel.* Nature, 1995. 375(6532): p. 599-603.
237. Pines, G., et al., *Cloning and expression of a rat brain L-glutamate transporter.* Nature, 1992. 360(6403): p. 464-7.
238. Storck, T., et al., *Structure, expression, and functional analysis of a Na(+)-dependent glutamate/aspartate transporter from rat brain.* Proc Natl Acad Sci U S A, 1992. 89(22): p. 10955-9.
239. Klockner, U., et al., *Electrogenic L-glutamate uptake in Xenopus laevis oocytes expressing a cloned rat brain L-glutamate/L-aspartate transporter (GLAST-1).* J Biol Chem, 1993. 268(20): p. 14594-6.
240. Levy, L.M., O. Warr, and D. Attwell, *Stoichiometry of the glial glutamate transporter GLT-1 expressed inducibly in a Chinese hamster ovary cell line selected for low endogenous Na+-dependent glutamate uptake.* J Neurosci, 1998. 18(23): p. 9620-8.
241. Owe, S.G., P. Marcaggi, and D. Attwell, *The ionic stoichiometry of the GLAST glutamate transporter in salamander retinal glia.* J Physiol, 2006. 577(Pt 2): p. 591-9.
242. Zerangue, N. and M.P. Kavanaugh, *Flux coupling in a neuronal glutamate transporter.* Nature, 1996. 383(6601): p. 634-7.
243. Bannai, S., *Exchange of cystine and glutamate across plasma membrane of human fibroblasts.* J Biol Chem, 1986. 261(5): p. 2256-63.
244. Sato, H., et al., *Cloning and expression of a plasma membrane cystine/glutamate exchange transporter composed of two distinct proteins.* J Biol Chem, 1999. 274(17): p. 11455-8.
245. Gameiro, A., et al., *The Discovery of Slowness: Low-Capacity Transport and Slow Anion Channel Gating by the Glutamate Transporter EAAT5.* Biophysical Journal, 2011. 100(11): p. 2623-2632.
246. Mim, C., et al., *The glutamate transporter subtypes EAAT4 and EAATs 1-3 transport glutamate with dramatically different kinetics and voltage dependence but share a common uptake mechanism.* J Gen Physiol, 2005. 126(6): p. 571-89.
247. Schneider, N., et al., *Functional properties of the retinal glutamate transporters GLT-1c and EAAT5.* J Biol Chem, 2014. 289(3): p. 1815-24.
248. Veruki, M.L., S.H. Morkve, and E. Hartveit, *Activation of a presynaptic glutamate transporter regulates synaptic transmission through electrical signaling.* Nat Neurosci, 2006. 9(11): p. 1388-96.
249. de Vivo, L., et al., *GLT-1 Promoter Activity in Astrocytes and Neurons of Mouse Hippocampus and Somatic Sensory Cortex.* Front Neuroanat, 2010. 3: p. 31.
250. Dehnes, Y., et al., *The glutamate transporter EAAT4 in rat cerebellar Purkinje cells: a glutamate-gated chloride channel concentrated near the synapse in parts of the dendritic membrane facing astroglia.* J Neurosci, 1998. 18(10): p. 3606-19.
251. Holmseth, S., et al., *The density of EAAC1 (EAAT3) glutamate transporters expressed by neurons in the mammalian CNS.* J Neurosci, 2012. 32(17): p. 6000-13.
252. Massie, A., et al., *High-affinity Na+/K+-dependent glutamate transporter EAAT4 is expressed throughout the rat fore- and midbrain.* J Comp Neurol, 2008. 511(2): p. 155-72.
253. Rothstein, J.D., et al., *Localization of neuronal and glial glutamate transporters.* Neuron, 1994. 13(3): p. 713-25.

254. Shashidharan, P., et al., *Immunohistochemical localization of the neuron-specific glutamate transporter EAAC1 (EAAT3) in rat brain and spinal cord revealed by a novel monoclonal antibody.* Brain Res, 1997. 773(1-2): p. 139-48.
255. Berger, U.V., et al., *Cellular and subcellular mRNA localization of glutamate transporter isoforms GLT1a and GLT1b in rat brain by in situ hybridization.* J Comp Neurol, 2005. 492(1): p. 78-89.
256. Chaudhry, F.A., et al., *Glutamate transporters in glial plasma membranes: highly differentiated localizations revealed by quantitative ultrastructural immunocytochemistry.* Neuron, 1995. 15(3): p. 711-20.
257. Danbolt, N.C., J. Storm-Mathisen, and B.I. Kanner, *An [Na+ + K+]coupled L-glutamate transporter purified from rat brain is located in glial cell processes.* Neuroscience, 1992. 51(2): p. 295-310.
258. Holmseth, S., et al., *The concentrations and distributions of three C-terminal variants of the GLT1 (EAAT2; slc1a2) glutamate transporter protein in rat brain tissue suggest differential regulation.* Neuroscience, 2009. 162(4): p. 1055-71.
259. Lehre, K.P., et al., *Differential expression of two glial glutamate transporters in the rat brain: quantitative and immunocytochemical observations.* J Neurosci, 1995. 15(3 Pt 1): p. 1835-53.
260. Levy, L.M., et al., *A monoclonal antibody raised against an [Na(+)+K+]coupled L-glutamate transporter purified from rat brain confirms glial cell localization.* FEBS Lett, 1993. 317(1-2): p. 79-84.
261. Rauen, T., *Diversity of glutamate transporter expression and function in the mammalian retina.* Amino Acids, 2000. 19(1): p. 53-62.
262. Yamada, K., et al., *Glutamate transporter GLT-1 is transiently localized on growing axons of the mouse spinal cord before establishing astrocytic expression.* J Neurosci, 1998. 18(15): p. 5706-13.
263. Chen, W., et al., *The glutamate transporter GLT1a is expressed in excitatory axon terminals of mature hippocampal neurons.* J Neurosci, 2004. 24(5): p. 1136-48.
264. Furness, D.N., et al., *A quantitative assessment of glutamate uptake into hippocampal synaptic terminals and astrocytes: new insights into a neuronal role for excitatory amino acid transporter 2 (EAAT2).* Neuroscience, 2008. 157(1): p. 80-94.
265. Melone, M., M. Bellesi, and F. Conti, *Synaptic localization of GLT-1a in the rat somatic sensory cortex.* Glia, 2009. 57(1): p. 108-17.
266. Melone, M., et al., *Cellular and Synaptic Localization of EAAT2a in Human Cerebral Cortex.* Front Neuroanat, 2011. 4: p. 151.
267. Eliasof, S., et al., *Localization and function of five glutamate transporters cloned from the salamander retina.* Vision Res, 1998. 38(10): p. 1443-54.
268. Hertz, L., et al., *Astrocytes: glutamate producers for neurons.* J Neurosci Res, 1999. 57(4): p. 417-28.
269. Patel, M.S., *The effect of ketone bodies on pyruvate carboxylation by rat brain mitochondria.* J Neurochem, 1974. 23(4): p. 865-7.
270. Schousboe, A., et al., *Trafficking between glia and neurons of TCA cycle intermediates and related metabolites.* Glia, 1997. 21(1): p. 99-105.
271. Shank, R.P., et al., *Pyruvate carboxylase: an astrocyte-specific enzyme implicated in the replenishment of amino acid neurotransmitter pools.* Brain Res, 1985. 329(1-2): p. 364-7.
272. Yu, A.C., et al., *Pyruvate carboxylase activity in primary cultures of astrocytes and neurons.* J Neurochem, 1983. 41(5): p. 1484-7.
273. Bak, L.K., A. Schousboe, and H.S. Waagepetersen, *The glutamate/GABA-glutamine cycle: aspects of transport, neurotransmitter homeostasis and ammonia transfer.* J Neurochem, 2006. 98(3): p. 641-53.

274. Schousboe, A., L.K. Bak, and H.S. Waagepetersen, *Astrocytic Control of Biosynthesis and Turnover of the Neurotransmitters Glutamate and GABA.* Front Endocrinol (Lausanne), 2013. 4: p. 102.
275. Boulland, J.L., et al., *Cell-specific expression of the glutamine transporter SN1 suggests differences in dependence on the glutamine cycle.* Eur J Neurosci, 2002. 15(10): p. 1615-31.
276. Boulland, J.L., et al., *Highly differential expression of SN1, a bidirectional glutamine transporter, in astroglia and endothelium in the developing rat brain.* Glia, 2003. 41(3): p. 260-75.
277. Broer, S. and N. Brookes, *Transfer of glutamine between astrocytes and neurons.* J Neurochem, 2001. 77(3): p. 705-19.
278. Chaudhry, F.A., R.J. Reimer, and R.H. Edwards, *The glutamine commute: take the N line and transfer to the A.* J Cell Biol, 2002. 157(3): p. 349-55.
279. Cubelos, B., et al., *Amino acid transporter SNAT5 localizes to glial cells in the rat brain.* Glia, 2005. 49(2): p. 230-44.
280. Broer, A., et al., *Regulation of the glutamine transporter SN1 by extracellular pH and intracellular sodium ions.* J Physiol, 2002. 539(Pt 1): p. 3-14.
281. Deitmer, J.W., A. Bröer, and S. Bröer, *Glutamine efflux from astrocytes is mediated by multiple pathways.* Journal of Neurochemistry, 2003. 87(1): p. 127-135.
282. Kvamme, E., I.A. Torgner, and B. Roberg, *Kinetics and localization of brain phosphate activated glutaminase.* J Neurosci Res, 2001. 66(5): p. 951-8.
283. Varoqui, H., et al., *Cloning and functional identification of a neuronal glutamine transporter.* J Biol Chem, 2000. 275(6): p. 4049-54.
284. Chaudhry, F.A., et al., *Glutamine uptake by neurons: interaction of protons with system a transporters.* J Neurosci, 2002. 22(1): p. 62-72.
285. Behrens, P.F., et al., *Impaired glutamate transport and glutamate-glutamine cycling: downstream effects of the Huntington mutation.* Brain, 2002. 125(Pt 8): p. 1908-22.
286. Kanamori, K. and B.D. Ross, *Chronic electrographic seizure reduces glutamine and elevates glutamate in the extracellular fluid of rat brain.* Brain Res, 2011. 1371: p. 180-91.
287. Melo, T.M., A. Nehlig, and U. Sonnewald, *Metabolism is normal in astrocytes in chronically epileptic rats: a (13)C NMR study of neuronal-glial interactions in a model of temporal lobe epilepsy.* J Cereb Blood Flow Metab, 2005. 25(10): p. 1254-64.
288. Melo, T.M., et al., *Cortical glutamate metabolism is enhanced in a genetic model of absence epilepsy.* J Cereb Blood Flow Metab, 2006. 26(12): p. 1496-506.
289. Sechi, G., et al., *Co-variation of free amino acids in brain interstitial fluid during pentylenetetrazole-induced convulsive status epilepticus.* Brain Res, 1997. 764(1-2): p. 230-6.
290. Lin, A.P., et al., *Reduced glutamate neurotransmission in patients with Alzheimer's disease -- an in vivo (13)C magnetic resonance spectroscopy study.* Magma, 2003. 16(1): p. 29-42.
291. Berthet, C., et al., *Early predictive biomarkers for lesion after transient cerebral ischemia.* Stroke, 2011. 42(3): p. 799-805.
292. Haberg, A., et al., *Differences in neurotransmitter synthesis and intermediary metabolism between glutamatergic and GABAergic neurons during 4 hours of middle cerebral artery occlusion in the rat: the role of astrocytes in neuronal survival.* J Cereb Blood Flow Metab, 2001. 21(12): p. 1451-63.
293. Kontro, P., K.M. Marnela, and S.S. Oja, *Free amino acids in the synaptosome and synaptic vesicle fractions of different bovine brain areas.* Brain Res, 1980. 184(1): p. 129-41.
294. Palkovits, M., et al., *Taurine levels in discrete brain nuclei of rats.* J Neurochem, 1986. 47(5): p. 1333-5.
295. Pow, D.V., et al., *Localization of taurine transporters, taurine, and (3)H taurine accumulation in the rat retina, pituitary, and brain.* Glia, 2002. 37(2): p. 153-68.

296. Hussy, N., et al., *Osmotic regulation of neuronal activity: a new role for taurine and glial cells in a hypothalamic neuroendocrine structure.* Prog Neurobiol, 2000. 62(2): p. 113-34.
297. Kreisman, N.R. and J.E. Olson, *Taurine enhances volume regulation in hippocampal slices swollen osmotically.* Neuroscience, 2003. 120(3): p. 635-42.
298. Oja, S.S. and P. Saransaari, *Taurine as osmoregulator and neuromodulator in the brain.* Metab Brain Dis, 1996. 11(2): p. 153-64.
299. Pasantes-Morales, H., et al., *Osmosensitive release of neurotransmitter amino acids: relevance and mechanisms.* Neurochem Res, 2002. 27(1-2): p. 59-65.
300. Jasper, H.H. and I. Koyama, *Rate of release of amino acids from the cerebral cortex in the cat as affected by brainstem and thalamic stimulation.* Canadian Journal of Physiology and Pharmacology, 1969. 47(10): p. 889-905.
301. Wu, J.Y. and H. Prentice, *Role of taurine in the central nervous system.* J Biomed Sci, 2010. 17 Suppl 1: p. S1.
302. Belluzzi, O., et al., *Selective neuroinhibitory effects of taurine in slices of rat main olfactory bulb.* Neuroscience, 2004. 124(4): p. 929-44.
303. Oja, S.S., E.R. Korpi, and P. Saransaari, *Modification of chloride flux across brain membranes by inhibitory amino acids in developing and adult mice.* Neurochem Res, 1990. 15(8): p. 797-804.
304. Kontro, P. and S.S. Oja, *Taurine and GABA release from mouse cerebral cortex slices: potassium stimulation releases more taurine than GABA from developing brain.* Brain Res, 1987. 465(1-2): p. 277-91.
305. Menendez, N., et al., *Taurine release evoked by NMDA receptor activation is largely dependent on calcium mobilization from intracellular stores.* Eur J Neurosci, 1993. 5(10): p. 1273-9.
306. Saransaari, P. and S.S. Oja, *Excitatory amino acids evoke taurine release from cerebral cortex slices from adult and developing mice.* Neuroscience, 1991. 45(2): p. 451-9.
307. Saransaari, P. and S.S. Oja, *Taurine release from the developing and ageing hippocampus: stimulation by agonists of ionotropic glutamate receptors.* Mech Ageing Dev, 1997. 99(3): p. 219-32.
308. Saransaari, P. and S.S. Oja, *Characterization of N-methyl-D-aspartate-evoked taurine release in the developing and adult mouse hippocampus.* Amino Acids, 2003. 24(1-2): p. 213-21.
309. Semba, J., S. Kito, and M. Toru, *Characterisation of extracellular amino acids in striatum of freely moving rats by in vivo microdialysis.* J Neural Transm Gen Sect, 1995. 100(1): p. 39-52.
310. Kamisaki, Y., et al., *Effects of taurine on depolarization-evoked release of amino acids from rat cortical synaptosomes.* Brain Res, 1993. 627(2): p. 181-5.
311. Olson, J.E. and E. Martinho, Jr., *Regulation of taurine transport in rat hippocampal neurons by hypo-osmotic swelling.* J Neurochem, 2006. 96(5): p. 1375-89.
312. Benrabh, H., J.M. Bourre, and J.M. Lefauconnier, *Taurine transport at the blood-brain barrier: an in vivo brain perfusion study.* Brain Res, 1995. 692(1-2): p. 57-65.
313. El Idrissi, A. and E. Trenkner, *Growth factors and taurine protect against excitotoxicity by stabilizing calcium homeostasis and energy metabolism.* J Neurosci, 1999. 19(21): p. 9459-68.
314. Molchanova, S., S.S. Oja, and P. Saransaari, *Characteristics of basal taurine release in the rat striatum measured by microdialysis.* Amino Acids, 2004. 27(3-4): p. 261-8.
315. Boadle-Biber, M.C., *Regulation of serotonin synthesis.* Prog Biophys Mol Biol, 1993. 60(1): p. 1-15.

316. Fernstrom, J.D. and M.H. Fernstrom, *Tyrosine, phenylalanine, and catecholamine synthesis and function in the brain.* J Nutr, 2007. 137(6 Suppl 1): p. 1539S-1547S; discussion 1548S.
317. Fernstrom, J.D., *Aromatic amino acids and monoamine synthesis in the central nervous system: influence of the diet.* J Nutr Biochem, 1990. 1(10): p. 508-17.
318. Tagliamonte, A., et al., *Free tryptophan in serum controls brain tryptophan level and serotonin synthesis.* Life Sciences, 1973. 12(6, Part 2): p. 277-287.
319. Bacci, A., et al., *Block of glutamate-glutamine cycle between astrocytes and neurons inhibits epileptiform activity in hippocampus.* J Neurophysiol, 2002. 88(5): p. 2302-10.
320. Levine, J., et al., *Increased cerebrospinal fluid glutamine levels in depressed patients.* Biol Psychiatry, 2000. 47(7): p. 586-93.
321. Albrecht, J. and E.A. Jones, *Hepatic encephalopathy: molecular mechanisms underlying the clinical syndrome.* J Neurol Sci, 1999. 170(2): p. 138-46.
322. Brusilow, S.W., et al., *Astrocyte glutamine synthetase: importance in hyperammonemic syndromes and potential target for therapy.* Neurotherapeutics, 2010. 7(4): p. 452-70.
323. Wendon, J. and W. Lee, *Encephalopathy and cerebral edema in the setting of acute liver failure: pathogenesis and management.* Neurocrit Care, 2008. 9(1): p. 97-102.
324. Lavoie, J., et al., *Amino acid changes in autopsied brain tissue from cirrhotic patients with hepatic encephalopathy.* J Neurochem, 1987. 49(3): p. 692-7.
325. Mans, A.M., M.R. DeJoseph, and R.A. Hawkins, *Metabolic abnormalities and grade of encephalopathy in acute hepatic failure.* J Neurochem, 1994. 63(5): p. 1829-38.
326. Yamamoto, H., *Hyperammonemia, increased brain neutral and aromatic amino acid levels, and encephalopathy induced by cyanide in mice.* Toxicol Appl Pharmacol, 1989. 99(3): p. 415-20.
327. Zanchin, G., et al., *Cerebral amino acid levels and uptake in rats after portocaval anastomosis: II. Regional studies in vivo.* J Neurosci Res, 1979. 4(4): p. 301-10.
328. Dejong, C.H., N.E. Deutz, and P.B. Soeters, *Cerebral cortex ammonia and glutamine metabolism in two rat models of chronic liver insufficiency-induced hyperammonemia: influence of pair-feeding.* J Neurochem, 1993. 60(3): p. 1047-57.
329. Hilgier, W. and J.E. Olson, *Brain ion and amino acid contents during edema development in hepatic encephalopathy.* J Neurochem, 1994. 62(1): p. 197-204.
330. Strauss, G.I., et al., *Cerebral metabolism of ammonia and amino acids in patients with fulminant hepatic failure.* Gastroenterology. 121(5): p. 1109-1119.
331. Kanamori, K. and B.D. Ross, *Suppression of glial glutamine release to the extracellular fluid studied in vivo by NMR and microdialysis in hyperammonemic rat brain.* J Neurochem, 2005. 94(1): p. 74-85.
332. Watanabe, A., et al., *Glutamic acid and glutamine levels in serum and cerebrospinal fluid in hepatic encephalopathy.* Biochem Med, 1984. 32(2): p. 225-31.
333. Jalan, R., et al., *Moderate hypothermia in patients with acute liver failure and uncontrolled intracranial hypertension.* Gastroenterology, 2004. 127(5): p. 1338-46.
334. Vaquero, J., C. Chung, and A.T. Blei, *Cerebral blood flow in acute liver failure: a finding in search of a mechanism.* Metab Brain Dis, 2004. 19(3-4): p. 177-94.
335. Hediger, M.A., et al., *The ABCs of solute carriers: physiological, pathological and therapeutic implications of human membrane transport proteinsIntroduction.* Pflugers Arch, 2004. 447(5): p. 465-8.
336. Broer, S., *Amino acid transport across mammalian intestinal and renal epithelia.* Physiol Rev, 2008. 88(1): p. 249-86.
337. Christensen, H.N., *Organic ion transport during seven decades. The amino acids.* Biochim Biophys Acta, 1984. 779(3): p. 255-69.

338. Christensen, H.N., *Role of amino acid transport and countertransport in nutrition and metabolism.* Physiol Rev, 1990. 70(1): p. 43-77.
339. Oxender, D.L. and H.N. Christensen, *DISTINCT MEDIATING SYSTEMS FOR THE TRANSPORT OF NEUTRAL AMINO ACIDS BY THE EHRLICH CELL.* J Biol Chem, 1963. 238: p. 3686-99.
340. Christensen, H.N., et al., *Gene-product designations for amino acid transporters.* J Exp Biol, 1994. 196: p. 51-7.
341. Collarini, E.J. and D.L. Oxender, *Mechanisms of transport of amino acids across membranes.* Annu Rev Nutr, 1987. 7: p. 75-90.
342. Bannai, S., et al., *Amino acid transport systems.* Nature, 1984. 311(5984): p. 308.
343. Guastella, J., et al., *Cloning and expression of a rat brain GABA transporter.* Science, 1990. 249(4974): p. 1303-6.
344. Kim, J.W., et al., *Transport of cationic amino acids by the mouse ecotropic retrovirus receptor.* Nature, 1991. 352(6337): p. 725-8.
345. Wang, H., et al., *Cell-surface receptor for ecotropic murine retroviruses is a basic amino-acid transporter.* Nature, 1991. 352(6337): p. 729-31.
346. Palacin, M., et al., *Molecular biology of mammalian plasma membrane amino acid transporters.* Physiol Rev, 1998. 78(4): p. 969-1054.
347. Verrey, F., et al., *CATs and HATs: the SLC7 family of amino acid transporters.* Pflugers Arch, 2004. 447(5): p. 532-42.
348. Bode, B.P., *Recent molecular advances in mammalian glutamine transport.* J Nutr, 2001. 131(9 Suppl): p. 2475S-85S; discussion 2486S-7S.
349. McGivan, J.D. and C.I. Bungard, *The transport of glutamine into mammalian cells.* Front Biosci, 2007. 12: p. 874-82.
350. Mackenzie, B., et al., *Functional properties and cellular distribution of the system A glutamine transporter SNAT1 support specialized roles in central neurons.* J Biol Chem, 2003. 278(26): p. 23720-30.
351. Yao, D., et al., *A novel system A isoform mediating Na+/neutral amino acid cotransport.* J Biol Chem, 2000. 275(30): p. 22790-7.
352. Baird, F.E., et al., *Bidirectional substrate fluxes through the system N (SNAT5) glutamine transporter may determine net glutamine flux in rat liver.* J Physiol, 2004. 559(Pt 2): p. 367-81.
353. Broer, A., et al., *The astroglial ASCT2 amino acid transporter as a mediator of glutamine efflux.* J Neurochem, 1999. 73(5): p. 2184-94.
354. Broer, A., et al., *The orphan transporter v7-3 (slc6a15) is a Na+-dependent neutral amino acid transporter (B0AT2).* Biochem J, 2006. 393(Pt 1): p. 421-30.
355. Yanagida, O., et al., *Human L-type amino acid transporter 1 (LAT1): characterization of function and expression in tumor cell lines.* Biochim Biophys Acta, 2001. 1514(2): p. 291-302.
356. Mastroberardino, L., et al., *Amino-acid transport by heterodimers of 4F2hc/CD98 and members of a permease family.* Nature, 1998. 395(6699): p. 288-91.
357. Segawa, H., et al., *Identification and functional characterization of a Na+-independent neutral amino acid transporter with broad substrate selectivity.* J Biol Chem, 1999. 274(28): p. 19745-51.
358. Rossier, G., et al., *LAT2, a new basolateral 4F2hc/CD98-associated amino acid transporter of kidney and intestine.* J Biol Chem, 1999. 274(49): p. 34948-54.
359. Rajan, D.P., et al., *Cloning and functional characterization of a Na+-independent, broad-specific neutral amino acid transporter from mammalian intestine.* Biochimica et Biophysica Acta (BBA) - Biomembranes, 2000. 1463(1): p. 6-14.
360. Broer, A., J.W. Deitmer, and S. Broer, *Astroglial glutamine transport by system N is upregulated by glutamate.* Glia, 2004. 48(4): p. 298-310.

361. Broer, A., et al., *The heterodimeric amino acid transporter 4F2hc/y+LAT2 mediates arginine efflux in exchange with glutamine.* Biochem J, 2000. 349 Pt 3: p. 787-95.
362. Gonzalez-Gonzalez, I.M., et al., *Immunohistochemical localization of the amino acid transporter SNAT2 in the rat brain.* Neuroscience, 2005. 130(1): p. 61-73.
363. Gliddon, C.M., et al., *Cellular distribution of the neutral amino acid transporter subtype ASCT2 in mouse brain.* J Neurochem, 2009. 108(2): p. 372-83.
364. Hagglund, M.G., et al., *B(0)AT2 (SLC6A15) is localized to neurons and astrocytes, and is involved in mediating the effect of leucine in the brain.* PLoS One, 2013. 8(3): p. e58651.
365. Braun, D., et al., *Developmental and cell type-specific expression of thyroid hormone transporters in the mouse brain and in primary brain cells.* Glia, 2011. 59(3): p. 463-71.
366. Hagglund, M.G., et al., *Identification of SLC38A7 (SNAT7) protein as a glutamine transporter expressed in neurons.* J Biol Chem, 2011. 286(23): p. 20500-11.
367. Bae, S.Y., et al., *Y+ and y+ L arginine transporters in neuronal cells expressing tyrosine hydroxylase.* Biochim Biophys Acta, 2005. 1745(1): p. 65-73.
368. Tanaka, K., A. Yamamoto, and T. Fujita, *Functional expression and adaptive regulation of Na+ -dependent neutral amino acid transporter SNAT2/ATA2 in normal human astrocytes under amino acid starved condition.* Neurosci Lett, 2005. 378(2): p. 70-5.
369. Boado, R.J., et al., *Selective expression of the large neutral amino acid transporter at the blood-brain barrier.* Proc Natl Acad Sci U S A, 1999. 96(21): p. 12079-84.
370. Agarwal, N., E.S. Lippmann, and E.V. Shusta, *Identification and expression profiling of blood-brain barrier membrane proteins.* J Neurochem, 2010. 112(3): p. 625-35.
371. Xiang, J., et al., *Glutamine transport at the blood-brain and blood-cerebrospinal fluid barriers.* Neurochem Int, 2003. 43(4-5): p. 279-88.
372. Sanchez del Pino, M.M., D.R. Peterson, and R.A. Hawkins, *Neutral amino acid transport characterization of isolated luminal and abluminal membranes of the blood-brain barrier.* J Biol Chem, 1995. 270(25): p. 14913-8.
373. Hawkins, R.A., et al., *Structure of the blood-brain barrier and its role in the transport of amino acids.* J Nutr, 2006. 136(1 Suppl): p. 218s-26s.
374. Duelli, R., et al., *Expression of large amino acid transporter LAT1 in rat brain endothelium.* J Cereb Blood Flow Metab, 2000. 20(11): p. 1557-62.
375. Mackenzie, B. and J.D. Erickson, *Sodium-coupled neutral amino acid (System N/A) transporters of the SLC38 gene family.* Pflugers Arch, 2004. 447(5): p. 784-95.
376. Christensen, H.N., et al., *The use of N-methylation to direct route of mediated transport of amino acids.* J Biol Chem, 1965. 240(9): p. 3609-16.
377. Shotwell, M.A., et al., *Neutral amino acid transport systems in Chinese hamster ovary cells.* J Biol Chem, 1981. 256(11): p. 5422-7.
378. McGivan, J.D. and M. Pastor-Anglada, *Regulatory and molecular aspects of mammalian amino acid transport.* Biochemical Journal, 1994. 299(Pt 2): p. 321-334.
379. Sugawara, M., et al., *Structure and function of ATA3, a new subtype of amino acid transport system A, primarily expressed in the liver and skeletal muscle.* Biochim Biophys Acta, 2000. 1509(1-2): p. 7-13.
380. Takanaga, H., et al., *ATA2 is predominantly expressed as system A at the blood-brain barrier and acts as brain-to-blood efflux transport for L-proline.* Mol Pharmacol, 2002. 61(6): p. 1289-96.
381. Uhl, G.R. and P.S. Johnson, *Neurotransmitter transporters: three important gene families for neuronal function.* J Exp Biol, 1994. 196: p. 229-36.
382. Takanaga, H., et al., *Characterization of a branched-chain amino-acid transporter SBAT1 (SLC6A15) that is expressed in human brain.* Biochem Biophys Res Commun, 2005. 337(3): p. 892-900.

383. Fei, Y.J., et al., *Primary structure, genomic organization, and functional and electrogenic characteristics of human system N 1, a Na+- and H+-coupled glutamine transporter.* J Biol Chem, 2000. 275(31): p. 23707-17.
384. Nakanishi, T., et al., *Cloning and functional characterization of a new subtype of the amino acid transport system N.* Am J Physiol Cell Physiol, 2001. 281(6): p. C1757-68.
385. Chaudhry, F.A., et al., *Coupled and uncoupled proton movement by amino acid transport system N.* The EMBO Journal, 2001. 20(24): p. 7041-7051.
386. Chaudhry, F.A., et al., *Molecular Analysis of System N Suggests Novel Physiological Roles in Nitrogen Metabolism and Synaptic Transmission.* Cell, 1999. 99(7): p. 769-780.
387. Chesler, M. and K. Kaila, *Modulation of pH by neuronal activity.* Trends Neurosci, 1992. 15(10): p. 396-402.
388. Deitmer, J.W. and C.R. Rose, *pH regulation and proton signalling by glial cells.* Prog Neurobiol, 1996. 48(2): p. 73-103.
389. Kilberg, M.S., M.E. Handlogten, and H.N. Christensen, *Characteristics of an amino acid transport system in rat liver for glutamine, asparagine, histidine, and closely related analogs.* J Biol Chem, 1980. 255(9): p. 4011-9.
390. Umapathy, N.S., et al., *Expression and function of system N glutamine transporters (SN1/SN2 or SNAT3/SNAT5) in retinal ganglion cells.* Invest Ophthalmol Vis Sci, 2008. 49(11): p. 5151-60.
391. Xiang, J., et al., *Glutamine transport at the blood–brain and blood–cerebrospinal fluid barriers.* Neurochemistry International, 2003. 43(4-5): p. 279-288.
392. Nakanishi, T., et al., *Structure, function, and tissue expression pattern of human SN2, a subtype of the amino acid transport system N.* Biochem Biophys Res Commun, 2001. 281(5): p. 1343-8.
393. Ennis, S.R., et al., *Glutamine uptake at the blood-brain barrier is mediated by N-system transport.* J Neurochem, 1998. 71(6): p. 2565-73.
394. Christensen, H.N., M. Liang, and E.G. Archer, *A distinct Na+-requiring transport system for alanine, serine, cysteine, and similar amino acids.* J Biol Chem, 1967. 242(22): p. 5237-46.
395. Kanai, Y. and M.A. Hediger, *The glutamate/neutral amino acid transporter family SLC1: molecular, physiological and pharmacological aspects.* Pflugers Arch, 2004. 447(5): p. 469-79.
396. Zander, C.B., T. Albers, and C. Grewer, *Voltage-dependent processes in the electroneutral amino acid exchanger ASCT2.* J Gen Physiol, 2013. 141(6): p. 659-72.
397. Wagner, C.A., F. Lang, and S. Broer, *Function and structure of heterodimeric amino acid transporters.* Am J Physiol Cell Physiol, 2001. 281(4): p. C1077-93.
398. Christensen, H.N., et al., *A Bicyclic Amino Acid to Improve Discriminations among Transport Systems.* Journal of Biological Chemistry, 1969. 244(6): p. 1510-1520.
399. Kanai, Y., et al., *Expression cloning and characterization of a transporter for large neutral amino acids activated by the heavy chain of 4F2 antigen (CD98).* J Biol Chem, 1998. 273(37): p. 23629-32.
400. Pineda, M., et al., *Identification of a membrane protein, LAT-2, that Co-expresses with 4F2 heavy chain, an L-type amino acid transport activity with broad specificity for small and large zwitterionic amino acids.* J Biol Chem, 1999. 274(28): p. 19738-44.
401. Fotiadis, D., Y. Kanai, and M. Palacin, *The SLC3 and SLC7 families of amino acid transporters.* Mol Aspects Med, 2013. 34(2-3): p. 139-58.
402. Deitmer, J.W., A. Broer, and S. Broer, *Glutamine efflux from astrocytes is mediated by multiple pathways.* J Neurochem, 2003. 87(1): p. 127-35.
403. Deves, R., P. Chavez, and C.A. Boyd, *Identification of a new transport system (y+L) in human erythrocytes that recognizes lysine and leucine with high affinity.* J Physiol, 1992. 454: p. 491-501.

404. Kanai, Y., et al., *Transport properties of a system y+L neutral and basic amino acid transporter. Insights into the mechanisms of substrate recognition.* J Biol Chem, 2000. 275(27): p. 20787-93.
405. Pfeiffer, R., et al., *Amino acid transport of y+L-type by heterodimers of 4F2hc/CD98 and members of the glycoprotein-associated amino acid transporter family.* The EMBO Journal, 1999. 18(1): p. 49-57.
406. Torrents, D., et al., *Identification and characterization of a membrane protein (y+L amino acid transporter-1) that associates with 4F2hc to encode the amino acid transport activity y+L. A candidate gene for lysinuric protein intolerance.* J Biol Chem, 1998. 273(49): p. 32437-45.
407. Rooman, I., et al., *Amino acid transporters expression in acinar cells is changed during acute pancreatitis.* Pancreatology, 2013. 13(5): p. 475-85.
408. Pascal, L.E., et al., *Correlation of mRNA and protein levels: cell type-specific gene expression of cluster designation antigens in the prostate.* BMC Genomics, 2008. 9: p. 246.
409. Vogel, C. and E.M. Marcotte, *Insights into the regulation of protein abundance from proteomic and transcriptomic analyses.* Nat Rev Genet, 2012. 13(4): p. 227-232.
410. Nie, L., G. Wu, and W. Zhang, *Correlation of mRNA expression and protein abundance affected by multiple sequence features related to translational efficiency in Desulfovibrio vulgaris: a quantitative analysis.* Genetics, 2006. 174(4): p. 2229-43.
411. Tian, Q., et al., *Integrated genomic and proteomic analyses of gene expression in Mammalian cells.* Mol Cell Proteomics, 2004. 3(10): p. 960-9.
412. Schwanhausser, B., et al., *Global quantification of mammalian gene expression control.* Nature, 2011. 473(7347): p. 337-42.
413. Sharova, L.V., et al., *Database for mRNA half-life of 19 977 genes obtained by DNA microarray analysis of pluripotent and differentiating mouse embryonic stem cells.* DNA Res, 2009. 16(1): p. 45-58.
414. Mayr, C. and D.P. Bartel, *Widespread shortening of 3'UTRs by alternative cleavage and polyadenylation activates oncogenes in cancer cells.* Cell, 2009. 138(4): p. 673-84.
415. Sandberg, R., et al., *Proliferating cells express mRNAs with shortened 3′ untranslated regions and fewer microRNA target sites.* Science, 2008. 320(5883): p. 1643-7.
416. Kehr, J., *Monitoring Chemistry of Brain Microenvironment: Biosensors, Microdialysis and Related Techniques*, in *Modern Techniques in Neuroscience Research*, U. Windhorst and H. Johansson, Editors. 1999, Springer Berlin Heidelberg. p. 1149-1198.
417. Zhang, X., R.D. Myers, and W.R. Wooles, *New triple microbore cannula system for push-pull perfusion of brain nuclei of the rat.* J Neurosci Methods, 1990. 32(2): p. 93-104.
418. Zhang, X., E. Wulfert, and I. Hanin, *Development of a sensitive and inexpensive micropush—pull technique for the continuous analysis of brain neurotransmitters and metabolites in vivo.* Journal of Neuroscience Methods, 1992. 42(1–2): p. 139-147.
419. Kottegoda, S., I. Shaik, and S.A. Shippy, *Demonstration of low flow push–pull perfusion.* Journal of Neuroscience Methods, 2002. 121(1): p. 93-101.
420. Justice, J., *Voltammetry in the Neurosciences: Principles, Methods, and Applications*. 1987: Humana Press.
421. Kawagoe, K.T., J.B. Zimmerman, and R.M. Wightman, *Principles of voltammetry and microelectrode surface states.* Journal of Neuroscience Methods, 1993. 48(3): p. 225-240.
422. Müller, M., *Microdialysis in Drug Development*. 2012: Springer New York.
423. Chefer, V.I., et al., *Overview of brain microdialysis.* Curr Protoc Neurosci, 2009. Chapter 7: p. Unit7 1.
424. Pardridge, W.M., *Drug transport in brain via the cerebrospinal fluid.* Fluids and Barriers of the CNS, 2011. 8: p. 7-7.

425. Stephan, J., *Heterogeneous distribution and utilization of inhibitory neurotransmitter transporters.* Neurotransmitter, 2015. 2(1): p. 1-7.
426. Lee, V. and J. Maguire, *The impact of tonic GABA(A) receptor-mediated inhibition on neuronal excitability varies across brain region and cell type.* Frontiers in Neural Circuits, 2014. 8: p. 3.
427. Lammel, S., B.K. Lim, and R.C. Malenka, *Reward and aversion in a heterogeneous midbrain dopamine system.* Neuropharmacology, 2014. 76, Part B(0): p. 351-359.
428. Mergenthaler, P., et al., *Sugar for the brain: the role of glucose in physiological and pathological brain function.* Trends in Neurosciences, 2013. 36(10): p. 587-597.
429. Simpson, I.A., A. Carruthers, and S.J. Vannucci, *SUPPLY AND DEMAND IN CEREBRAL ENERGY METABOLISM: THE ROLE OF NUTRIENT TRANSPORTERS.* Journal of cerebral blood flow and metabolism : official journal of the International Society of Cerebral Blood Flow and Metabolism, 2007. 27(11): p. 1766-1791.
430. Burant, C.F. and G.I. Bell, *Mammalian facilitative glucose transporters: evidence for similar substrate recognition sites in functionally monomeric proteins.* Biochemistry, 1992. 31(42): p. 10414-20.
431. Cerdán, S., et al., *The redox switch/redox coupling hypothesis.* Neurochemistry International, 2006. 48(6–7): p. 523-530.
432. Grewal, S., et al., *SNAT2 amino acid transporter is regulated by amino acids of the SLC6 gamma-aminobutyric acid transporter subfamily in neocortical neurons and may play no role in delivering glutamine for glutamatergic transmission.* J Biol Chem, 2009. 284(17): p. 11224-36.
433. Bagga, P., et al., *Characterization of cerebral glutamine uptake from blood in the mouse brain: implications for metabolic modeling of 13C NMR data.* J Cereb Blood Flow Metab, 2014. 34(10): p. 1666-72.
434. Erecinska, M. and D. Nelson, *Activation of glutamate dehydrogenase by leucine and its nonmetabolizable analogue in rat brain synaptosomes.* J Neurochem, 1990. 54(4): p. 1335-43.
435. Fahien, L.A., et al., *Regulation of glutamate dehydrogenase by Mg2+ and magnification of leucine activation by Mg2+.* Mol Pharmacol, 1990. 37(6): p. 943-9.
436. Betz, A.L., J.A. Firth, and G.W. Goldstein, *Polarity of the blood-brain barrier: distribution of enzymes between the luminal and antiluminal membranes of brain capillary endothelial cells.* Brain Res, 1980. 192(1): p. 17-28.
437. Kubo, Y., et al., *Quantitative Determination of Luminal and Abluminal Membrane Distributions of Transporters in Porcine Brain Capillaries by Plasma Membrane Fractionation and Quantitative Targeted Proteomics.* Journal of Pharmaceutical Sciences, 2015: p. n/a-n/a.
438. Verrey, F., *System L: heteromeric exchangers of large, neutral amino acids involved in directional transport.* Pflugers Arch, 2003. 445(5): p. 529-33.
439. Poncet, N., et al., *The catalytic subunit of the system L1 amino acid transporter (slc7a5) facilitates nutrient signalling in mouse skeletal muscle.* PLoS One, 2014. 9(2): p. e89547.
440. Chan K., B.S.M., Wagner C.A., *CHARACTERIZATION OF A SLC38A3 (SNAT3) DEFICIENT MOUSE.* Acta Physiologica, 2011. 201(Supplement 682).
441. Monvoisin, A., et al., *VE-cadherin-CreERT2 transgenic mouse: a model for inducible recombination in the endothelium.* Dev Dyn, 2006. 235(12): p. 3413-22.
442. Katayama, Y., et al., *Massive increases in extracellular potassium and the indiscriminate release of glutamate following concussive brain injury.* J Neurosurg, 1990. 73(6): p. 889-900.

8. Curriculum Vitae

ELENA DOLGODILINA

PERSONAL DATA

Date of Birth	23/11/1986
Nationality	Belarusian
	Residence permit B (Switzerland)
Address	Berninastrasse 9, 8057 Zürich, Switzerland
Mobile phone	+41(0)786035465
E-mail	elena.dolgodilina@uzh.ch

EDUCATION

08/2010 - present	University of Zürich, Institute of Physiology, Switzerland **PhD in Integrative Molecular Medicine** Regulation of amino acid homeostasis in the brain interstitial fluid
09/2009 – 06/2010	Belarusian State University, Department of Biochemistry, Belarus **Master Thesis in Biochemistry** Antioxidant and prooxidant properties of some flavonoids
09/2004 – 06/2009	Belarusian State University, Department of Biochemistry, Belarus **Specialist degree in Biotechnology, Biochemistry**
09/1993 – 06/2004	Kolodischanskaya Secondary School, Belarus

EXPERIENCE

08/2010 - present **Graduate researcher**

- Work with laboratory animals (cranial surgeries, microdialysis in rodents, breeding, genotyping, terminal perfusion)
- Routine cell culture techniques
- Molecular-biological and biochemical methods (cloning, DNA and RNA isolation, western-blotting, immunofluorescence)
- Microscopy (bright field, confocal)
- Analytical methods (uHPLC)

09/2009 – 06/2010 **Undergraduate researcher**

- General biochemical measurement assays
- Spectrophotometric kinetic assay

PROFESSIONAL SKILLS

- Design and conduction of experiments
- Collection, processing and analysis of experimental data
- Performance of collaborative projects
- Scientific writing
- Data presentation
- Teaching assistance for medical students

LANGUAGES

Russian, Belarusian	Native
English	C1
German	B1

COMPUTER SKILLS	Windows OS, Mac OS X, Microsoft Office 2000/XP
GRAPHICS EDITORS	Adobe Photoshop, Imaris, ImageJ
OTHER SOFTWARE	GraphPad Prism, Clone Manager

PUBLICATION LIST	E.Dolgodilina, S. Imobersteg, T. Welt, E. Laczko, V. Makrides, F. Verrey (2015) Brain interstitial fluid glutamine homeostasis is controlled by blood-brain barrier SLC7A5/LAT1 amino acid transporter (submitted in JCBFM)

PRIZES AND AWARDS

2013	Swiss Physiological Society travel grant
2012	Hartmann Müller-Stiftung travel grant

9. Acknowledgements

So, this is it. And here I would like to thank people without whom this adventure called PhD would never happen.

First of all, I would like to thank François Verrey for the unique possibility to perform this exciting and challenging project and critical scientific inputs during "jour fixe" and early Monday morning labmeetings.

Many thanks to my thesis committee members Britta Engelhardt, Jean-Marc Fritschy and Carsten Wagner for constructive discussions and important suggestions during our meetings.

A special thank to Victoria Makrides, who has been carefully supervising my work for all these years, for endless discussions and great help in improving my skills in time management, presentation and exercising my patience in research.

I am grateful to the imMed PhD program for nice retreats and possibility to gather with PhD students from other Institutes.

I would like to thank past and present people not only from our lab, but also from the whole J-floor, who created nice working atmosphere. I am grateful to Nadine for being a patient and knowledgeable guide for me during my first months in the lab. Thanks a lot to Sandra, who joined the BBB subgroup and shared the "love" for glutamine uptake by SNAT5. Many thanks to Philipp Gysin for his assistance with visa issues; Helen for finding my first accommodation and great help on my first day in Zurich; Brigitte for her invaluable assistance in OHB (I will always remember never ending search of cages) and with mD stuff orders; Simone for sharing love for SNAT5 antibody and glutamine measurement; Ian for a proper introduction for "the needles pulling" and moreover for his hospitality during nice pizza/movie nights; Katja for sharing some tricks for western blotting and precious protocols for bacterial cells production (lab duties). I am happy that here I met Marta, not only a lab mate, but also a reliable friend, who has been patiently listening to my "super lucky" stories and shared happiness and difficulties for all these years in and outside the lab. Thanks to Luca, Adriano and Selene, who have transformed our office to a small Italian speaking country; Alok(ino) for his optimism and chips/popcorn parties; Evelyne for the important encouragement, an establishment a nice "Zvieri" tradition and correcting my numerous mistakes in German and translation of Zusammenfassung. Many thanks to Nicola, Lorenz, Tina, Olga, Raphael, Daniel, Carlos, Lukas, Felipe, Christian, Laura, Sam, Lalita (especially for her truthfulness and outstanding waving skills), Emilia, Liviu, Julia (for great help with the Disney "sammelaktion" from COOP), Nadège, Eva, Stine, Mehdi. Special

thank to Sabrine, with whom we had amazing experience and nice discussions during BBB conferences in the US and Hungary.

Moreover I extremely thankful to people who I met in the lab of Prof. Roger Nitsch and in FGCZ. Thanks to Tobias Welt for introducing me to the world of mD experiments, also Claudia, Fabian and Anna who helped a lot during my time in Burgwies and then in Schlieren (Wagi). I am eternally grateful to Stufi, who has been supporting me during my *in vivo* experiments for the last three years, for his outstanding sense of humor, kindness, readiness to help, sharing knowledge, creativity (newly designed lab items) and cheering up. Many thanks to Peter Hunziker and Birgit Roth for introducing to uHPLC analysis, useful advices and encouraging optimism.

I would like to thank people, who I met in Zurich and who made my staying here gorgeous and full of joy. Thanks to Zori for her enthusiasm, long discussions, unconditional support and great friendship; to Eli for her wise advises and lovely BBQs at the balcony and to both of them for amazing time at Zumba. Many thanks to Carmen and Patrick for fantastic skiing experience and relaxing time together; Benedetta and Rebeccita for warm and encouraging words and making me laugh; Fede for being an excellent flatmate, her tolerance and delicious strawberry cup cakes; Paola for long chats and all the time readiness to listen to. Particularly I am grateful to Tias for being always patient with me, for his love and encouragement.

Я также признательна Лешке и Паше, которых я встретила в самом начале этого длиного пути и с которыми я разделила много радостных и не очень событий. Спасибо за долгие беседы за чашкой чая, дельные советы, возможность выговориться и быть выслушаной и, наконец, за всегда своевременную помощь с компьютером. Кроме того, спасибо Катику и Настику за приятное время, проведенное вместе, и за приобщение к прекрасной музыке. Спасибо моим друзьям Кате Т, Половешке (Тане П.), Наде, Танюшке и Ленке за дружбу, выдержавшую испытание не только временем, но и расстоянием. И, конечно же, я безгранично благодарна моему брату, маме и папе за поддержку моих самых сумасшедших идей, веру в мои силы и безграничную любовь.